NASA TECHNICAL NOTE

NASA TN D-4051

NASA TN D-4051

ANALYSIS OF RADIATIVE HEAT TRANSFER FOR LARGE OBJECTS AT METEORIC SPEEDS

by Kenneth K. Yoshikawa

Ames Research Center
Moffett Field, Calif.

NATIONAL AERONAUTICS AND SPACE ADMINISTRATION • WASHINGTON, D. C. • JUNE 1967

NASA TN D-4051

ANALYSIS OF RADIATIVE HEAT TRANSFER FOR LARGE OBJECTS AT METEORIC SPEEDS

By Kenneth K. Yoshikawa

Ames Research Center
Moffett Field, Calif.

NATIONAL AERONAUTICS AND SPACE ADMINISTRATION

For sale by the Clearinghouse for Federal Scientific and Technical Information
Springfield, Virginia 22151 – CFSTI price $3.00

TABLE OF CONTENTS

ANALYSIS OF RADIATIVE HEAT TRANSFER FOR LARGE OBJECTS AT METEORIC SPEEDS

By Kenneth K. Yoshikawa

Ames Research Center

SUMMARY

An explicit closed-form solution has been obtained for radiative heat transfer to a body in flight in the earth's atmosphere at speeds such that radiation is the dominant mode of heat transfer. The solution was attained by assuming a gray-gas radiator and then linearizing the radiative transfer equation. Approximations to the one-dimensional flow equations are developed which allow the solution to be applied to the stagnation region of a shock layer on an axisymmetric body. Because of its characteristics, the linearized solution is readily applicable to multilayer heat transfer encountered during very high speed flights, when the interactions among the cold air ahead of the shock wave, the heated air behind the shock wave, and the layer of ablation gases adjacent to the body surface must be considered.

The development of the first-order linearized solution for radiative heat transfer is described, and some applications are presented and discussed. The results demonstrate the effects, on radiative and convective heat transfer to the body surface, of shock-layer energy loss by radiation, absorption of radiation within the multiple layers, blockage of radiative heating by blowing of ablative vapors, and the absorption and emission of radiation by the body.

INTRODUCTION

For atmospheric entry at meteor velocities, radiation is the dominant mode of energy transfer. Many investigators have emphasized the importance of understanding and predicting the radiant heat transfer to bodies at these speeds (e.g., refs. 1-3). These investigators have pointed out that energy loss by radiation from the shock layer and the reabsorption of radiation in the shock layer itself, in the free stream, and in ablation products will affect both the radiative and convective heat transfer to the body.

Both simplifying flow assumptions and intricate numerical techniques have been used to solve the gasdynamic problem. Examples of the flow assumptions that have been used are: one-dimensional porous flow (ref. 4) and a linear velocity distribution and constant pressure in the shock layer (ref. 5). Reference 6 showed that the mass flow distribution on the stagnation streamline, rather than the velocity distribution, is relatively insensitive to radiative heat transfer. Examples of numerical techniques are local similarity (ref. 7) and the integral method (ref. 8).

Most investigators have emphasized the effects of radiation cooling rather than self-absorption on shock-layer structure. The inclusion of self-absorption into the problem introduces additional complexities that require further simplification of either the equations or the forms of their solutions. These simplifications generally involve the substitution of an exponential function for the exponential integral that appears in the solutions of the transfer equation, and/or the use of successive approximations employing combinations of simple functions (refs. 9-13).

Substituting the exponential function is the simplest means of evaluating reentry radiation, including self-absorption, with reasonable accuracy.

At relatively high free-stream density, where the radiation mean free path is comparable to or smaller than the body size, one can assume that radiation flux is absorbed by the media just ahead of the shock front (preheating). The structure of the strong shock front has been investigated (refs. 14-17) for plane shock flow of a perfect gas. Such analyses explicitly consider thermal radiation effects on the structure of the shock wave rather than the influence of preheating energy on radiative heating.

The ablative mass loss from large meteors entering the atmosphere was considered (ref. 18) assuming a porous-flow analogy and the Rosseland approximation. The increase in total shock stand-off distance due to a sizable amount of ablation or injection has been shown, both theoretically and experimentally, to obey a linear correlation formula (refs. 19 and 20); this provides a basis for calculating radiative interaction between shock and ablation layers.

Our primary interest here is to obtain the simplest form of an analytical solution for radiative transfer in the shock layer, especially explicit expressions for radiative net fluxes at the body and at the shock. This solution includes the effect of self-absorption in a strong shock layer, the interaction of thermal radiation with the shock layer, the preheating zone, and the ablated vapor layer. The results will be used to relate the convective heating rates in adiabatic and nonadiabatic flow.

SYMBOLS

a_n	coefficient of series expansion (eqs. (15))
B	Stefan-Boltzmann function (eq. (2b)) or blowing parameter (eqs. (101b))
B_ν	Planck's function, $\frac{2h}{c^2}\frac{\nu^3}{e^{h\nu/kT}-1}$
$C_\nu(\theta), C_{-\nu}(\theta)$	indefinite integral of modified Bessel function (eqs. 37)
$C_\nu, C_{-\nu}$	definite integral of modified Bessel function (eqs. (38b))

c_p	specific heat at constant pressure
c_1, c_2	constants associated with equation (26a)
E_n	exponential integral function of order n (eq. (6))
F	thermal function defined by equation (14)
$\bar{F}'$	$\frac{dF}{d\bar{\theta}}$
f	auxiliary function defined by equations (18c)
f_w	blowing rate, $\frac{\rho_w v_w}{\rho_\infty V_\infty}$
g	parameter defined by equations (101b)
H	altitude
h	enthalpy
$\bar{h}$	enthalpy ratio, $\frac{h}{h_s}$
I	specific intensity (eq. (1))
I_ν	modified Bessel function of first kind (order ν)
$K_1, K_2, K_3, K_4, K_5, K_6$	functions defined by equations (32c) and (38a)
K_ν	modified Bessel function of second kind (order ν)
k	constant associated with shock stand-off distance (eqs. (76)) or the Boltzmann constant
k_b	constant associated with blowing thickness (eq. (94))
L, L_b	nonadiabatic shock stand-off distance and nonadiabatic blowing thickness
L_o, L_{bo}	adiabatic shock and blowing thickness
L_t	total shock-layer thickness
L_ν	modified Struve function (eq. (C14a))
M	molecular weight

$M_0, M_1, M_2, M_3, M_4, M_5$	functions defined by equations (26), (33), and (40)
m	constant (1/2), mass, or power of pressure ratio
n	exponential constant
O	order of
p	pressure
$\bar{p}$	pressure ratio, $\frac{p}{p_s}$
Q_1, Q_2	function defined in equations (55)
q	net radiative flux
q_c	convective heat
q_{co}	convective heat with no radiation loss
q_o	adiabatic radiative heat, $2\rho_s \kappa_s \sigma T_s^4 L_o$
R	dimensionless boundary value (inward direction is positive) (eqs. (8b) and (c)) or body radius
R^*	dimensionless boundary value based on T_f, $\frac{q}{2\pi B(T_f)}$
$R^\dagger$	dimensionless boundary value based on T_{sp}, $\frac{q}{2\pi B(T_{sp})}$
r	reflectivity
T	temperature
T_{ef}	effective surface temperature (eqs. (54a) and (b))
T_o	surface temperature ahead of shock
$\bar{T}$	temperature ratio, $\frac{T}{T_s}$
$\bar{T}_s$	temperature ratio, unity or $\frac{T_o}{T_s}$ (eqs. (68))
$\bar{T}_w$	temperature ratio, $\frac{T_w}{T_s}$
t	dummy variable
u	x component of velocity

V_∞	free-stream velocity
v	y component of velocity
W	Wronskian operator
X	linear solution defined by equation (26a)
x	distance along body
Y	linear solution defined by equation (26a) or adiabatic distance (eq. (74a))
y	normal distance from shock to wall
$Z_\nu(\theta), Z_{-\nu}(\theta)$	Bessel function defined by $\theta^\nu I_\nu(n\theta)$, $\theta^\nu K_\nu(n\theta)$
$Z_\nu, Z_{-\nu}, Z^*_{-\nu}$	values of Bessel function defined by equations (38b)
z, z_o	constant defined by equations (F2b)
$\bar{\alpha}$	average value of $\frac{\partial \bar{T}^4}{\partial F}$ (eq. (15d))
β_1, β_2	characteristic constants (eqs. (28))
Γ	dimensionless radiative flux function (eq. (8a)) or gamma function as designated
$\Delta\Gamma_s$	radiative flux absorbed by preheating zone ($\Gamma_{sp} - \Gamma_\infty$)
γ	constant that characterizes flows (zero for plane shock flow, one for stagnation flow)
Δ	determinant (eqs. (33) and (40))
δ	boundary-layer thickness (eq. (105))
ϵ	emissivity of boundary (eqs. (67))
ζ	heat of vaporization
η	variable defined by equation (F1c)
η_o	quantity defined by equation (F3b)
θ	independent variable $\tau_w - \tau$ (eqs. (18c)), angle of directional cosine, or apex angle
κ	mass absorption coefficient (eq. (2a))

λ ratio of radiative heat to total flow energy, $\frac{q}{(1/2)\rho_\infty v_\infty^3} \left(\simeq \frac{q}{\rho_\infty v_\infty h_s} \right)$

λ_a ratio of black-body radiation loss to total energy, $\frac{2\sigma T_s^4}{\rho_\infty v_\infty h_s}$

λ_b $\frac{2\sigma T_w^4}{\rho_\infty v_\infty h_w}$

λ_m recurrence formula (eqs. (C14c))

λ_o adiabatic radiation loss parameter, $\frac{4\rho_s \kappa_s \sigma T_s^4 L_o}{\rho_\infty V_\infty h_s}$

λ_o^* modified radiation loss parameter, $\left(\frac{v_{ref}}{V_\infty}\right) \lambda_o$

μ direction cosine or viscosity

μ_o quantity defined by equation (F3b)

ν order of Bessel function (eq. (35b)), or frequency

ν_o parameter, $mn\bar{\alpha}\tau_w$

ρ density

$\rho\kappa$ absorption coefficient, cm^{-1}

σ Stefan-Boltzmann constant

τ optical thickness defined by equation (2a)

$\bar{\tau}$ $\frac{\tau}{\tau_w}$

τ_i optical thickness at interface

τ_w, τ_{wb} optical thickness at wall

Φ_w, Φ_{wb} radiative blockage function at wall (eq. (107))

Φ_∞ radiative leakage function, $\frac{\Gamma_\infty}{\Gamma_{sp}}$

φ thermal function defined in equations (18c)

φ_o Euler's constant (0.57721 . . .) + 2 ln 2 (eqs. (55))

χ	dimensionless mass flow rate, $\rho v/\rho_\infty V_\infty$ (eqs. (11))
ω	absorption parameter (eq. (82))

Superscript

$\pm$	direction toward free stream or downstream
I,II	reference properties based on region I or region II
*	preheating zone, or limiting value of Bessel function
†	modified function of dimensionless quantities (dimensionless function based on temperature behind shock)

Subscript

b	blowing layer
e	edge of gas layer
f	just ahead of shock wave, shock front
i	interface
l	local
p	preheating effect
o	adiabatic, no absorption, no ablation, no preheating effect
r,ref	reference condition
s	immediately behind the shock wave
sl	sea level
sp	shock wave due to preheating effect
t	total
w	wall
wo	wall without preheating and injection
wp	wall with preheating effect
∞	free stream

ANALYSIS

The equation of radiative transfer will be combined with a simplified gasdynamic energy equation for one-dimensional flow, and the thermodynamic properties of air will be introduced in such a way as to make the resulting equation linear. Solutions for this linear equation will be obtained for plane shock flow and stagnation stream-tube flows. The extension of the technique to multiple gas layers (e.g., a zone of preheating or of injected or ablated species) will be considered. The calculation of radiative heat-transfer rates at boundaries will be emphasized. However, auxiliary results, such as the distribution of enthalpy and temperature in the shock layer and the reduction of shock-layer thickness as a result of radiative transfer will be obtained. Details of the analyses are deferred to appendixes wherever possible. The notation used follows closely that of reference 5 or of reference 21 with minor differences.

Assumptions and Geometry

The following assumptions are basic to the analysis:

1. One-dimensional flow (plane shock flow and stagnation stream flow)

2. Local thermodynamic equilibrium

3. Gray-gas approximation

4. Viscosity and heat transfer by thermal conduction are neglected. (However, the effect of radiation on convective heating will be estimated in a later section.)

5. In the solution of the transfer equation, the exponential integrals are replaced by exponential functions.

6. The term T^4 is assumed to be locally a linear function of enthalpy, and a thermal function is defined which incorporates this relation (locally linear thermal relation).

Figures 1(a) and 1(b) show the geometry used in the analysis.

Basic Radiative Equation

If the absorption coefficient of the gas is assumed to be independent of frequency (gray gas) and the gas to be in local thermodynamic equilibrium, the radiative transfer equation for plane parallel flow is

$$\mu \frac{dI}{d\tau} + I = B \tag{1}$$

where I is the specific intensity (rate of radiative energy flow per unit area and solid angle), and μ is the direction cosine relative to the free stream (upstream direction is positive). The optical thickness τ and the Stefan-Boltzmann function B are defined by

$$\tau = \int_0^y \rho\kappa \, dy \tag{2a}$$

$$B = \int_0^\infty B_\nu \, d\nu = \frac{\sigma}{\pi} T^4 \tag{2b}$$

where B_ν is Planck's function and κ, the mass absorption coefficient.

The formal solution to equation (1) is

$$I^-(\tau,\mu) = I^-(0)e^{-(\tau/-\mu)} + \int_0^\tau Be^{-(\tau-t)/-\mu} \, dt/-\mu \tag{3a}$$

$$I^+(\tau,\mu) = I^+(\tau_w)e^{-(\tau_w-\tau)/\mu} + \int_\tau^{\tau_w} Be^{-(t-\tau)/\mu} \, dt/\mu \tag{3b}$$

where I^+ is the specific intensity in the upstream direction (positive μ) and I^- in the downstream direction (negative μ); τ_w is the optical thickness at the downstream boundary.

The rate of radiative energy transport per unit area (fig. 1(b)) is

$$q^-(\tau) = 2\pi \int_0^{-1} I^-(\tau,\mu)\mu \, d\mu \tag{4a}$$

$$q^+(\tau) = 2\pi \int_0^1 I^+(\tau,\mu)\mu \, d\mu \tag{4b}$$

It follows that

$$q^-(\tau) = 2q_s^- E_3(\tau) + 2\pi \int_0^\tau BE_2(\tau - t)dt \tag{5a}$$

$$q^+(\tau) = 2q_w^+ E_3(\tau_w - \tau) + 2\pi \int_\tau^{\tau_w} BE_2(t - \tau)dt \tag{5b}$$

where $q_s^- = \pi I^-(0)$, $q_w^+ = \pi I^+(\tau_w)$, and the exponential integral function E_n (refs. 9 and 22) is

$$E_n(\tau) \equiv \int_0^1 e^{-\tau/\mu}\, \mu^{n-2}\, d\mu = \int_1^\infty e^{-\tau x}/x^n\, dx \tag{6}$$

The net flux transferred per unit area q is

$$q(\tau) = q^+(\tau) - q^-(\tau) \tag{7}$$

If the dimensionless notations

$$\Gamma \equiv \Gamma(\tau) = q(\tau)/2\pi B_s \tag{8a}$$

$$\Gamma_s^- \equiv q_s^-/2\pi B_s = R_s \tag{8b}$$

$$\Gamma_w^+ \equiv q_w^+/2\pi B_s = R_w \tag{8c}$$

$$\bar{T} \equiv T/T_s \tag{8d}$$

are introduced into equation (7), we obtain

$$\Gamma(\tau) = -2R_s E_3(\tau) + 2R_w E_3(\tau_w - \tau) - \int_0^\tau \bar{T}^4 E_2(\tau - t)dt + \int_\tau^{\tau_w} \bar{T}^4 E_2(t - \tau)dt \tag{9a}$$

The subscript s refers to position immediately behind shock wave. The first and second terms in equation (9a) represent the radiative fluxes at τ from the upstream and downstream boundaries, respectively, attenuated by the gas between τ and the boundaries. The third and fourth terms represent the radiative fluxes at τ from the gas between τ and the upstream and downstream boundaries, respectively, attenuated by self-absorption. At the upstream and downstream boundaries, equation (9a) reduces to

$$\Gamma_s \equiv \Gamma(0) = -2R_s E_3(0) + 2R_w E_3(\tau_w) + \int_0^{\tau_w} \bar{T}^4 E_2(t)dt = \Gamma_s^+ - R_s \tag{9b}$$

$$\Gamma_w \equiv \Gamma(\tau_w) = -2R_s E_3(\tau_w) + 2R_w E_3(0) - \int_0^{\tau_w} \bar{T}^4 E_2(\tau_w - t)dt = R_w - \Gamma_w \tag{9c}$$

where $E_3(0) = 1/2$.

Equation (9a) is applicable to multiple radiating and absorbing layers as well as single layers (e.g., a preheating zone in front of a shock wave or a layer of injected or ablated gases from a surface). However, the exact calculation of fluxes is complicated by the interaction between layers. To simplify the calculation an approximation is introduced whereby the actual boundary fluxes are replaced by "equivalent wall" fluxes. This approximation concentrates the effects of other layers at the boundaries of the layer for which the solution is desired and allows equations (9) to be applied to each layer of the multilayer separately. The details of the procedure are presented in appendix A.

Pseudo One-Dimensional Flow Model and Thermal Function

In hypersonic flow, as the gas travels downstream from the shock wave, its enthalpy decreases as a result of radiative loss to the surroundings. Since this study is concerned with flight conditions for which radiative heating is the dominant mode of energy transfer (e.g., for a meteoric object entering the atmosphere), the energy equation in the shock layer may be written

$$\rho v \, dh = dq \tag{10}$$

where heat conduction and changes in the gas kinetic energy have been neglected. The mass flow along the stagnation streamline is expressed in terms of optical thickness. First, we introduce the mass flow distribution

$$\chi = \rho v / \rho_\infty V_\infty \tag{11a}$$

Many authors (e.g., refs. 5, 13, 23) have assumed a linear relation between mass flow distribution and physical thickness

$$\chi = (1 - y/L)^\gamma \tag{11b}$$

where γ is a constant (zero or one) that characterizes the flow. Flow with $\gamma = 0$ corresponds to plane shock flow such as in shock tubes, piston problems, and porous type flows; flow with $\gamma = 1$ corresponds to stagnation streamline flow. For present purposes, it is convenient to replace physical thickness in equation (11b) with optical thickness. Thus, we assume in this paper that

$$\chi = \left(1 - \frac{\tau}{\tau_w}\right)^\gamma \tag{11c}$$

where γ has the same meaning as before. The validity of this replacement is discussed in a later section, where it is shown that equation (11c) is as good an approximation to the actual mass flow distribution as equation (11b) or better. With the mass flow distribution of equation (11c) the energy equation becomes

$$\rho_\infty V_\infty (1 - \tau/\tau_w)^\gamma \, dh = dq \tag{12}$$

The thermodynamic variables are now expressed by a dimensionless function (thermal function) F so that

$$dF \equiv \frac{\rho_\infty V_\infty \, dh}{2\sigma T_s^4} \tag{13}$$

or

$$F_s - F = \frac{\rho_\infty V_\infty}{2\sigma T_s^4} (h_s - h) = \frac{1}{\lambda_a} (1 - \bar{h}) \tag{14}$$

where λ_a is the ratio of the black-body radiation at the shock wave to the total flow energy.

$$\lambda_a = 2\pi B_s / \rho_\infty V_\infty h_s$$

$$\bar{h} = h/h_s$$

After integrating this last equation for a constant pressure process (or constant density), one can readily obtain (ref. 4)

$$\bar{T}^4 = \sum_{n=o}^{N} a_n (F_s - F)^n \tag{15a}$$

where

$$\left.\begin{aligned} a_o &= 1 \\ a_1 &= -8\sigma T_s^3 / \rho_\infty V_\infty c_{p_s} \\ &\text{etc.} \end{aligned}\right\} \tag{15b}$$

The variations of $\bar{h}$ and F with temperature are shown in figure 2 for two reference conditions.

It can be seen from figure 2 that the temperature variation can be further simplified for wide ranges of enthalpy as

$$\bar{T}^4 = 1 - \bar{\alpha}(F_s - F) \tag{15c}$$

if $\bar{\alpha}$ is taken from the average slope of $(\partial \bar{T}^4 / \partial F)$ at the designated reference point. Thus,

$$\bar{\alpha} = \left(\frac{\partial \bar{T}^4}{\partial F}\right)_{av} = \lambda_a \left(\frac{\partial \bar{T}^4}{\partial \bar{h}}\right)_{av} \tag{15d}$$

Appendix B gives a more detailed discussion of the thermal function.

From equations (13) and (12) the dimensionless thermal function is thus related to the radiative function by

$$dF = \frac{d\Gamma}{\left(1 - \frac{\tau}{\tau_w}\right)^{\gamma}} \tag{16}$$

Linearization of Radiative Transfer Equation

The differential form of equations (9) is

$$\frac{d\Gamma}{d\tau} = 2R_s E_2(\tau) + 2R_w E_2(\tau_w - \tau) - 2\bar{T}^4 + \int_0^{\tau_w} \bar{T}^4 E_1(|t - \tau|)dt \tag{17}$$

Substituting equations (15c) and (16) into equation (17), we obtain a linear integrodifferential equation with a singular kernel

$$-\left(\frac{\theta}{\tau_w}\right)^{\gamma} \frac{d\varphi}{d\theta} + 2\bar{\alpha}\varphi - \bar{\alpha}\int_0^{\tau_w} \varphi E_1(|\theta - \theta'|)d\theta' = f(\theta) \tag{18a}$$

with an initial value of

$$\varphi(\tau_w) = 0 \tag{18b}$$

where

$$\left.\begin{aligned} \varphi &= F_s - F \\ \theta &= \tau_w - \tau \\ f &= (1 - 2R_s)E_2(\tau_w - \theta) + (1 - 2R_w)E_2(\theta) \end{aligned}\right\} \tag{18c}$$

No attempt is made to find a general solution for equation (18a) except for $\gamma = 0$, for which several numerical calculations have been carried out by a successive iteration method merely to compare it with the approximate solution.

Approximate Solutions for a Single Layer

In the present paper an approximate solution to the transfer equation is given explicitly in analytic and closed form when the exponential integral function $E_3(\tau)$ is replaced by an exponential function. We introduce the commonly used approximation

$$E_3(\tau) \simeq me^{-n\tau} \tag{19}$$

where choice of m and n will depend on the optical thickness at the wall (τ_w) of the plane layer, and will be constant for given τ_w. The values of m and n are discussed later; meanwhile, the solution is carried out without assigning values to these constants.

It follows from equation (19) and the properties of the exponential integrals that

$$E_2(\tau) = -E_3'(\tau) \simeq mne^{-n\tau} \tag{20}$$

The integral equation (9a) then becomes

$$\Gamma = -2mR_s e^{-n\tau} + 2mR_w e^{-n(\tau_w-\tau)} - mn\int_0^\tau \bar{T}^4 e^{-n(\tau-t)}dt + mn\int_\tau^{\tau_w} \bar{T}^4 e^{-n(t-\tau)}\,dt \tag{21}$$

After differentiating the above equation twice, we obtain the following second-order nonlinear differential equation:

$$\frac{d^2\Gamma}{d\tau^2} + 2mn\frac{d\bar{T}^4}{d\tau} - n^2\Gamma = 0 \tag{22}$$

(Equation (22) is equivalent to the Milne-Eddington approximation except with different constants.) From equation (16) the derivative of the temperature becomes

$$\frac{d\bar{T}^4}{d\tau} = -\frac{\partial\bar{T}^4}{\partial(F_s - F)}\frac{\partial F}{\partial\Gamma}\frac{d\Gamma}{d\tau} = -\frac{\partial\bar{T}^4}{\partial(F_s - F)}\frac{1}{\chi}\frac{d\Gamma}{d\tau} \tag{23}$$

With the simplified equations (11c) and (15c) and the transformation

$$\theta = \tau_w - \tau \tag{24a}$$

$$\frac{d\Gamma}{d\theta} = -\frac{d\Gamma}{d\tau} \tag{24b}$$

A linearized form of equation (22) is now obtained as

$$\frac{d^2\Gamma}{d\theta^2} - 2mn\bar{\alpha}\left(\frac{\tau_w}{\theta}\right)^{\gamma} \frac{d\Gamma}{d\theta} - n^2\Gamma = 0 \tag{25a}$$

with boundary values, from equation (21),

$$\Gamma_s = -2mR_s + 2mR_w e^{-n\tau_w} + mn \int_0^{\tau_w} \bar{T}^4 e^{-nt}\, dt \tag{25b}$$

$$\Gamma_w = -2mR_s e^{-n\tau_w} + 2mR_w - mn \int_0^{\tau_w} \bar{T}^4 e^{-n(\tau_w - t)}\, dt \tag{25c}$$

(For consistency, $E_3(0) = m$ is used instead of 1/2.)

The general solution of equation (25a) has the form

$$\Gamma = c_1 X_\gamma(n\theta) + c_2 Y_\gamma(n\theta) \tag{26a}$$

where c_1 and c_2 are constants and X and Y are functions to be determined. In equation (26a) X and Y for $\gamma = 0$ are the ordinary exponential functions, and for $\gamma = 1$, the modified Bessel functions. Solutions will be obtained in explicit and closed form for these two cases.

It will be shown that the solutions of equation (25a) lead to the following important linear[1] relations between the boundary values R_s and R_w and the fluxes at the boundaries:

$$\Gamma_s = M_0 + M_1 R_s + M_2 R_w \tag{26b}$$

$$\Gamma_w = M_3 + M_4 R_s + M_5 R_w \tag{26c}$$

Expressions for the M functions will be given in terms of $\bar{\alpha}$ and optical thickness τ_w.

Plane shock flow ($\gamma = 0$).- The differential equation (25a) for $\gamma = 0$ becomes

$$\frac{d^2\Gamma}{d\tau^2} + 2mn\bar{\alpha} \frac{d\Gamma}{d\tau} - n^2\Gamma = 0 \tag{27}$$

[1]This is a consequence of choosing a linear thermal function (eq. (15c)) and does not require the exponential approximation (eq. (19)).

Its solution is

$$\Gamma = c_1 e^{-n\beta_1 \tau} + c_2 e^{-n\beta_2(\tau_w - \tau)} \tag{28a}$$

where

$$\beta_1 = m\bar{\alpha} + \sqrt{(m\bar{\alpha})^2 + 1} \tag{28b}$$

$$\beta_2 = -m\bar{\alpha} + \sqrt{(m\bar{\alpha})^2 + 1} \tag{28c}$$

Fluxes at the boundaries are

$$\Gamma_s = c_1 + c_2 e^{-n\beta_2 \tau_w} \tag{29a}$$

$$\Gamma_w = c_1 e^{-n\beta_1 \tau_w} + c_2 \tag{29b}$$

To evaluate the constants c_1 and c_2, combine equations (29) with equations (25b) and (25c)

$$c_1 + c_2 e^{-n\beta_2 \tau_w} = -2mR_s + 2mR_w e^{-n\tau_w} + mn \int_0^{\tau_w} \bar{T}^4 e^{-nt}\, dt \tag{30a}$$

$$c_1 e^{-n\beta_1 \tau_w} + c_2 = -2mR_s e^{-n\tau_w} + 2mR_w - mn \int_0^{\tau_w} \bar{T}^4 e^{-n(\tau_w - t)}\, dt \tag{30b}$$

where $(\bar{T})^4$ may be expressed in terms of c_1 and c_2 by substituting equations (28) into equation (16) and integrating between 0 and τ. Thus, with equation (15c),

$$F_s - F = \frac{1}{\bar{\alpha}} (1 - \bar{T}^4) = c_1(1 - e^{-n\beta_1 \tau}) + c_2 e^{-n\beta_2 \tau_w}(1 - e^{n\beta_2 \tau}) \tag{31}$$

Substituting equation (31) into equations (30) gives two simultaneous algebraic equations for c_1 and c_2 of the form

$$K_1 c_1 + K_2 c_2 = K_5 \tag{32a}$$

$$K_3 c_1 + K_4 c_2 = K_6 \tag{32b}$$

where

$$
\left.
\begin{aligned}
K_1 &= 1 + m\bar{\alpha}\left\{1 - e^{-n\tau_w} - \frac{1}{1+\beta_1}\left[1 - e^{-n(1+\beta_1)\tau_w}\right]\right\} \\
K_2 &= e^{-n\beta_2\tau_w}\left(1 + m\bar{\alpha}\left\{1 - e^{-n\tau_w} - \frac{1}{1-\beta_2}\left[1 - e^{-n(1-\beta_2)\tau_w}\right]\right\}\right) \\
K_3 &= e^{-n\beta_1\tau_w} - m\bar{\alpha}\left[1 - e^{-n\tau_w} + \frac{1}{1-\beta_1}\left(e^{-n\tau_w} - e^{-n\beta_1\tau_w}\right)\right] \\
K_4 &= 1 - m\bar{\alpha}\left\{e^{-n\beta_2\tau_w}(1 - e^{-n\tau_w}) - \frac{1}{1+\beta_2}\left[1 - e^{-n(1+\beta_2)\tau_w}\right]\right\} \\
K_5 &= 2m\left(\frac{1}{2} - R_s\right) - 2me^{-n\tau_w}\left(\frac{1}{2} - R_w\right) \\
K_6 &= -2m\left(\frac{1}{2} - R_w\right) + 2me^{-n\tau_w}\left(\frac{1}{2} - R_s\right)
\end{aligned}
\right\} \qquad (32c)
$$

$$
\left.
\begin{aligned}
c_1 &= (-K_2K_6 + K_4K_5)/(K_1K_4 - K_2K_3) \\
c_2 &= -(-K_1K_6 + K_3K_5)/(K_1K_4 - K_2K_3)
\end{aligned}
\right\} \qquad (32d)
$$

With some algebraic manipulation, equations (29) and (32) can be expressed in the linear form:

$$\Gamma_s = M_o + M_1R_s + M_2R_w \qquad (26b)$$

$$\Gamma_w = M_3 + M_4R_s + M_5R_w \qquad (26c)$$

where the M values depend only on m, n, $\bar{\alpha}$, and τ_w, and are given by

$$
\left.
\begin{aligned}
M_0 &= \frac{1}{\Delta}\, m\left(1 - e^{-n\tau_w}\right)\left[(K_2 + K_4) - e^{-n\beta_2\tau_w}(K_1 + K_3)\right] \\
M_1 &= \frac{1}{\Delta}\, 2m\left[e^{-n\tau_w}\left(K_2 - e^{-n\beta_2\tau_w}K_1\right) - \left(K_4 - e^{-n\beta_2\tau_w}K_3\right)\right] \\
M_2 &= \frac{-1}{\Delta}\, 2m\left[\left(K_2 - e^{-n\beta_2\tau_w}K_1\right) - e^{-n\tau_w}\left(K_4 - e^{-n\beta_2\tau_w}K_3\right)\right] \\
M_3 &= \frac{-1}{\Delta}\, m\left(1 - e^{-n\tau_w}\right)\left[(K_1 + K_3) - e^{-n\beta_1\tau_w}(K_2 + K_4)\right] \\
M_4 &= \frac{-1}{\Delta}\, 2m\left[e^{-n\tau_w}\left(K_1 - e^{-n\beta_1\tau_w}K_2\right) - \left(K_3 - e^{-n\beta_1\tau_w}K_4\right)\right] \\
M_5 &= \frac{1}{\Delta}\, 2m\left[\left(K_1 - e^{-n\beta_1\tau_w}K_2\right) - e^{-n\tau_w}\left(K_3 - e^{-n\beta_1\tau_w}K_4\right)\right] \\
\Delta &= K_1K_4 - K_2K_3
\end{aligned}
\right\} \qquad (33)
$$

The terms M_0 and M_3 are fluxes from the shock layer without boundary conditions; M_1 and M_4 show the effects of reflection or emission from the shock wave (at $\tau = 0$); similarly, M_2 and M_5 show the effects of reflection or emission at $\tau = \tau_w$. For the present case, $\gamma = 0$, it can be shown that $M_1 = -M_5$.

Stagnation streamline flow ($\gamma = 1$).- The differential equation (25a) for $\gamma = 1$ becomes

$$\frac{d^2\Gamma}{d\theta^2} - \frac{2mn\bar{\alpha}\tau_w}{\theta}\frac{d\Gamma}{d\theta} - n^2\Gamma = 0 \qquad (34)$$

which can be transformed to the modified Bessel equation of order ν (refs. 24 and 25); its general solution is

$$\Gamma = \theta^{\nu}[c_1 I_{\nu}(n\theta) + c_2 K_{\nu}(n\theta)] \qquad (35a)$$

where I_{ν} and K_{ν} are modified Bessel functions of the first and second kind, respectively, and

$$\nu = mn\bar{\alpha}\tau_w + 1/2 \qquad (35b)$$

The constants c_1 and c_2 are evaluated by a procedure similar to that for plane shock flow. (Appendixes C and D give detailed evaluations of properties of the Bessel functions required for the present analysis.)

Since $dF = d\Gamma/(\theta/\tau_w)$, for $\Gamma_\nu \equiv \Gamma(\theta)$, it follows that

$$\frac{dF}{d\theta} = n\tau_w \Gamma_{\nu-1} \tag{36a}$$

where

$$\Gamma_{\nu-1} \equiv \theta^{\nu-1}[c_1 I_{\nu-1}(n\theta) - c_2 K_{\nu-1}(n\theta)] \tag{36b}$$

By integration one obtains

$$\int_F^{F_s} dF = n\tau_w \int_\theta^{\tau_w} \Gamma_{\nu-1}\, d\theta = n\tau_w \left[c_1 C_{\nu-1}(\theta) - c_2 C_{-(\nu-1)}(\theta) \right]_\theta^{\tau_w}$$

Thus,

$$F_s - F = n\tau_w \left\{ c_1 C_{\nu-1}(\tau_w) - c_2 C_{-(\nu-1)}(\tau_w) - \left[c_1 C_{\nu-1}(\theta) - c_2 C_{-(\nu-1)}(\theta) \right] \right\} \tag{37a}$$

where

$$C_{\nu-1}(\theta) \equiv \int_o^\theta t^{\nu-1} I_{\nu-1}(nt)dt \tag{37b}$$

$$C_{-(\nu-1)}(\theta) \equiv \int_o^\theta t^{\nu-1} K_{\nu-1}(nt)dt \tag{37c}$$

Then K takes the following forms:

$$
\left.
\begin{aligned}
K_1 &= -mn\bar{\alpha}\tau_w e^{-n\tau_w} C_{\nu-1} + \frac{1}{2} Z_\nu + \frac{1}{2} \tau_w Z_{\nu-1} \\
K_2 &= mn\bar{\alpha}\tau_w e^{-n\tau_w} C_{-(\nu-1)} + \frac{1}{2} Z_{-\nu} - \frac{1}{2} \tau_w Z_{-(\nu-1)} + \frac{1}{2} e^{-n\tau_w} Z^*_{-\nu} \\
K_3 &= -mn\bar{\alpha}\tau_w C_{\nu-1} + \frac{1}{2} e^{-n\tau_w} Z_\nu + \frac{1}{2} e^{-n\tau_w} \tau_w Z_{\nu-1} \\
K_4 &= mn\bar{\alpha}\tau_w C_{-(\nu-1)} + \frac{1}{2} e^{-n\tau_w} Z_{-\nu} - \frac{1}{2} e^{-n\tau_w} \tau_w Z_{-(\nu-1)} + \frac{1}{2} Z^*_{-\nu} \\
K_5 &= 2m\left(\frac{1}{2} - R_s\right) - 2me^{-n\tau_w}\left(\frac{1}{2} - R_w\right) \\
K_6 &= -2m\left(\frac{1}{2} - R_w\right) + 2me^{-n\tau_w}\left(\frac{1}{2} - R_s\right)
\end{aligned}
\right\} \qquad (38a)
$$

where

$$
\left.
\begin{aligned}
C_{\nu-1} &\equiv C_{\nu-1}(\tau_w) \\
C_{-(\nu-1)} &\equiv C_{-(\nu-1)}(\tau_w) \\
Z_\nu &\equiv Z_\nu(\tau_w) \equiv \tau_w{}^\nu I_\nu(n\tau_w) \\
Z_{-\nu} &\equiv Z_{-\nu}(\tau_w) \equiv \tau_w{}^\nu K_\nu(n\tau_w) \\
Z^*_{-\nu} &\equiv Z_{-\nu}(0) = \frac{1}{2}\left(\frac{2}{n}\right)^\nu \Gamma(\nu)
\end{aligned}
\right\} \qquad (38b)
$$

where $\Gamma(\nu)$ in equations (38b) is a gamma function. Boundary fluxes are

$$\Gamma_s = c_1 Z_\nu + c_2 Z_{-\nu} \qquad (39a)$$

$$\Gamma_w = c_2 Z^*_{-\nu} \qquad (39b)$$

The relation between fluxes and boundary values is again

$$\Gamma_s = M_o + M_1 R_s + M_2 R_w \tag{26b}$$

$$\Gamma_w = M_3 + M_4 R_s + M_5 R_w \tag{26c}$$

where M now has the following forms:

$$\left.\begin{aligned}
M_o &= \frac{1}{\Delta} m \left(1 - e^{-n\tau_w}\right) \left[(K_2 + K_4)Z_\nu - (K_1 + K_3)Z_{-\nu}\right] \\
M_1 &= \frac{1}{\Delta} 2m\left[\left(e^{-n\tau_w}K_2 - K_4\right) Z_\nu - \left(e^{-n\tau_w}K_1 - K_3\right) Z_{-\nu}\right] \\
M_2 &= \frac{-1}{\Delta} 2m\left[\left(K_2 - e^{-n\tau_w}K_4\right) Z_\nu - \left(K_1 - e^{-n\tau_w}K_3\right) Z_{-\nu}\right] \\
M_3 &= \frac{-1}{\Delta} m \left(1 - e^{-n\tau_w}\right) (K_1 + K_3)Z^*_{-\nu} \\
M_4 &= \frac{-1}{\Delta} 2m \left(e^{-n\tau_w}K_1 - K_3\right) Z^*_{-\nu} \\
M_5 &= \frac{1}{\Delta} 2m \left(K_1 - e^{-n\tau_w}K_3\right) Z^*_{-\nu} \\
\Delta &= K_1K_4 - K_2K_3
\end{aligned}\right\} \tag{40}$$

The same physical interpretation can be ascribed to these values of M as to those in equations (33). From equation (35a) it follows that the flux gradient at the wall is

$$\Gamma'_w = 0 \tag{41}$$

The enthalpy gradient at the wall from equations (36) depends on ν

$$F_w' = \bar{F}_w'/\tau_w = \begin{cases} \infty & \text{for } \nu < 1 \quad (42a) \\ -(1/2)n^2\tau_w\Gamma_w/(\nu - 1) & \text{for } \nu \geq 1 \quad (42b) \end{cases}$$

where

$$\bar{F}' \equiv \frac{dF}{d\bar{\theta}}$$

The physical interpretation of this dependence of enthalpy gradient on ν will be considered in a later section.

Approximate Solutions for Optically Thin and Thick Layers

In this section, the solutions to equations (26) are simplified for optically thin and optically thick shock layers. Only the major results of these simplifications are presented here. Details are presented in appendixes.

Plane shock flow ($\gamma = 0$).- The following are the results for two limiting cases.

Optically thin layers ($\tau_w \ll 1$): If the exponentials are approximated by Taylor series, the quantities K in equations (32c) become, to order τ_w^2,

$$\left.\begin{aligned} K_1 &\simeq 1 + \frac{1}{2} mn\bar{\alpha}\beta_1\tau_w^2 \\ K_2 &\simeq 1 - n\beta_2\tau_w + \frac{1}{2} n^2\beta_2(\beta_2 - m\bar{\alpha})\tau_w^2 \\ K_3 &\simeq 1 - n\beta_1\tau_w + \frac{1}{2} n^2\beta_1(\beta_1 - m\bar{\alpha})\tau_w^2 \\ K_4 &\simeq 1 + \frac{1}{2} mn\bar{\alpha}\beta_2\tau_w^2 \\ K_5 &\simeq -2m(R_s - R_w) + mn(1 - 2R_w)\tau_w \\ K_6 &\simeq -2m(R_s - R_w) - mn(1 - 2R_s)\tau_w \\ \Delta &\simeq n(\beta_1 + \beta_2)\tau_w(1 - n\beta_2\tau_w) \end{aligned}\right\} \quad (43)$$

With the relation derived from equations (28)

$$\beta_1 - \beta_2 = 2m\bar{\alpha} \tag{44}$$

The M values then directly follow from equations (33) and are

$$\left.\begin{aligned} M_0 &\simeq mn\tau_w\left[1 - \frac{n}{2}(1 + 2m\bar{\alpha})\tau_w\right] \\ M_1 &\simeq -2m + O(\tau_w^2) \\ M_2 &\simeq 2m(1 - n\tau_w) \\ M_3 &\simeq -mn\tau_w\left[1 - \frac{1}{2}n(1 + 2m\bar{\alpha})\tau_w\right] \\ M_4 &\simeq -2m(1 - n\tau_w) \\ M_5 &\simeq 2m + O(\tau_w^2) \end{aligned}\right\} \tag{45}$$

The fluxes at the boundaries for $m = 1/2$ and $n = 2$ are

$$\Gamma_s \simeq [1 - (1 + \bar{\alpha})\tau_w]\tau_w - R_s + (1 - 2\tau_w)R_w \tag{46a}$$

$$\Gamma_w \simeq -[1 - (1 + \bar{\alpha})\tau_w]\tau_w - (1 - 2\tau_w)R_s + R_w \tag{46b}$$

Here, we have omitted second order terms from the boundary fluxes because, in practice, R_s and R_w will usually be small. The choices of m and n will be justified later.

Optically thick layers ($\tau_w \gg 1$): For large optical thickness, K takes the following forms (the second and third identities for K_1 follow from eqs. (28)):

$$\left.\begin{aligned} K_1 &\simeq 1 + m\bar{\alpha}\beta_1/(1 + \beta_1) = K_4 \simeq (1/2)(1 + \beta_1) \\ K_2 &\simeq (1/2)(1 - \beta_2)e^{-n\beta_2\tau_w} \sim 0 \\ K_3 &\simeq -m\bar{\alpha} \\ K_4 &\simeq 1 + m\bar{\alpha}[1/(1 + \beta_2)] \\ K_5 &\simeq m(1 - 2R_s) \\ K_6 &\simeq -m(1 - 2R_w) \end{aligned}\right\} \tag{47}$$

The determinant Δ becomes

$$\Delta \simeq \frac{1}{4}(1 + \beta_1)^2 \tag{48}$$

Values of M follow directly

$$\left.\begin{aligned} M_0 &\simeq 2m/(1 + \beta_1) \\ M_1 &\simeq -4m/(1 + \beta_1) \\ M_2 &\simeq [4m/(1 + \beta_1)][(\beta_1 + \beta_2)/(1 + \beta_1)]e^{-n\beta_2\tau_w} \sim 0 \\ M_3 &\simeq -2m\beta_2/(1 + \beta_1) \\ M_4 &\simeq -4m(1 - \beta_2)/(1 + \beta_1) \\ M_5 &\simeq 4m/(1 + \beta_1) \end{aligned}\right\} \tag{49}$$

Net fluxes at both boundaries from equations (26) are

$$\Gamma_s \simeq \frac{2m}{1 + \beta_1}(1 - 2R_s) \tag{50a}$$

$$\Gamma_w \simeq -\frac{2m}{1 + \beta_1}\beta_2[1 + 2(\beta_1 - 1)R_s - 2\beta_1 R_w] \tag{50b}$$

Flux variation and temperature variation for $1 \ll \tau \ll \tau_w$ are

$$\Gamma \simeq \frac{2m}{1 + \beta_1}(1 - 2R_s)e^{-n\beta_1\tau} \tag{51}$$

$$\bar{T}^4 \simeq \beta_2 + (1 - \beta_2)e^{-n\beta_1\tau} + 2(1 - \beta_2)(1 - e^{-n\beta_1\tau})R_s \tag{52}$$

The gas temperature at the wall ($\tau = \tau_w \gg 1$) is

$$\bar{T}_e^4 \simeq \beta_2^2 + 2\beta_2(1 - \beta_2)R_s + 2(1 - \beta_2)R_w \tag{53}$$

Effective surface temperatures that emit equivalent radiant fluxes from both boundaries are

$$(T_{ef})_s = (2\Gamma_s)^{1/4}T_s \tag{54a}$$

$$(T_{ef})_w = (2\Gamma_w)^{1/4}T_s \tag{54b}$$

It is noted from equations (50b) and (53) that radiant flux toward the wall for an optically thick layer with no boundary effect is always greater than the local black-body radiation at the edge of the layer. This was also shown in references 4 and 12.

Stagnation streamline flow ($\gamma = 1$).- Appendixes E and F give details of the derivations for $\tau_w \ll 1$ and $\tau_w \gg 1$, respectively, since the manipulation of the Bessel functions becomes complicated. The following are the results.

Optically thin layers ($\tau_w \ll 1$): For $\nu = [(1/2) + mn\bar{\alpha}\tau_w]$ fixed and the argument of the Bessel functions approaching zero, the values of K in equations (38a) are

$$\left.\begin{aligned}
K_1 &\simeq n\tau_w^2[1 - mn\bar{\alpha}\tau_w]Q_1 \\
K_2 &\simeq [1 - (2mn\bar{\alpha}\varphi_o + n\tau_w^{2\nu_o})\tau_w]Q_2 \\
&\simeq Z_{-\nu} \\
K_3 &\simeq -n(mn\bar{\alpha})\tau_w^3\left[1 - \left(\frac{n}{4} + 2mn\bar{\alpha}\right)\tau_w\right]Q_1 \\
K_4 &\simeq (1 - 2mn\bar{\alpha}\varphi_o\tau_w)Q_2 \\
&\simeq Z^*_{-\nu} \\
K_5 &\simeq -2m(R_s - R_w) + mn(1 - 2R_w)\tau_w \\
K_6 &\simeq -2m(R_s - R_w) - mn(1 - 2R_s)\tau_w \\
\Delta &\simeq n\tau_w^2(1 - 2mn\bar{\alpha}\varphi_o\tau_w)Q_1Q_2
\end{aligned}\right\} \qquad (55a)$$

where

$$\left.\begin{aligned}
\varphi_o &= 2\ \ln 2 + 0.57721 \quad \text{(where second term is Euler's constant)} \\
\nu_o &= mn\bar{\alpha}\tau_w \\
Q_1 &= \left(\frac{2}{n}\right)^{1-\nu}\frac{1}{\Gamma(\nu)}\tau_w^{-2(1-\nu)} \\
Q_2 &= \frac{1}{2}\left(\frac{2}{n}\right)^{1-\nu}\Gamma(1 - \nu)
\end{aligned}\right\} \qquad (55b)$$

$\Gamma(\nu)$ and $\Gamma(1 - \nu)$ in equations (55b) are gamma functions. The values of M are

$$\left.\begin{aligned} M_0 &\simeq mn\tau_w\left[1 - \tfrac{1}{2}\, n(1 + 4m\bar{\alpha})\tau_w\right] \\ M_1 &\simeq -2m[1 - O(\tau_w{}^2)] \\ M_2 &\simeq 2m(1 - n\tau_w) \\ M_3 &\simeq -mn\tau_w\left[1 - \tfrac{1}{2}\, n(1 + 4m\bar{\alpha})\tau_w\right] \\ M_4 &\simeq -2m(1 - n\tau_w) \\ M_5 &\simeq 2m[1 - O(\tau_w{}^2)] \end{aligned}\right\} \tag{56}$$

The boundary fluxes for $m = 1/2$ and $n = 2$ are

$$\Gamma_s \simeq \tau_w[1 - (1 + 2\bar{\alpha})\tau_w] - R_s + (1 - 2\tau_w)R_w \tag{57a}$$

$$\Gamma_w \simeq -\tau_w[1 - (1 + 2\bar{\alpha})\tau_w] - (1 - 2\tau_w)R_s + R_w \tag{57b}$$

The thermal function is

$$F_s - F \simeq (1/\bar{\alpha})\{1 - [1 - (\tau/\tau_w)]^{2\nu_o}\}\{1 - n\nu_o\tau_w{}^{2\nu_o} - [1 - \nu_o(n + 2\varphi_o)\tau_w{}^{2\nu_o}]R_s$$

$$- [1 - \nu_o(n - 2\varphi_o)\tau_w{}^{2\nu_o}]R_w\} \tag{58a}$$

which, to order τ_w, can be further simplified as

$$F_s - F \simeq (1/\bar{\alpha})\{1 - [1 - (\tau/\tau_w)]^{2\nu_o}\}(1 - R_s - R_w) \tag{58b}$$

From equation (14), and letting $R_s = R_w = 0$ in equation (58b) the enthalpy profile within the layer becomes

$$\bar{h} \simeq 1 - (\lambda_a/\bar{\alpha})\{1 - [1 - (\tau/\tau_w)]^{2\nu_o}\} \tag{59}$$

which is similar to the expression in equation (15) of reference 23 for $\tau_w \ll 1$.

The temperature distribution follows directly from equation (15c)

$$\bar{T} \simeq [1 - (\tau/\tau_w)]^{\nu_o/2} \tag{60}$$

which is equivalent to that of reference 5 for $\tau_w \ll 1$.

It is interesting that the boundary fluxes for plane shock flow (eqs. (46)) and stagnation flow (eqs. (57)) differ only in second order of τ_w for $\tau_w \ll 1$.

Optically thick layers ($\tau_w \gg 1$): Asymptotic expressions for K and M are:

$$\left.\begin{aligned}
K_1 &\simeq \frac{1}{2}(1 + \beta_1)Z_\nu \\
K_2 &\simeq \frac{1}{2}(1 - \beta_2)Z_{-\nu} \\
K_3 &\simeq -\frac{1}{2}(1 + \beta_1)(1 - \beta_2)Z_\nu \\
K_4 &\simeq \frac{1}{2}(1 + \sqrt{\pi\nu})Z^*_{-\nu} \\
K_5 &\simeq 2m\left(\frac{1}{2} - R_s\right) \\
K_6 &\simeq -2m\left(\frac{1}{2} - R_w\right) \\
\Delta &\simeq \frac{1}{4}(1 + \beta_1)(1 + \sqrt{\pi\nu})Z_\nu Z^*_{-\nu}
\end{aligned}\right\} \tag{61}$$

$$
\left.
\begin{aligned}
M_0 &\simeq \frac{2m}{1+\beta_1} \\
M_1 &\simeq \frac{-4m}{1+\beta_1} \\
M_2 &\simeq \frac{4m}{1+\beta_1}\,\frac{\beta_1+\beta_2}{1+\sqrt{\pi\nu}}\,\frac{Z_{-\nu}}{Z^*_{-\nu}} \sim 0 \\
M_3 &\simeq -2m\,\frac{\beta_2}{1+\sqrt{\pi\nu}} \\
M_4 &\simeq -4m\,\frac{1-\beta_2}{1+\sqrt{\pi\nu}} \\
M_5 &\simeq \frac{4m}{1+\sqrt{\pi\nu}}
\end{aligned}
\right\} \qquad (62)
$$

Thus, the boundary fluxes are

$$\Gamma_s \simeq \frac{2m}{1+\beta_1}\,(1-2R_s) \qquad (63a)$$

$$\Gamma_w \simeq -2m\,\frac{\beta_2}{1+\sqrt{\pi\nu}}\,[1+2(\beta_1-1)R_s-2\beta_1 R_w] \qquad (63b)$$

As noted from equations (62) and (49), fluxes with no boundary effects (M_0 and M_3) are nearly independent of the constant n (M_3 in eqs. (62) is very weakly dependent on n). The major contributing factor to the flux calculation comes from the constant m. Note that the asymptotic values of Γ_w for stagnation flow decrease inversely as the square root of τ_w whereas Γ_w for plane shock flow reaches finite asymptotic values.

Asymptotic radiant flux variations for $1 \ll \tau \ll \tau_w$ are

$$\Gamma \simeq M_0(1-2R_s)Z_\nu(\theta)/Z_\nu$$

$$\simeq \Gamma_s e^{-n\beta_1\tau} \qquad (64)$$

and the thermal function becomes

$$F_s - F \simeq M_o(1 - 2R_s)\left[1 - \frac{\tau_w}{\theta}\frac{Z_\nu(\theta)}{Z_\nu}\right]$$

$$\simeq \Gamma_s(1 - e^{-n\beta_1\tau}) \tag{65}$$

Finally, the temperature distribution is written[2]

$$\bar{T}^4 \simeq 1 - M_o(1 - 2R_s)\bar{\alpha}\left[1 - \frac{\tau_w}{\theta}\frac{Z_\nu(\theta)}{Z_\nu}\right]$$

$$\simeq \beta_2 + (1 - \beta_2)e^{-n\beta_1\tau} + 2(1 - \beta_2)(1 - e^{-n\beta_1\tau})R_s \tag{66}$$

The asymptotic values of the radiant functions above yield identical results to those for $\gamma = 0$ which shows that the asymptotic values of radiant properties are independent of velocity profile for $1 \ll \tau \ll \tau_w$.

---

[2]For an optically thick layer, the Rosseland approximation of net flux is

$$\Gamma \simeq + \frac{2}{3}\left[\frac{\partial \bar{T}^4}{\partial \tau}\right]$$

Applying this equation to equation (66), we obtain

$$\Gamma \simeq - \frac{2}{3} n\beta_1\bar{\alpha}M_o(1 - 2R_s)e^{-n\beta_1\tau}$$

which differs from equation (64) when combined with equation (63a) by a factor $(2/3)n\beta_1\bar{\alpha}$. If the Rosseland approximation is to apply, higher derivatives of temperature distribution must vanish, or $n\beta_1 \ll 1$. Since $\bar{\alpha}$ is a finite constant, it is required that $(2/3)(n\beta_1)\bar{\alpha} \ll 1$. Now it is obvious that the coefficient $(n\beta_1)\bar{\alpha}$ cannot be unity, in fact, $\beta_1 \geq 1$; consequently, the Rosseland approximation for a high enthalpy flow field with radiation, in general, is not applicable. This also implies that agreement with Rosseland approximation for an optically thick layer in a flow field is not a property of the asymptotic solution (this approximation can be commonly used for non-flow cases) and it may sometimes lead to incorrect solutions if proper care is not exercised.

Calculation of Boundary Conditions

Boundary values R_s and R_w may be expressed in terms of emissivity and reflectivity of boundaries since the boundary values introduced in equations (8b) and (c) can be written[3]

$$q_s^- = \underbrace{\epsilon_s \sigma T_o^4}_{\left[\begin{smallmatrix}\text{flux from}\\ \text{shock wave}\end{smallmatrix}\right]} + \underbrace{r_s q_s^+}_{\left[\begin{smallmatrix}\text{flux reflected}\\ \text{from shock wave}\end{smallmatrix}\right]} + (\text{external fluxes from upstream}) \tag{67a}$$

$$q_w^+ = \underbrace{\epsilon_w \sigma T_w^4}_{\left[\begin{smallmatrix}\text{flux from}\\ \text{wall}\end{smallmatrix}\right]} + \underbrace{r_w q_w^-}_{\left[\begin{smallmatrix}\text{flux reflected}\\ \text{from wall}\end{smallmatrix}\right]} + (\text{external fluxes from the wall}) \tag{67b}$$

In dimensionless form, equations (67a) and (b) may be written (for no external fluxes)

$$R_s = \frac{\epsilon_s}{2} \bar{T}_s^4 + r_s \Gamma_s^+ \tag{68a}$$

$$R_w = \frac{\epsilon_w}{2} \bar{T}_w^4 + r_w \Gamma_w^- \tag{68b}$$

where $\bar{T}_s = T_o/T_s$ and $\bar{T}_w = T_w/T_s$. From equations (9) and (26) it follows that

$$\Gamma_s^+ = M_o + (1 + M_1)R_s + M_2 R_w \tag{69a}$$

$$\Gamma_w^- = -M_3 - M_4 R_s + (1 - M_5)R_w \tag{69b}$$

Combining equations (68a) and (b) with equations (69a) and (b) gives

$$R_s = \frac{\frac{1}{2}\{[1 - r_w(2m - M_5)]\epsilon_s \bar{T}_s^4 + r_s M_2 \epsilon_w \bar{T}_w^4\} + r_s\{[1 - r_w(2m - M_5)]M_o - r_w M_2 M_3\}}{\{[1 - r_s(2m + M_1)][1 - r_w(2m - M_5)] + r_s r_w M_2 M_4\}} \tag{70a}$$

[3]Radiative flux will be reflected back into the shock layer, for example, just prior to an impact. Radiative flux from a surface placed just ahead of the shock can be treated similarly.

$$R_W = \frac{\frac{1}{2}\{[1 - r_S(2m + M_1)]\epsilon_W \bar{T}_W^4 - r_W M_4 \epsilon_S \bar{T}_S^4\} - r_W\{[1 - r_S(2m + M_1)]M_3 + r_S M_O M_4\}}{\{[1 - r_S(2m + M_1)][1 - r_W(2m - M_5)] + r_S r_W M_2 M_4\}} \tag{70b}$$

Boundary temperatures T_O and T_W may be taken as effective temperatures so that they could include fluxes impinging from external sources added independently from the system.

Selection of Constants m and n

Replacing the exponential integral function by an exponential function is essential to the present analysis and is commonly used as an analytic approximation for radiative transfer problems. Here the relation

$$E_3(\tau) \simeq me^{-n\tau} \tag{19}$$

is introduced where m and n are constants chosen in some plausible fashion.

Although many different values for m and n are found in the literature, depending on the applications, the first constant, m, is not arbitrary; it must be 1/2 to satisfy the asymptotic solutions for both optically thin and thick layers. This is clear for optically thin layers since

$$E_3(0) = m = \frac{1}{2} \tag{71}$$

For optically thick layers, m must also be 1/2, as will be shown in Results and Discussion where exact and approximate solutions of the equations are compared. The exponential constant n is less restricted, and proposed values of n between 3/2 and 2 are found in the literature. The value 3/2 is associated with Eddington's approximation and has been preferred for astrophysical problems (ref. 21). In this paper, values of n which depend on total optical thickness τ_W are used to provide correct results for both optically thin and thick layers. The criterion is chosen to match the area under E_3 with the area under the exponential function:

$$\int_O^{\tau_W} E_3(\tau)d\tau = m\int_O^{\tau_W} e^{-n\tau}\, d\tau$$

or

$$n = \frac{m(1 - e^{-n\tau_W})}{\frac{1}{3} - E_4(\tau_W)} \tag{72}^4$$

[4]Quick convergence results if equation (72) is rearranged as $\epsilon = e^{-n\tau_W} - 1 + 2n[(1/3) - E_4(\tau_W)]$ and solved for $\epsilon = 0$.

Thus, for $\tau_w \to \infty$, $E_4(\tau_w) \to 0$, and $n = 3/2$ when $m = 1/2$. For $\tau_w \to 0$, $-E_3'(0) = E_2(0) = mn$ and $n = 2$ when $m = 1/2$. A set of exponential constants is tabulated in table I for various values of τ_w and for $m = 1/2$.

This completes the solution of the radiative transfer equation in terms of optical thickness.

Conversion of Optical Thickness to Physical Thickness

To facilitate application of the solution to physical problems the optical thickness must be converted to physical thickness. Physical distance into the shock layer is related to optical depth by

$$dy = d\tau/\rho\kappa \tag{73a}$$

Integrating equation (73a) between 0 and τ_w gives the nonadiabatic standoff distance L as

$$L = \int_0^{\tau_w} d\tau/\rho\kappa \tag{73b}$$

For stagnation flow, Goulard (ref. 5) has shown that the nonadiabatic distance into the shock layer, y, is related to the adiabatic distance Y by

$$dY = (\rho/\rho_s)^{1/2}\, dy = (\rho/\rho_s)^{1/2}\, d\tau/\rho\kappa \tag{74a}$$

Therefore, the adiabatic standoff distance L_o is

$$L_o = \int_0^{\tau_w} (\rho/\rho_s)^{1/2}\, d\tau/\rho\kappa \tag{74b}$$

From equations (73a) and (74a) the ratio of nonadiabatic to adiabatic standoff distance is

$$L/L_o = \int_0^1 (\rho_s/\rho)^{1/2}\, d(Y/L_o) \tag{75a}$$

An approximate relation between adiabatic distance and optical thickness (ref. 5) is

$$d(Y/L_o) \simeq d(\tau/\tau_w) = d\bar{\tau} \tag{75b}$$

Incorporating this approximation into equation (75a) gives the following simple expression for standoff distance, which is consistent with the present approximation for mass flow, equation (11c).

$$\frac{L}{L_o} \simeq \int_o^1 \left(\frac{\rho_s}{\rho}\right)^{1/2} d\bar{\tau} \tag{75c}$$

In order to use equations (74b) and (75c) the density ratio (ρ/ρ_s) and absorption coefficient $(\rho\kappa)$ can be expressed in terms of power series of enthalpy ratio (ref. 26), and the shock-layer thickness readily evaluated by numerical calculation. Finally, the Hayes-Probstein formula relates L_o to body radius and density ratio across the normal shock wave (ref. 27) by

$$\frac{L_o}{R} = k \frac{\rho_\infty}{\rho_s} \tag{76a}$$

where

$$k = \frac{1}{1 + \sqrt{\frac{8}{3}\frac{\rho_\infty}{\rho_s} - \frac{\rho_\infty}{\rho_s}}} \tag{76b}$$

and an average value is

$$k \simeq \frac{3}{4} \quad \text{for} \quad \frac{\rho_s}{\rho_\infty} \simeq 16 \tag{76c}$$

(See also ref. 28.)

Approximate Solutions for Multilayers

Absorption of radiation by the free-stream (preheating).- If appreciable amounts of radiation are absorbed by the free-stream media just ahead of the strong shock front, there is an important effect on the structure of the shock layer and the radiative heating to the body is changed significantly. (Emission effect from upstream is somewhat similar to increasing the reflectivity of the shock front.) Following references 16 and 29 the present paper assumes negligible change in kinetic energy and nearly constant density ahead of the shock wave[5] (as opposed to nearly constant pressure in the shock layer); the thermal function for air in the preheating zone is therefore determined by a constant density process. Furthermore, the flow in front of the shock wave is planar and the analysis previously presented for $\gamma = 0$ can be applied to the preheating region. Therefore, with the "equivalent wall" approximation (appendix A) for the boundary conditions at the shock wave, the flow can be separated into two regions with variable boundary conditions:

[5]These assumptions are considered in more detail in reference 29.

Region * is the preheated free stream with $\rho \simeq \rho_\infty$ (constant) and $\gamma = 0$. Region I is the shock layer with $p \simeq p_s$ (constant) and $\gamma = 1$.

In the preheating zone, the energy equation is

$$\rho_\infty V_\infty (h^* - h_\infty) - (q^* - q_\infty) \simeq 0 \tag{77}$$

where q^* is the net radiant heat flux in the preheating zone and q_∞ is the radiant heat flux escaping from the zone (sketch (a)). Physically, this model is adopted because, in real air, only the far ultraviolet portion of the flux leaving the shock wave will be absorbed in the free stream near the shock layer. Consequently, in the present analysis the portion of the radiation leaving the shock front (q_∞) is allowed to escape from the system. No attempt is made to compute q_∞, but it simply becomes a parameter in the analysis.

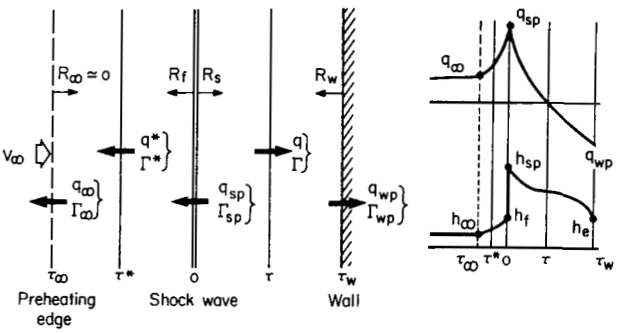

Sketch (a) Preheating and shock layer.

In the shock layer the energy equation may be written from equation (10) as

$$\rho v \, d(h_{sp} - h) = d(q_{sp} - q) \tag{78}$$

where q_{sp} is the net radiative heating at the shock wave due to preheating. Equation (78) shows that preheating changes the enthalpy level in the shock layer. This increase is proportional to $(q_{sp} - q_\infty)$ since energy balance at the shock wave ($\gamma = 0$) is

$$\rho_\infty V_\infty \left(h_\infty + \frac{1}{2} V_\infty^2 \right) - q_\infty = \rho_\infty V_\infty \left(h_{sp} + \frac{1}{2} v_s^2 \right) - q_{sp}$$

which can be rewritten as

$$\rho_\infty V_\infty (h_{sp} - h_s) = q_{sp} - q_\infty \tag{79a}$$

since

$$h_s = \frac{1}{2} V_\infty^2 + h_\infty - \frac{1}{2} v_s^2$$

Thus, the increases in enthalpy immediately ahead and behind the shock are obtained.

From equations (78) and (79a) three types of energy profiles can be established.

(a) $q_{sp} \simeq q_\infty$

(b) $q_\infty \simeq q_w \simeq 0$

(c) $q_{sp} > q_\infty \geq 0$

Case (a) is for no preheating and is the case previously discussed. Case (b) is for infinite layers that reach adiabatic equilibrium Rankine-Hugoniot temperature as $\tau_w \to \infty$ (for $1 \ll \tau \ll \tau_w$). Case (c) is a general one, and contains strong absorption, or a preheating effect and will be discussed here. In dimensionless form equation (79a) becomes

$$F_{sp} - F_s \simeq \Gamma_{sp} - \Gamma_\infty \tag{79b}$$

where $\Gamma_{sp} = q_{sp}/2\pi B_s$. From equation (15c), the corresponding temperature rise behind the shock wave is

$$\bar{T}_{sp}^4 \simeq 1 + \bar{\alpha}(\Gamma_{sp} - \Gamma_\infty) \tag{80}$$

Temperature in the preheating zone is usually relatively small compared to that in the shock layer; thus emission from this zone may be neglected. (An extension of this part of the analysis which includes emission from the preheating zone is given in appendix G.) With this assumption and further assuming negligible wall emission ($R_s = R_w = 0$), we have, for given τ_w and $\bar{\alpha}$, from equation (26b)

$$\Gamma_{sp} = \bar{T}_{sp}^4 M_o \tag{81a}$$

where $\bar{T}_{sp}^4$ must be inserted to account for the higher temperature behind the shock wave due to preheating. Similarly, from equation (26c), the flux at the wall is

$$\Gamma_{wp} = \bar{T}_{sp}^4 M_3 \tag{81b}$$

We now define

$$\omega \equiv \frac{\Gamma_{sp} - \Gamma_\infty}{\Gamma_{sp}} \tag{82}$$

Combining this definition with equations (80) and (81) gives

$$\Gamma_{sp} = \frac{M_o}{1 - \bar{\alpha} M_o \omega} \tag{83a}$$

$$\Gamma_{wp} = \frac{M_3}{1 - \bar{\alpha} M_o \omega} \tag{83b}$$

$$\Gamma_\infty = \frac{(1 - \omega)M_o}{1 - \bar{\alpha}M_o\omega} \tag{83c}$$

Since emission in the preheating zone has been neglected, the transfer equation (9a) in this zone takes on the particularly simple form

$$\Gamma^* = \Gamma_{sp}2E_3(\tau^*) \tag{84}$$

We use equation (84) to define τ_∞ so that $\tau_\infty = \tau^*$ when $\Gamma^* = \Gamma_\infty$. Hence

$$\Gamma_\infty = \Gamma_{sp}2E_3(\tau_\infty) \tag{85}$$

and τ_∞ is fixed by ω through the relation

$$E_3(\tau_\infty) = \frac{1}{2}(1 - \omega) \tag{86}$$

Finally, the enthalpy distribution in the preheating zone (from eq. (77)) is

$$\frac{h^* - h_\infty}{h_s} = \lambda_a(\Gamma^* - \Gamma_\infty) \tag{87a}$$

which at the shock front becomes

$$\frac{h_f - h_\infty}{h_s} = \lambda_a(\Gamma_{sp} - \Gamma_\infty) \tag{87b}$$

where h_f is enthalpy immediately ahead of the shock. Pressure and temperature in this zone are now obtained directly from the thermodynamic chart for constant density ($\rho^* \simeq \rho_\infty$). The distribution of thermal properties in the shock layer with preheating may be found by adjusting the thermal function previously found (eqs. (14) and (15c)) to account for the higher temperature due to preheating immediately behind the shock wave. If the normalization temperature for the thermal function F and the function Γ is changed from T_s to T_{sp}, then the previous analysis of the shock layer, equations (35) and (37), may be applied directly. Therefore we define a new thermal function in the shock layer, $F^\dagger$, normalized with respect to $\bar{T}_{sp}^4$ by $F^\dagger = F/\bar{T}_{sp}^4$, or

$$(F_{sp} - F)^\dagger = (F_{sp} - F)/\bar{T}_{sp}^4 \tag{88a}$$

This new thermal function is related to the original thermal function $F_s - F$ (without preheating) by

$$\begin{aligned} F_s - F &= (F_s - F_{sp}) + (F_{sp} - F) \\ &= -(\Gamma_{sp} - \Gamma_\infty) + \bar{T}_{sp}^4(F_{sp} - F)^\dagger \end{aligned} \tag{88b}$$

The enthalpy and temperature distributions in the shock layer obtained in a similar manner are

$$\bar{h} = 1 + \lambda_a[(\Gamma_{sp} - \Gamma_\infty) - \bar{T}_{sp}^4(F_{sp} - F)^\dagger] \tag{89}$$

$$\bar{T}^4 = \bar{T}_{sp}^4[1 - \bar{\alpha}(F_{sp} - F)^\dagger] \tag{90}$$

Injection and ablation layers.- It is assumed that a secondary layer of vaporization materials from the wall is separated from the primary shock layer by an interface. Experimental observations support this assumption (refs. 20 and 30). Figure 1 indicates the geometry with a stagnation point in the flow at the interface. The analysis of the vaporization layer is similar to the analysis for a shock layer in that constant pressure with $\gamma = 1$ (stagnation flow) is assumed. As in the shock layer, it is assumed that the thermal properties in the vaporization layer can be correlated by a linear equation relating T^4 and enthalpy. The reference temperature for this correlation is taken as the temperature of the vapor at the wall. It is further assumed that the injected gases are relatively cool compared to the air in the shock layer; therefore, the emission from the injected vapors may be neglected. An extension of the analysis in which this last assumption is relaxed is presented in appendix H.

We define a radiative blockage function as

$$\Phi_{wb} = \frac{q_{wb}}{q_{wo}} = \frac{\Gamma_{wb}}{\Gamma_{wo}} \tag{91}$$

where Γ_{wb} is radiative flux penetrating to the wall through the vapor layer and Γ_{wo} is the radiative flux for the same flight conditions without a vapor layer but, for consistency, with the same wall temperature with and without vaporization.

The optical thickness of the vapor layer is measured from the wall to the interface and conditions in the vapor layer are denoted by the subscript b. Thus, $\tau_b = 0$ at the wall and τ_{wb} is the optical thickness of the vapor layer at the interface.

If the emission from the vapor layer is assumed to be small compared to the emission from the shock layer, it follows that the properties in the shock layer are not changed significantly by the presence of the vapor layer. Therefore, from equations (9),

$$\Gamma_{wb} \simeq \Gamma_{wo} 2E_3(\tau_{wb}) \simeq \Gamma_{wo} e^{-n\tau_{wb}} \tag{92}$$

Consequently,

$$\Phi_{wb} = e^{-n\tau_{wb}} \tag{93}$$

The physical thickness of the vapor layer depends on the mass flow rate of the vapors; in adiabatic flow the thickness of the vapor layer is correlated by a simple expression (refs. 20 and 31).

$$\frac{L_t}{L_o} \simeq 1 + k_b \sqrt{\frac{\rho_s}{\rho_\infty} \frac{M_\infty}{M_b}}\, f_w \tag{94}$$

where $L_t = L_o + L_{bo}$, or the total distance between shock wave and wall; $k_b \simeq 1$ for a spherical nose (ref. 20); M_∞ and M_b are the molecular weights of air and vapor layers; L_o and L_{bo} are the thicknesses of air and vapor layers for adiabatic flow; ρ_b is the density of the injected gas at the wall; and f_w is the blowing ratio $(\rho_b v_b / \rho_\infty V_\infty)$.

The correlation law (eq. (94)) further provides a simple relation between vapor layer thickness and the blowing parameter; thus,

$$\frac{L_{bo}}{L_o} \simeq k_b \sqrt{\frac{\rho_s}{\rho_\infty} \frac{M_\infty}{M_b}}\, f_w \tag{95a}$$

$$\frac{L_{bo}}{R} \simeq k_s \sqrt{\frac{\rho_\infty}{\rho_s} \frac{M_\infty}{M_b}}\, f_w \tag{95b}$$

where $k_s \simeq 0.75$ for spherical noses (see eqs. (76)) and R is the radius of the spherical body. The nonadiabatic thickness of the vaporization layer is approximated by equations (74b) and (75c) in a manner similar to the calculation of nonadiabatic shock-layer distance.

For forced injection of vapors from the surface, the blowing rate parameter f_w is given a priori and the solution is then straightforward. For ablation, however, the blowing rate parameter f_w depends on the heat reaching the wall Γ_{wb}, and the solution is therefore coupled. We assume that the mass loss rate of ablation vapors per unit area is given by

$$-\frac{dm}{dt} \equiv \rho_b v_b = \frac{q_{wb}}{\zeta} \tag{96}$$

where ζ is the heat capacity of ablation products. The net radiant heat through the entire system at the wall is

$$q_{wb} = 2\sigma T_s^4 \Gamma_{wb} = \Phi_{wb} q_{wo} \tag{97}$$

thus, the blowing parameter, $f_w = \rho_b v_b / \rho_\infty V_\infty$, becomes

$$f_w = \lambda_a \left(\frac{h_s}{\zeta}\right) \Gamma_{wb} \tag{98}$$

where $\lambda_a = (2\sigma T_s^4/\rho_\infty V_\infty h_s)$ as in equation (14). The coefficient α_b in the thermal function for the ablation layer is coupled with the blowing parameter f_w, since Γ_{wb} in equation (98) depends on $\bar{\alpha}_b$ for given optical thickness and boundary conditions as given below:

$$\bar{\alpha}_b = \frac{2\sigma}{\rho_b v_b}\left(-\frac{\partial T^4}{\partial h}\right)_w = \frac{\lambda_b\left(\frac{\partial \bar{T}^4}{\partial \bar{h}}\right)_w}{f_w} \tag{99}$$

where

$$\lambda_b = \frac{2\sigma T_w^4}{\rho_\infty V_\infty h_w}$$

and

$$\left(\frac{\partial \bar{T}^4}{\partial \bar{h}}\right)_w = \frac{\partial (T/T_w)^4}{\partial (h/h_w)}$$

With equations (95), (98), and (99) and the solutions previously presented for $\gamma = 1$, including equation (74b), an iterative procedure is used to determine Γ_{wb} and f_w and the ablation vapor-layer thickness L_{bo} (see appendix H).

A simpler and useful approximation for Φ_{wb} may be obtained if it is further assumed that the absorption coefficient $(\rho_b \kappa_b)$ in the ablation layer is constant and that the blowing parameter f_w is very small.

Then, by the definition of optical depth,

$$\tau_{wb} = \rho_b \kappa_b L_b \tag{100}$$

where L_b is nonadiabatic vapor layer thickness, equation (100) may be rewritten as

$$\tau_{wb} = \frac{1}{2} \lambda_o \Gamma_{wo} g \frac{L_b}{L_{bo}} B \tag{101a}$$

where

$$\left.\begin{aligned} \lambda_o &= \frac{4\rho_s \kappa_s \sigma T_s^4 L_o}{\rho_\infty V_\infty h_s} \\ g &= k_b\left(\frac{\rho_b \kappa_b}{\rho_s \kappa_s}\right)\sqrt{\frac{\rho_s}{\rho_\infty}\frac{M_\infty}{M_b}} \\ B &= \frac{\rho_\infty V_\infty f_w h_s}{q_{wo}} \end{aligned}\right\} \tag{101b}$$

With equation (93), Φ_w becomes

$$\Phi_{wb} = e^{-\frac{n}{2}\lambda_o \Gamma_{wo} g \frac{L_b}{L_{bo}} B} \tag{102}$$

From equations (97) and (98) and by the definition of B in equations (101b), Φ_{wb} can be written

$$\Phi_{wb} = \frac{\zeta}{h_s} B \tag{103}$$

Equations (102) and (103) may be combined to eliminate B and therefore to obtain Φ_{wb} (or vice versa) for ablation. For $B \ll 1$ (small ablation), equation (102) may be expanded in the first order of power series and combined with equation (103) to obtain the approximate formula

$$\Phi_{wb} \simeq \frac{1}{1 + \lambda_o \Gamma_{wo} g \frac{h_s}{\zeta}} \tag{104}$$

where n has been set equal to 2 and $L_b/L_{bo} = 1$. Equation (104) is useful in that the absorption coefficients of the shock layer and vapor layer (which are generally unknown) are combined into a ratio. This allows parametric studies for assessing the effects of radiative blockage.

RESULTS FOR A SINGLE LAYER

Calculations of radiative flux at the boundaries and of profiles of radiative flux, enthalpy, and temperature in the shock layer have been made for selected flight conditions. The equilibrium air properties used in making these calculations are given in appendix I. The results are used to assess the effect of radiative energy loss on shock standoff distance, the effect of preheating and absorption in ablation layers on the radiative heat transfer

to the body, and the effect of radiative energy loss on the convective heat transfer. Where possible, the effects of the assumptions on the present results are considered by making comparisons with other solutions.

Comparisons With More Exact Analyses

Plane shock wave flow ($\gamma = 0$).- To evaluate the error introduced in the present solutions by replacing the exponential integrals with exponential functions, equation (18a) (the integrodifferential equation) was solved numerically[6] and this solution compared with solutions of equation (25a) (the differential equation obtained by using the exponential approximation). Various commonly used values of the constants m and n were used in these calculations. The results are shown in figure 3(a) for $\gamma = 0$, where Γ_w and Γ_s, the radiative heat to the wall and free stream, respectively, are plotted as functions of τ_w. This figure shows that the exact and approximate solutions agree well for $m = 1/2$ and n varying from 3/2 to 2 (but constant for a given value of τ_w) as provided by equation (72). As mentioned in the analysis, m is not arbitrary but should be 1/2 as required by the asymptotic values for optically thin and thick layers and by the equivalent wall approximation. This becomes particularly apparent (fig. 3(a)) for Γ_s as optical thickness is increased since the results for values of m different from 1/2 deviate from the correct asymptotic flux. The other constant n is less restricted, except that it should take on the value of 2 as τ_w approaches zero because it must take $mn = 1$ for $\tau_w \to 0$. Note that the approximate solution for $m = 1/2$ and $n = 3/2$ shows rather good agreement with the exact solution except, as expected, for small optical thickness.

Stagnation flow ($\gamma = 1$).- A comparison similar to that of figure 3(a) but for $\gamma = 1$ has not been made primarily because of numerical difficulties associated with the singularities in equation (18a). However, Howe and Viegas' (ref. 7) elaborate viscous solutions are available for comparison with the present solution. They do not assume a linear thermal function, a linear mass flow relation, or the exponential approximation (as does the present work). However, their solutions are for a gray gas, with the same absorption coefficients as used in the present work. Furthermore, the solutions of reference 7 are for relatively small values of τ_w and thus energy loss by radiation is emphasized rather than energy redistribution by self-absorption. The comparison is presented in figure 3(b) which shows very good agreement between the two treatments except, of course, near the wall where viscous effects predominate. The approximate boundary-layer edge, δ, is indicated in figure 3(b) as estimated from the empirical equation (ref. 32) as

$$\frac{\delta}{\sqrt{\frac{\mu_s}{2\rho_s (du/dx)_o}}} \simeq 3 \qquad (105)$$

[6]In the iteration process for equation (18a) the approximate solution is substituted as an initial input function. This reduces the difficulty of convergence associated with the equation and is very effective in controlling oscillations of the solution.

The stagnation streamline mass-flow distribution used in the present work is shown in figure 3(c). The calculated mass-flow distributions for various optical thicknesses τ_w are plotted as a function of physical depth into the shock layer and are compared with both a linear equation and the more realistic quadratic equation (nonadiabatic compressible flow) presented in reference 6. This figure shows that the present results agree well with the quadratic equation for most optical thicknesses but approach the linear equation for small optical thickness. As a first approximation, the present mass-flow distribution (eq. (11c)) provides the advantage of a closed form, simple solution for the radiative heat transfer.

Radiative Flux Results

The principal results of this report are illustrated in figures 4 and 5. The radiative fluxes at the shock wave Γ_s, and at the wall, Γ_w, as determined from the present closed-form solution are plotted as functions of τ_w in figures 4(a) and 4(b) for a temperature $T_s = 15{,}000^\circ$ K and pressures $p_s = 1$ and 10 atm, respectively. Results are presented for both plane shock flow and stagnation streamline flow; the corresponding flight conditions are shown on the figure. As mentioned in the analysis, radiative fluxes for plane shock flow and stagnation flow differ only to second order in optical thickness when τ_w is small. Furthermore, the asymptotic values of Γ_s for large τ_w are the same for both flows. The asymptotic absolute values of Γ_w for stagnation flow, however, decrease inversely as the square root of τ_w, whereas Γ_w for plane shock flow decreases very slowly to its finite symptotic value.

The results shown in figures 4(a) and 4(b) for stagnation flow are replotted in figure 4(c) where the ratio of nonadiabatic to adiabatic radiative heat transfer Γ_w/Γ_o is plotted as a function of the ratio of adiabatic radiative heat transfer to flow energy (λ_o). Existing numerical machine solutions are also shown on figure 4(c). For $p_s = 1$, where absorption effects are small, the present method agrees well with the results of references 7 and 8 except when λ_o is small. This can be anticipated because for small λ_o and fixed free-stream conditions Γ_o must be small, which in turn corresponds to small nose radius. Therefore, the Reynolds numbers for these conditions are low and the shock layer is primarily viscous. Thus, the temperature profile deviates sharply from that for a radiating field alone, and the present method overestimates radiative heating. It is probable that the present results for $p_s = 1$ in figure 4(c) represent a correlation curve for all flight conditions as long as τ_w is small and thus absorption effects are small. (This has also been pointed out in ref. 8.) However, when self-absorption becomes pronounced, as is the case for $p_s = 10$, Γ_w/Γ_o deviates from this correlation curve. Thus, the correlation curve should not be used for large values of λ_o, since large values of λ_o eventually correspond to large τ_w.

Results similar to those presented in figure 4, but for a much higher velocity (30 km/sec) and for stagnation flow only, are presented in figure 5. The ratio of radiative heat to total flow energy $q/(1/2)\rho_\infty V_\infty^3$ is plotted in figures 5(a) and 5(b) for $p_s = 1$ and 10 atm, respectively. The same trends

are evident in these figures as in figures 4(a) and 4(b). Figure 5(c) shows parameters similar to those in figure 4(c) except that the parameter is modified by $\lambda_o^* = (v_{ref}/V_\infty)\lambda_o$, where the reference is chosen for the flight condition, $p_s = 1$ atm and $V_{ref} = 15$ km/sec. An explanation of the correlation is that the modified parameter λ_o^* depends weakly on the flight velocity since

$$\rho_s \kappa_s \propto p_s \ , \qquad T_s^4 \propto h_s^2 \quad \text{and} \quad \rho_\infty V_\infty h_s \propto p_s \sqrt{h_s}$$

or

$$\lambda_o \propto \sqrt{h_s} \simeq V_\infty$$

Thus, parameter $\lambda_o^* = (v_{ref}/V_\infty)\lambda_o$ becomes relatively independent of the flight speed. For the higher velocity flight condition, and for both pressures, values of λ_o^* less than about 1 correspond to small values of τ_w. Thus, the results correlate well with each other and with the correlation curve from figure 4(c).

Shock-Layer Profiles

Enthalpy distributions in the shock layer for various values of τ_w are shown in figures 6(a) and 6(b). For large τ_w the major change in enthalpy occurs relatively near the shock wave; for small τ_w the major change in enthalpy occurs near the wall. Enthalpy, when plotted in terms of optical thickness τ (rather than $\bar{\tau} = \tau/\tau_w$), is always higher for larger τ_w.

Because of the nearly constant enthalpy near the wall for large τ_w, radiation heat transfer to the wall for this case (i.e., for large bodies or high free-stream densities) is nearly black-body radiation σT_l^4 where T_l is the local temperature near the wall. Such radiation is proportional to local enthalpy, as can be seen from the thermal function, and therefore is proportional to a reduced velocity v_l defined by

$$h_l \simeq \frac{1}{2} v_l^2 \tag{106a}$$

The absorption effect thus reduces radiative heat by an amount which corresponds to a velocity change similar for a conical body with apex angle

$$\theta_l = \sin\left(\frac{v_l}{V_\infty}\right) \tag{106b}$$

An important parameter in the analysis for $\gamma = 1$ is ν (the order of the modified Bessel function where $\nu = (1/2) + mn\bar{\alpha}\tau_w$) since the character of the solutions depends on whether ν is greater or less than 1. In figure 7,

profiles of $\bar{T}$, Γ, and $d\Gamma/d\bar{\tau}$ are presented for $\nu > 1$ and $\nu < 1$. The temperature distribution for $\nu < 1$ shows a very sharp drop near the wall and, in fact, has infinite slope at the wall, whereas the temperature distribution for $\nu > 1$ has a finite slope near the wall (eqs. (42)). The temperature itself at the wall is greater for $\nu > 1$ than for $\nu < 1$. The flux distribution shows no infinite slope; in fact, the derivative of the flux is zero at the wall regardless of the value of ν (eq. (41)).

In figure 8, the variation of the gas temperature at the wall, T_e (with optical thickness, τ_w), shows considerable differences between stagnation flow and plane shock flow. These differences occur because for stagnation flow the flow time (and thus the emission time) near the stagnation point is infinite. For stagnation flow of an optically thin layer ($\tau_w \ll 1$) the gas does not absorb strongly enough to block the radiant energy, and the edge temperature, therefore, is relatively low. As the optical thickness increases, as a result of increasing either the absorption coefficient or the body radius, T_e increases with increasing τ_w since now the gas near the wall absorbs flux from upstream more effectively. A further increase of τ_w, however, causes a gradual drop in T_e, and T_e finally vanishes as τ_w approaches infinity. This occurs because the gas particles then have sufficient distance to travel, thus time in which to cool, even in a strongly absorbing layer. Because the velocity approaches zero at the wall in stagnation flow, there is a coupling effect between self-absorption and emission time for the gas near the stagnation point. Plane shock flow does not show this coupling effect (as illustrated in the same figure) because the velocity behind the shock is approximately constant and therefore the emission time is very short compared to that for stagnation flow. In actual flight, the boundary layer plays a significant role near the wall, so the trend of T_e described above exists, but is interrupted by heat conduction in the boundary layer before the T_e reaches its final value by radiation alone.

The effects of absorption in radiating flow discussed above will also occur for the case of nongray gas radiation where cooler gas near the stagnation point (with or without boundary layer) is heated by the absorption of U-V radiation from the rest of the shock layer. In other words, the optical thickness is in effect increased locally, and thus will act to prevent a sharp drop of edge temperature.

Shock Standoff Distance

Figure 9 presents the ratio of nonadiabatic to adiabatic shock standoff distance; this ratio illustrates the effect of density increase due to temperature drop by radiation loss. The results of reference 7 are included in this figure for comparison. The curves of L/L_o flatten out as the body radius increases and absorption effects become significant. For small bodies, the shock standoff distance depends primarily on radiation loss and is less sensitive to the effects of absorption.

APPLICATIONS TO MULTILAYERS

Blockage of Radiation by Injected or Ablated Vapors

The effect of injected or ablated vapors on the heat that reaches the wall from an intensely radiating shock layer will be considered; convective heat will be assumed negligible compared to radiative heat. The radiation blockage parameter Φ_{wb} (defined in eq. (91)) is the ratio of the net radiation flux reaching the wall with blockage Γ_{wb} to that reaching the wall without blockage Γ_{wo}. It is assumed that the intensity of the shock-layer radiation is so high compared to that of the ablation layer that the major effect is absorption of shock-layer radiation and therefore emission from the ablation vapor is negligible. The emission term for the injected vapors becomes comparable to the absorption term when τ_{wb} for the vapors becomes very large; however, that occurs only when values of Φ_{wb} are small and thus radiative heating at the wall has already been greatly reduced. (It should be noted that emission from the ablated vapor increases the net radiative heating at the wall.) Furthermore, convective heating can increase the temperature and consequently the emission from the ablation layer.

Figure 10(a) presents the radiative blockage function Φ_{wb} for injection, which is similar to the blockage function for convective heat. The solid line on the figure was obtained by considering only absorption in the injected vapor, equation (102), while the dashed line was obtained by considering both absorption and emission with various optical thicknesses of the shock layer, τ_w^I. A rather good correlation curve resulted for these calculations. It can be seen that the effect of emission is negligible for $\tau_{wb} \ll 1$. The calculations were obtained with carbon as the injected vapor.

Figure 10(b) presents the radiative blockage function, Φ_{wb}, for ablation as a function of the ratio of absorption coefficient in the ablation layer to that of the air behind the normal shock wave for body radii of 1 and 10 meters. Increasing the body radius reduces the radiative blockage parameter for a given absorption coefficient. To block radiative heat effectively a small body (1 m) requires higher absorption coefficients than a large body because the small body receives less radiative heat; consequently it has a relatively thin ablation layer that will not block as much radiative heat. Radiative heat is sharply reduced as the absorption coefficient of the ablation vapor increases because the optical thickness in the ablation layer is increased by two factors:

(1) Higher absorption coefficients

(2) Increased physical thickness due to the absorption effect (i.e., the ablation layer is heated by absorption, and accordingly is thicker).

In connection with the flow field, temperature near the interface changes sharply; but it is continuous for stagnation type flow ($\gamma = 1$) since net flux and velocity at the interface are continuous. The theoretical

interface temperature for a similar situation in plane shock flows ($\gamma = 0$) is discontinuous because the velocity profile is discontinuous.

Preheating Zone

As the flight velocity approaches meteoric speed, most of the radiation from the strong shock layer is in the U-V region and can be strongly absorbed by free-stream air ahead of the shock. The absorption of the ultraviolet creates a preheating zone which raises the temperature both ahead of and behind the shock wave, thus increasing the radiative heat to the wall. To represent the actual (wavelength selective) absorption by the free stream with a gray-gas analysis, a portion (Γ_∞) of the flux entering the preheating zone from the shock layer (Γ_{sp}) is allowed to escape from the system (as described in the analysis). The escaping fraction is then $\Phi_\infty = \Gamma_\infty/\Gamma_{sp}$ which can be considered a radiative leakage function at the edge of the preheating zone. The fraction absorbed by the preheating zone is $1 - \Phi_\infty$. The increase in heating to the wall is given by Φ_{wp} where $\Phi_{wp} = \Gamma_{wp}/\Gamma_{wo}$, the ratio of radiative heating to the wall with and without preheating.

Figure 11 is a plot of Φ_{wp} versus body radius R, with Φ_∞ as a parameter. (Emission from the preheating zone was neglected in figure 11.) For $\Phi_\infty = 1$ there is no preheating effect and $\Phi_{wp} = 1$. For $\Phi_\infty = 0$ all radiative flux is trapped in the preheating zone, and there is a sizable increase in radiative heat with increasing body radius. This increase is primarily due to the increase of temperature behind the shock wave. For a given Φ_∞ (escaping radiation fraction), the larger bodies undergo a greater increase in radiative heat at the wall because the preheating zone can absorb more from the larger radiation associated with the thicker shock layers of the large bodies. Figure 11 also suggests that in actual flight a body can receive more than half the energy radiated from the system ($q_\infty + q_{wp}$). However, as the temperature ahead of the shock becomes comparable to that behind the shock, emission and other neglected effects (i.e., kinetic energy changes and heat conduction) may become important.

The approximate combined effects of both preheating and ablation on heat transfer to the body can be given as

$$\Phi_w \simeq \underbrace{\Phi_{wp}}_{\left[\begin{array}{c}\text{preheating effect}\\ \text{on nonablating body}\end{array}\right]} \quad \underbrace{\Phi_{wb}}_{\left[\begin{array}{c}\text{ablation vapor effect}\\ \text{without preheating}\end{array}\right]} \tag{107}$$

if absorption is the major mode of energy transfer in the ablation layers.

Effect of Nonadiabatic Flow on Convective Heating

While it is beyond the scope of this paper to analyze in detail the changes in convective heating that occur as a result of nonadiabatic radiative

flow, it is possible to make a simple estimate of the effect by modifying somewhat the criterion (first introduced by Goulard, ref. 33) of taking the enthalpy at the edge of the viscous boundary layer as the driving enthalpy for convective heating. (Later, Thomas (ref. 13) suggested taking the enthalpy at the edge of the gas layer, h_e (the enthalpy corresponding to T_e), as the driving enthalpy.) It is reasonable to assume that convection becomes important in energy transfer at the boundary-layer edge and finally becomes completely dominant in changing the fluid enthalpy at a certain distance into the boundary layer. The assumed distance at which convection becomes dominant[7] is $\delta/2$, where δ is the boundary-layer thickness given by equation (105). However, the additional loss of enthalpy by radiation in the transition layer should be considered where radiation and conduction are both important. To approximately account for this additional loss of enthalpy by radiation we will use the enthalpy at $\delta/2$ computed for radiation alone, $h_{\delta/2}$, as the driving enthalpy by convective heating. Thus, the convective heating q_c is reduced by

$$\frac{q_c}{q_{co}} \approx \frac{h_{\delta/2}}{h_s} \tag{108}$$

where q_{co} is convective heat without radiation effect. Figure 12 shows the ratio q_c/q_{co} as a function of τ_w. The results agree well with the results from reference 7.[8]

CONCLUDING REMARKS

The gray-gas approximation was used and the radiant heat-transfer equation was linearized to obtain analytical closed-form solutions for the radiative heating of a body for optical thicknesses from zero to infinity. It was shown that effects of absorption and energy loss are important. By virtue of the linearized solution, radiative heat transfer in multiple layers with various boundary conditions is simplified considerably. Some important characteristics of nonadiabatic flow were computed simply from adiabatic relations, for example, shock standoff distance in terms of density ratio and convective heating in terms of enthalpy ratio. A radiative blockage function for gas injection, similar to the convective blockage function, was introduced and computed for high-speed flows over ablating bodies in which radiant heat predominates over convective heat. It was also shown that the preheating effect in high-speed flight may contribute substantially to the heat transfer to a body.

Ames Research Center
National Aeronautics and Space Administration
Moffett Field, Calif., 94035, March 20, 1967
129-01-08-11-00-21

[7]The precise value was discussed in reference 29.

[8]The asymptotic value of q_c/q_{co} approaches zero slowly since T_e approaches zero.

APPENDIX A

RADIATIVE TRANSPORT EQUATION IN DOUBLE OR MULTILAYERS

A preheating layer with a shock layer and a shock layer with ablation or vapor injection from the body surface separated by an interface represent a typical two-gas layer problem. The radiative equation within the shock layer for this case becomes (from eq. (9a)), for $\tau < \tau_i$

$$\Gamma(\tau) = -2R_s E_3(\tau) + 2R_w E_3(\tau_w - \tau) - \int_0^\tau \bar{T}^4 E_2(\tau - t)dt + \int_\tau^{\tau_w} \bar{T}^4 E_2(t - \tau)dt \tag{9a}$$

which, in terms of each layer thickness, becomes

$$\Gamma(\tau) = -2R_s E_3(\tau) + 2R_w E_3(\tau_w - \tau_i + \tau_i - \tau) - \int_0^\tau \bar{T}^4 E_2(\tau - t)dt$$

$$+ \int_\tau^{\tau_i} \bar{T}^4 E_2(t - \tau)dt + \int_{\tau_i}^{\tau_w} \bar{T}^4 E_2(t - \tau)dt \tag{A1}$$

For $\tau > \tau_i$,

$$\Gamma(\tau) = 2R_s E_3(\tau - \tau_i + \tau_i) + 2R_w E_3(\tau_w - \tau)$$

$$- \int_0^{\tau_i} \bar{T}^4 E_2(\tau - t)dt - \int_{\tau_i}^\tau \bar{T}^4 E_2(\tau - t)dt + \int_\tau^{\tau_w} \bar{T}^4 E_2(t - \tau)dt \tag{A2}$$

Equivalent Wall Approximation

It is useful here to introduce the concept of an equivalent wall approximation, that is, the assumption of a thin wall that intercepts all incoming fluxes on this boundary, and reemits the same number of photons in the same direction across the wall. Thus, mathematically, equations (A1) and (A2) change form slightly and become, for $\tau < \tau_i$,

$$\Gamma(\tau) = -2R_s E_3(\tau) + 2R_1 E_3(\tau_i - \tau) - \int_0^\tau \bar{T}^4 E_2(\tau - t)dt + \int_\tau^{\tau_i} \bar{T}^4 E_2(t - \tau)dt \tag{A3}$$

for $\tau > \tau_i$,

$$\Gamma(\tau) = -2R_2E_3(\tau - \tau_i) + 2R_wE_3(\tau_w - \tau) - \int_o^{\tau} \bar{T}^4E_2(\tau - t)dt + \int_{\tau}^{\tau_w} \bar{T}^4E_2(t - \tau)dt \tag{A4}$$

where

$$R_1 = 2R_wE_3(\tau_w - \tau_i) + \int_{\tau_i}^{\tau_w} \bar{T}^4E_2(t - \tau_i)dt \tag{A5}$$

$$R_2 = 2R_sE_3(\tau_i) + \int_o^{\tau_i} \bar{T}^4E_2(\tau_i - t)dt \tag{A6}$$

Quantities R_1 and R_2 represent equivalent boundary conditions which include the effect of radiative flux from other gas slabs on the assumed thin wall. Consequently, if equivalent wall conditions are assumed, radiative transport of double layers is separable and can be considered as two independent single-layer problems with variable boundary conditions. The physical interpretation given by equations (A3) to (A6) can be justified mathematically as well. By Taylor's expansion, for $\tau \geq \tau_i$,

$$E_3(\tau) = E_3(\tau_i + \tau - \tau_i)$$

$$= E_3(\tau_i) - (\tau - \tau_i)E_2(\tau_i) + \ldots$$

and

$$E_3(\tau_i)2E_3(\tau - \tau_i) = E_3(\tau_i) - (\tau - \tau_i)2E_3(\tau_i) + \ldots$$

$$\simeq E_3(\tau_i) - (\tau - \tau_i)E_2(\tau_i) + \ldots$$

for the moderate range of τ_i (exact at $\tau = \tau_i$). Since the major contribution of the exponential integral function $E_3(\tau)$ comes when $\tau \simeq \tau_i$, and the magnitude of the difference of the above two functions becomes small for larger τ

$$|E_3(\tau) - E_3(\tau_i)2E_3(\tau - \tau_i)| \ll E_3(\tau_i)$$

for the entire range of τ. Thus, the above substitution of $E_3(\tau)$ by $E_3(\tau_i)2E_3(\tau - \tau_i)$ will provide a good approximation for all values of τ_i. In fact, when the integral exponential function is replaced by the exponential

function of constant m and n, the original transport equations (9) and modified equations (A3) and (A4) become identical; thus, from substitution of

$$E_3(\tau) = me^{-n\tau}$$

and its derivative ($E_2(\tau) = -E_3'(\tau)$)

$$E_2(\tau) = mne^{-n\tau}$$

it follows for $\tau \geq \tau_i$ that

$$E_3(\tau) = me^{-n(\tau-\tau_i)}e^{-n\tau_i}$$

$$E_3(\tau_i)2E_3(\tau - \tau_i) = 2m^2e^{-n\tau_i}e^{-n(\tau-\tau_i)}$$

Thus,

$$E_3(\tau) = E_3(\tau_i)2E_3(\tau - \tau_i) \tag{A7}$$

when $m = 1/2$. Similarly, for $\tau \leq \tau_i$,

$$E_3(\tau_w - \tau) = E_3(\tau_w - \tau_i)2E_3(\tau_i - \tau) \tag{A8}$$

With the exponential approximation substituted in the integral part of equation (A1)

$$\int_{\tau_i}^{\tau_w} \bar{T}^4 E_2(t - \tau)dt = \int_{\tau_i}^{\tau_w} \bar{T}^4 mne^{-n(t - \tau)}dt \qquad (\tau \leq \tau_i)$$

and

$$2E_3(\tau_i - \tau)\int_{\tau_i}^{\tau_w} \bar{T}^4 E_2(t - \tau_i)dt = 2me^{-n(\tau_i-\tau)}\int_{\tau_i}^{\tau_w} \bar{T}^4 mne^{-n(t - \tau_i)}dt$$

$$= 2m\int_{\tau_i}^{\tau_w} \bar{T}^4 mne^{-n(t - \tau)}dt \tag{A9}$$

One can readily see that these integrals are identical if $m = 1/2$. As discussed previously in the approximate solution, the constant m is found to be 1/2 from other criteria.

Equivalent Boundary Values

Since the transport equation in double or multiple gas layers can be divided into two or several separate layers, corresponding boundary conditions on the equivalent wall can be treated, from equations (26), if regions I and II are considered separately. Thus, region II can be considered entirely separate from region I so that its flow field and notation become consistent with that of the first layer (see sketch (b)). The superscripts I and II denote properties in the respective regions.

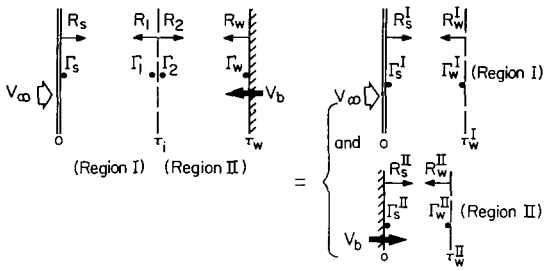

Sketch (b) Separation of shock layer (I) and injection layer (II).

The net flux Γ_1 from layer I at $\tau = \tau_i$, and Γ_2 from layer II are

$$\Gamma_1 = \Gamma_w{}^I = (M_3 + M_4 R_s + M_5 R_w)^I \tag{A10}$$

$$\Gamma_2 = -\bar{T}_w{}^4 \Gamma_w{}^{II} = -\bar{T}_w{}^4 (M_3 + M_4 R_s + M_5 R_w)^{II} \tag{A11}$$

Dimensionless quantities in region II are based on wall (injection) temperature T_w, and boundary values $R_w{}^I$ and $R_w{}^{II}$ are to be determined for given $R_s{}^I$ and $R_s{}^{II}$. With new definitions of

$$\left.\begin{aligned} R_1 &= R_w{}^I \\ R_2 &= \bar{T}_w{}^4 R_w{}^{II} \end{aligned}\right\} \tag{A12}$$

and energy balance at boundary τ_i,

$$\Gamma_1 = \Gamma_2 = R_1 - R_2 \tag{A13}$$

it follows that, from equations (A10), (A11), and (A13), equivalent boundary values are

$$R_1 \equiv R_w{}^I = \frac{(M_3 + M_4 R_s)^I (1 - M_5{}^{II}) + \bar{T}_w{}^4 (M_3 + M_4 R_s)^{II}}{M_5{}^I M_5{}^{II} - (M_5{}^I + M_5{}^{II})} \tag{A14}$$

$$\frac{R_2}{\bar{T}_w^4} \equiv R_w^{II} = \frac{(M_3 + M_4R_s)^I/\bar{T}_w^4 + (1 - M_5^I)(M_3 + M_4R_s)^{II}}{M_5^I M_5^{II} - (M_5^I + M_5^{II})} \tag{A15}$$

With these boundary conditions, flux toward the free stream, Γ_s, and flux toward the surface, Γ_w, from the whole system are calculated by

$$\Gamma_s = (M_o + M_1R_s + M_2R_w)^I \tag{A16}$$

$$\Gamma_{wb} = -\bar{T}_w^4\Gamma_s^{II} = -\bar{T}_w^4(M_o + M_1R_s + M_2R_w)^{II} \tag{A17}$$

The radiative blockage function Φ_{wb} is then

$$\Phi_{wb} = \frac{\Gamma_{wb}}{\Gamma_{wo}} \tag{91}$$

where Γ_{wo} is the radiative function at the wall without injection (or ablation) and is written

$$\Gamma_{wo} = (M_3 + M_4R_s + M_5R_w)^I \tag{A18}$$

APPENDIX B

THERMAL FUNCTION

From thermodynamic charts or tables (refs. 34 and 35), temperature variation with enthalpy for constant pressure (or constant density) can be expressed around reference temperature T_r as

$$T^4 = T_r^4 + \left(\frac{\partial T^4}{\partial h}\right)_r (h - h_r) + \frac{1}{2}\left(\frac{\partial^2 T^4}{\partial h^2}\right)_r (h - h_r)^2 + \cdots \tag{B1}$$

For the present work, only a few terms in equation (B1) are sufficient to cover the range of temperature of interest; however, average slope $(\overline{\partial T^4/\partial h})$ is effective and simple for general applications. Thus, with temperature behind the shock, T_s, as reference,

$$T^4 \simeq T_s^4 + \left(\overline{\frac{\partial T^4}{\partial h}}\right)(h - h_s) \tag{B2}$$

This equation, normalized by dividing by T_s^4 becomes

$$\bar{T}^4 \simeq 1 - \bar{\alpha}(F_s - F) \tag{B3}$$

where

$$\bar{\alpha} = \frac{2\sigma}{\rho_\infty V_\infty}\left(\overline{\frac{\partial T^4}{\partial h}}\right)_s = \lambda_a\left(\overline{\frac{\partial T^4}{\partial \bar{h}}}\right)_s \tag{B4}$$

This equation can be called the ideal or linear thermal relation since the transfer equation is linearized (in contrast to the linear relation between enthalpy and temperature for an ideal gas).

The temperature relation for constant density in the preheating zone can be written as

$$T^4 \simeq T_f^4 + \left(\overline{\frac{\partial T^4}{\partial h}}\right)_f (h - h_f) \tag{B5}$$

where T_f is the temperature just ahead of shock front and is to be determined; T_f is selected as reference temperature rather than free-stream temperature T_∞ since transport properties depend strongly on temperature near T_f. In normalized form, with T_f as reference temperature, equation (B5) becomes

$$(T/T_f)^4 \simeq 1 - \bar{\alpha}_f(F_f - F) \tag{B6}$$

Temperature T_f can be calculated from the relation derived for other reference gas temperature, T_r, as follows: from equation (87b) and for $h_f \simeq h_r$

$$\frac{h_r - h_\infty}{h_s} \simeq \lambda_a(\Gamma_{sp} - \Gamma_\infty)_r \tag{B7}$$

where

$$(\Gamma_{sp} - \Gamma_\infty)_r = \frac{M_o(1 - 2E_3\tau_\infty)}{1 - \bar{\alpha}M_o(1 - 2E_3\tau_\infty)} \tag{B8}$$

Equation (B8), which takes only absorption effects into account and thus neglects gas emission in the preheating layer, is calculated from equations (83) and (86) for given $\bar{\alpha}_r$ and τ_∞. The value of temperature T_r, which corresponds to enthalpy h_r, can be obtained from the real gas chart for constant density ($\rho^* \simeq \rho_\infty$). Since $T_f \simeq T_r$, one can use $(\overline{\partial T^4}/\partial h)_r$ for any temperature near $T \simeq T_f$ so that in the preheating zone

$$T_f^4 \simeq T_r^4 + \left(\frac{\overline{\partial T^4}}{\partial h}\right)_r (h_f - h_r) \tag{B9}$$

After equation (B7) is substituted into (B9) and divided by T_s^4,

$$\bar{T}_f^4 \simeq \bar{T}_r^4 + \bar{\alpha}_r[(\Gamma_{sp} - \Gamma_\infty) - (\Gamma_{sp} - \Gamma_\infty)_r] \tag{B10}$$

where Γ_{sp} and Γ_∞, including the effects of both self-absorption and gas emission, are now calculated for the same $\bar{\alpha}_r$ and τ_∞ as used in equation (B8). The thermal function is used to calculate the radiative flux with preheating and is presented in appendix G.

With this temperature T_f and $\bar{\alpha}_r \simeq \bar{\alpha}_f$, the temperature relation given in equation (B6) can be used to evaluate radiative transfer in the preheating zone by a procedure similar to that given for the shock-layer analysis.

Similar thermal relations can be used for the injection layer except now constant pressure over the layer is assumed; thus,

$$(T/T_w)^4 \simeq 1 - \bar{\alpha}_b(F_w - F) \tag{B11}$$

where $\bar{\alpha}_b$ is defined by equation (99), and wall temperature, T_w, is the reference temperature for normalizing the thermal function.

Note that the linear thermal relation may not apply in some gases; but it can be used to predict the importance of emission effects (from the preheating and the vapor layers) on radiative heat at the wall.

Temperature-Pressure Relation

The temperature variation for other pressures (fig. 2) can be written empirically as

$$\bar{T}^4 \simeq \bar{T}^4(P_s,h) + [1 - \bar{T}^4(P_s,h)][1 - (P/P_s)^{-m}] \qquad (B12)$$

where P_s is reference pressure near p, and m is constant; for example, $m \simeq 0.69$ for $T_s \simeq 15{,}000^\circ$ K and for pressure ranges of $P_s = 10^{-1}$ to 10^2 atm.

APPENDIX C

MODIFIED BESSEL FUNCTIONS OF THE FIRST AND SECOND KIND (I,K)

The differential equation of radiative transfer for stagnation flow ($\gamma = 1$) is (eq. (34))

$$\frac{d^2\Gamma}{d\theta^2} - \frac{2mn\tilde{\alpha}\tau_w}{\theta}\frac{d\Gamma}{d\theta} - n^2\Gamma = 0 \tag{C1}$$

which can be reduced to the modified Bessel equation. The general solution is

$$\Gamma = \theta^{\nu}[c_1 I_{\nu}(n\theta) + c_2 K_{\nu}(n\theta)] \tag{C2}$$

Definitions and properties for these functions are presented in many textbooks (refs. 24 and 25). The detailed calculation scheme involved in the present application is given in this appendix. Bessel functions in ascending series are (refs. 24 and 25)

$$I_{\nu}(n\theta) = \left(\frac{n\theta}{2}\right)^{\nu}\sum_{\kappa=0}^{\infty}\frac{\left(\frac{n\theta}{2}\right)^{2\kappa}}{\kappa!\Gamma(\nu + \kappa + 1)} \tag{C3}$$

where $\Gamma(\nu + \kappa + 1)$ is the gamma function.

$$K_{\nu}(n\theta) = \frac{\pi}{2}\frac{1}{\sin \pi\nu}[I_{-\nu}(n\theta) - I_{\nu}(n\theta)] \tag{C4}$$

Properties of the $\Gamma_{\nu}(\theta)$ Function

Differentiation formula.- Let the flux function $\Gamma_{\nu}(\theta)$ and $\Gamma_{\nu\pm1}(\theta)$ be defined by

$$\left.\begin{aligned}\Gamma_{\nu}(\theta) &\equiv c_1 Z_{\nu}(\theta) + c_2 Z_{-\nu}(\theta)\\ \Gamma_{\nu\pm1}(\theta) &\equiv c_1 Z_{\nu\pm1}(\theta) - c_2 Z_{-(\nu\pm1)}(\theta) \qquad (\nu \pm 1 \neq \nu)\end{aligned}\right\} \tag{C5a}$$

where

$$Z_\nu(\theta) \equiv \theta^\nu I_\nu(n\theta) \tag{C5b}$$

$$Z_{-\nu}(\theta) \equiv \theta^\nu K_\nu(n\theta) \tag{C5c}$$

Since derivatives of Z_ν functions are

$$\frac{\partial}{\partial\theta}\left[Z_\nu(\theta)\right] = n\theta Z_{\nu-1}(\theta) \tag{C6a}$$

$$\frac{\partial}{\partial\theta}\left[Z_{-\nu}(\theta)\right] = -n\theta Z_{-(\nu-1)}(\theta) \tag{C6b}$$

it follows that

$$\frac{\partial}{\partial\theta}\,\Gamma_\nu(\theta) = n\theta\left[c_1 Z_{\nu-1}(\theta) - c_2 Z_{-(\nu-1)}(\theta)\right]$$

or

$$\frac{\partial}{\partial\theta}\,\Gamma_\nu(\theta) = n\theta\Gamma_{\nu-1}(\theta) \tag{C7}$$

Recurrence relation.- The recurrence formulas of I_ν and K_ν are

$$2\nu I_\nu(n\theta) = n\theta I_{\nu-1}(n\theta) - n\theta I_{\nu+1}(n\theta) \tag{C8a}$$

$$2\nu K_\nu(n\theta) = -n\theta K_{\nu-1}(n\theta) + n\theta K_{\nu+1}(n\theta) \tag{C8b}$$

With slight modification of the last two equations it follows that

$$2\nu\Gamma_\nu(\theta) = n\theta^2\Gamma_{\nu-1}(\theta) - n\Gamma_{\nu+1}(\theta) \tag{C9}$$

From equation (C7) and (C9), one obtains

$$\theta\,\frac{\partial}{\partial\theta}\,\Gamma_\nu(\theta) = 2\nu\Gamma_\nu(\theta) + n\Gamma_{\nu+1}(\theta) \tag{C10}$$

But

$$\frac{\partial}{\partial\theta}\left[\theta\Gamma_\nu(\theta)\right] = \Gamma_\nu(\theta) + \theta\,\frac{\partial}{\partial\theta}\,\Gamma_\nu(\theta)$$

therefore with equation (C10) it becomes

$$\frac{\partial}{\partial\theta}\left[\theta\Gamma_\nu(\theta)\right] = (2\nu + 1)\Gamma_\nu(\theta) + n\Gamma_{\nu+1}(\theta) \tag{C11}$$

Integrals involving $\Gamma_\nu(\theta)$ functions.- The integration involving the Γ_ν function, which appeared in the evaluation of boundary conditions (eqs. (25b) and (c)), is

$$\int_0^{\tau_w} e^{\pm n\theta}\Gamma_{\nu-1}(\theta)d\theta$$

Integrating by part, one obtains

$$\int_0^{\tau_w} e^{\pm n\theta}\Gamma_{\nu-1}(\theta)d\theta = \left[\theta e^{\pm n\theta}\Gamma_{\nu-1}(\theta)\right]_0^{\tau_w} - \int_0^{\tau_w} e^{\pm n\theta}\left[\pm n\theta\Gamma_{\nu-1}(\theta) + \theta\Gamma'_{\nu-1}(\theta)\right]d\theta$$

where

$$\Gamma'_{\nu-1}(\theta) \equiv \frac{d}{d\theta}\Gamma_{\nu-1}(\theta)$$

From equations (C7) and (C10) it follows that

$$\int_0^{\tau_w} e^{\pm n\theta}\left[\pm n\theta\Gamma_{\nu-1}(\theta) + \theta\Gamma'_{\nu-1}(\theta)\right]d\theta$$

$$= 2(\nu - 1)\int_0^{\tau_w} e^{\pm n\theta}\Gamma_{\nu-1}(\theta)d\theta \pm \int_0^{\tau_w}\frac{d}{d\theta}\left[e^{\pm n\theta}\Gamma_\nu(\theta)\right]d\theta$$

or

$$\int_0^{\tau_w} e^{\pm n\theta}\Gamma_{\nu-1}(\theta)d\theta = \frac{1}{2\nu - 1}e^{\pm n\theta}\left[\theta\Gamma_{\nu-1}(\theta) \mp \Gamma_\nu(\theta)\right]_0^{\tau_w} \qquad \left(R\nu > \frac{1}{2}\right)$$

Finally, it becomes

$$\int_0^{\tau_w} e^{\pm n\theta}\Gamma_{\nu-1}(\theta)d\theta = \frac{1}{2\nu - 1}\left\{e^{\pm n\tau_w}\left[\tau_w\Gamma_{\nu-1}(\tau_w) \mp \Gamma_s\right] \pm \Gamma_w\right\} \tag{C12a}$$

Then integration associated with Γ_s in equation (25b) is

$$\int_0^{\tau_w} e^{-n\tau}\Gamma_{\nu-1}(\tau_w - \tau)d\tau = \frac{1}{2\nu - 1}\left\{\left[\tau_w\Gamma_{\nu-1}(\tau_w) - \Gamma_s\right] + e^{-n\tau_w}\Gamma_w\right\} \qquad (C12b)$$

and that of Γ_w in equation (25c) is

$$\int_0^{\tau_w} e^{-n(\tau_w-\tau)}\Gamma_{\nu-1}(\tau_w - \tau)d\tau = \frac{1}{2\nu - 1}\left\{e^{-n\tau_w}\left[\tau_w\Gamma_{\nu-1}(\tau_w) + \Gamma_s\right] - \Gamma_w\right\} \qquad (C12c)$$

Integral of the $Z_\nu(\theta)$ function.- By definition, $C_\nu(\theta)$ is expressed as

$$C_\nu(\theta) \equiv \int_0^\theta Z_\nu(\theta)d\theta \equiv \int_0^\theta \theta^\nu I_\nu(n\theta)d\theta$$

Similarly,

$$C_{-\nu}(\theta) \equiv \int_0^\theta Z_{-\nu}(\theta)d\theta \equiv \int_0^\theta \theta^\nu K_\nu(n\theta)d\theta$$

The term $C_{\nu-1}(n\theta)$ in equations (37) are calculated by

$$C_{\nu-1}(\theta) = \frac{1}{2}\left(\frac{2}{n}\right)^{\nu-1}\Gamma\left(\frac{1}{2}\right)\Gamma\left(\nu - \frac{1}{2}\right)\theta\left[I_{\nu-1}(n\theta)L_{\nu-2}(n\theta) - L_{\nu-1}(n\theta)I_{\nu-2}(n\theta)\right] \qquad (C13a)$$

also,

$$C_{-(\nu-1)}(\theta) = \frac{1}{2}\left(\frac{2}{n}\right)^{\nu-1}\Gamma\left(\frac{1}{2}\right)\Gamma\left(\nu - \frac{1}{2}\right)\theta\left[K_{\nu-1}(n\theta)L_{\nu-2}(n\theta) + L_{\nu-1}(n\theta)K_{\nu-2}(n\theta)\right] \qquad (C13b)$$

where $L_\nu(n\theta)$ is the modified Struve function (ref. 25) for which a series expansion can be written as

$$L_\nu(n\theta) = \left(\frac{n\theta}{2}\right)^{\nu+1}\sum_{m=0}^{\infty}\frac{(n\theta/2)^{2m}}{\Gamma[m + (3/2)]\Gamma[\nu + (3/2) + m]} \qquad (C14a)$$

In the recurrence formula

$$L_{\nu}(n\theta) = \left(\frac{n\theta}{2}\right)^{\nu+1} \frac{1}{\Gamma(3/2)\Gamma[\nu + (3/2)]} \left(1 + \sum_{m=1}^{\infty} \lambda_m\right) \tag{C14b}$$

where

$$\left.\begin{aligned} \lambda_o &= 1 \\ \lambda_m &= \frac{(n\theta)^2}{(2m + 1)(2\nu + 2m + 1)} \lambda_{m-1} \end{aligned}\right\} \tag{C14c}$$

APPENDIX D

EVALUATION OF BOUNDARY CONDITIONS

The equations required for calculating the boundary conditions are

$$\frac{d\Gamma}{d\theta^2} - 2mn\bar{\alpha}\left(\frac{\tau_w}{\theta}\right)^{\gamma}\frac{d\Gamma}{d\theta} - n^2\Gamma = 0 \tag{25a}$$

and the boundary conditions are

$$\Gamma_s = -2mR_s + 2mR_w e^{-n\tau_w} + mn\int_o^{\tau_w} \bar{T}^4 e^{-nt}\,dt \tag{25b}$$

$$\Gamma_w = -2mR_s e^{-n\tau_w} + 2mR_w - mn\int_o^{\tau_w} \bar{T}^4 e^{-n(\tau_w - t)}\,dt \tag{25c}$$

The general solution for the flux function can be expressed as

$$\Gamma(\theta) = c_1 X_\gamma(n\theta) + c_2 Y_\gamma(n\theta) \tag{26a}$$

where

$$X_o(n\theta) = e^{-n\beta_1(\tau_w - \theta)} \quad \text{and} \quad Y_o(n\theta) = e^{-n\beta_2\theta} \qquad (\gamma = 0)$$

$$X_1(n\theta) = \theta^{\nu} I_\nu(n\theta) \quad \text{and} \quad Y_1(n\theta) = \theta^{\nu} K_\nu(n\theta) \qquad (\gamma = 1)$$

The thermal function F is related to the flux function by

$$dF = \frac{d\Gamma}{(\theta/\tau_w)^{\gamma}} \tag{16}$$

and to the temperature by

$$\bar{T}^4 = 1 - \bar{\alpha}(F_s - F) \tag{15c}$$

The boundary condition can now be evaluated, say for $\gamma = 1$, from equations (25) as follows:

$$\Gamma_s = mn\int_o^{\tau_w} e^{-nt}(1 - \bar{\alpha}F_s)dt + mn\bar{\alpha}\int_o^{\tau_w} e^{-nt}F\,dt - 2mR_s + 2mR_w e^{-n\tau_w}$$

The second term on the right side of the equation becomes

$$\int_o^{\tau_w} e^{-nt}F\,dt = e^{-n\tau_w}\int_o^{\tau_w} e^{n\theta}F(\theta)d\theta$$

$$= \frac{1}{n}e^{-n\tau_w}\left(e^{n\theta}F\right)_o^{\tau_w} - \frac{1}{n}e^{-n\tau_w}\int_o^{\tau_w} e^{n\theta}F'(\theta)d\theta$$

By equations (36) and (C12) it follows that

$$\Gamma_s = m(1 - \bar{\alpha}F_s)(1 - e^{-n\tau_w}) + m\bar{\alpha}(F_s - e^{-n\tau_w}F_w) - 2mR_s$$

$$+ 2mR_w e^{-n\tau_w} - \frac{mn\bar{\alpha}\tau_w}{2\nu - 1}\left[\tau_w\Gamma_{\nu-1}(\tau_w) - \Gamma_s + e^{-n\tau_w}\Gamma_w\right]$$

But from equations (15c) and

$$\nu = mn\bar{\alpha}\tau_w + \frac{1}{2} \tag{35b}$$

after the terms are rearranged it follows that

$$\Gamma_s = m - me^{-n\tau_w}[1 - \bar{\alpha}(F_s - F_w)] - 2mR_s + 2mR_w e^{-n\tau_w} - \frac{1}{2}\left[\tau_w\Gamma_{\nu-1}(\tau_w) - \Gamma_s + e^{-n\tau_w}\Gamma_w\right] \tag{D1}$$

Similarly, the boundary conditions for Γ_w, with use of equation (C12a) or (C12c), can be written as

$$\Gamma_w = me^{-n\tau_w} - m[1 - \bar{\alpha}(F_s - F_w)] - 2mR_s e^{-n\tau_w} + 2mR_w - \frac{1}{2}\left\{e^{-n\tau_w}[\tau_w\Gamma_{\nu-1}(\tau_w) + \Gamma_s] - \Gamma_w\right\} \tag{D2}$$

Since equations (37), (C7), and (39) provide that

$$\left.\begin{aligned} \Gamma_s &= c_1 Z_\nu + c_2 Z_{-\nu} \,, \qquad \Gamma_w = c_2 Z^*_{-\nu} \\ \Gamma_{\nu-1}(\tau_w) &= c_1 Z_{\nu-1} - c_2 Z_{-(\nu-1)} \\ F_s - F_w &= n\tau_w [c_1 C_{\nu-1} - c_2 C_{-(\nu-1)}] \end{aligned}\right\} \tag{D3}$$

two simultaneous equations, with c_1 and c_2 as unknowns, are obtained from equations (D1) and (D2) as written in equations (32d) and (38a). Similar procedures were applied for evaluating boundary conditions for $\gamma = 0$, and these results were given in equations (32c) and (32d).

APPENDIX E

ASCENDING EXPANSION OF Z FUNCTION ($\tau_w \ll 1$)

For $\gamma = 1$, when ν is fixed and the argument approaches zero, the following ascending series of the modified Bessel functions are useful for evaluating fluxes for $\tau_w \ll 1$. From equations (C3) and (C4)

$$Z_\nu(\theta) \equiv \theta^\nu I_\nu(n\theta) \simeq \left(\frac{n}{2}\right)^\nu \frac{\theta^{2\nu}}{\Gamma(\nu+1)}\left[1 + \frac{(1/2)n\theta}{\nu+1} \cdots\right] \qquad (\nu \neq -1, -2, \ldots) \tag{E1a}$$

$$Z_{-\nu}(\theta) \equiv \theta^\nu K_\nu(n\theta) = \frac{\pi}{2}\frac{1}{\sin \pi\nu}\left[\theta^\nu I_{-\nu}(n\theta) - Z_\nu(n\theta)\right]$$

$$\approx \frac{1}{2}\left(\frac{2}{n}\right)^\nu \Gamma(\nu)\left\{1 + \frac{[(1/2)n\theta]^2}{1-\nu} \cdots\right\}$$

$$- \frac{1}{2}\left(\frac{n}{2}\right)^\nu \frac{\Gamma(1-\nu)}{\nu}\theta^{2\nu}\left\{1 + \frac{[(1/2)n\theta]^2}{1+\nu} + \cdots\right\} \tag{E1b}$$

$$Z^*_{-\nu} \equiv Z_{-\nu}(0) = \frac{1}{2}\left(\frac{2}{n}\right)^\nu \Gamma(\nu) \tag{E2}$$

$$C_{\nu-1}(\theta) \simeq \left(\frac{n}{2}\right)^{\nu-1} \frac{\theta^{2(\nu-1)}}{\Gamma(\nu)}\left[\frac{\theta}{2\nu-1} + \left(\frac{n}{2}\right)^2 \frac{\theta^3}{\nu(2\nu+1)} \cdots\right] \tag{E3a}$$

$$C_{-(\nu-1)}(\theta) \simeq \left(\frac{1}{2}\right)\left(\frac{2}{n}\right)^{1-\nu} \Gamma(1-\nu)\theta^{-2(1-\nu)}\left[\frac{\theta}{2\nu-1} + \left(\frac{n}{2}\right)^2 \frac{\theta^3}{\nu(2\nu+1)} \cdots\right]$$

$$- \frac{1}{2}\left(\frac{n}{2}\right)^{1-\nu} \frac{\Gamma(\nu)}{1-\nu}\left[\theta + \left(\frac{n}{2}\right)^2 \frac{\theta^3}{3(2-\nu)} \cdots\right] \tag{E3b}$$

With these supplementary forms, the quantities in equations (38b) are expressed by the notations:

$$Q_1 = \left(\frac{2}{n}\right)^{1-\nu} \frac{1}{\Gamma(\nu)} \tau_w^{-2(1-\nu)} \tag{E4a}$$

$$Q_2 = \frac{1}{2}\left(\frac{2}{n}\right)^{1-\nu}\Gamma(1-\nu) \tag{E4b}$$

Replacing θ by τ_w in equations (E1a) and (E3a), one obtains

$$Z_\nu \simeq \left(\frac{2}{n}\right)^{1-\nu}\frac{1}{\Gamma(\nu)}\left[\frac{n}{2}\frac{1}{\nu}\tau_w^{2\nu} + O(\tau_w^3)\right]$$

$$\simeq n\tau_w^2(1 - 2mn\bar{\alpha}\tau_w)Q_1 \tag{E5}$$

$$Z_{\nu-1} \simeq \left(\frac{2}{n}\right)^{1-\nu}\frac{1}{\Gamma(\nu)}\left[\tau_w^{-2(1-\nu)} + \left(\frac{n}{2}\right)^2\frac{1}{\nu}\tau_w^{2\nu} + O(\tau_w^3)\right]$$

$$\simeq \left(1 + \frac{1}{2}n^2\tau_w^2\right)Q_1 \tag{E6}$$

$$C_{\nu-1} \simeq \left(\frac{2}{n}\right)^{1-\nu}\frac{1}{\Gamma(\nu)}\left[\frac{1}{2\nu-1}\tau_w^{2\nu-1} + O(\tau_w^2)\right]$$

$$\simeq \left[\frac{1}{2mn\bar{\alpha}} + O(\tau_w^3)\right]Q_1 \tag{E7}$$

From equation (E1b) one can write

$$Z_{-\nu} \simeq \left[\frac{1}{2}\left(\frac{2}{n}\right)^{\nu}\Gamma(\nu)\right][1 + O(\tau_w^2)] - \left[\frac{\pi}{2}\frac{1}{\sin\pi\nu}\left(\frac{n}{2}\right)^{\nu}\frac{1}{\Gamma(\nu+1)}\right]\tau_w^{2\nu}[1 + O(\tau_w^2)] \tag{E8}$$

by using the following properties of the gamma function (refs. 24 and 25)

$$\Gamma(\nu+1) = \nu\Gamma(\nu)\ , \qquad \frac{1}{\Gamma(\nu)} = \frac{\sin\pi\nu}{\pi}\Gamma(1-\nu)$$

and

$$\Gamma\left(\frac{1}{2} \pm \nu_o\right) \simeq \sqrt{\pi}(1 \mp \varphi_o\nu_o) \qquad \text{for} \qquad \nu_o \ll 1$$

where $\nu_o = mn\bar{\alpha}\tau_w$ and $\varphi_o = 2\ln 2 + \gamma$ (Euler's constant). Consider the first bracketed term in equation (E8); one obtains

$$\frac{1}{2}\left(\frac{2}{n}\right)^{\nu}\Gamma(\nu) \equiv Z_{-\nu}(0) = \left[\left(\frac{2}{n}\right)^{2\nu-1}\frac{\Gamma(\nu)}{\Gamma(1-\nu)}\right]Q_2$$

$$\simeq (1 - 2\varphi_o\nu_o)Q_2 \qquad \text{(E9)}$$

Consider the leading part of the second term in equation (E8). One obtains

$$\frac{1}{2}\left(\frac{n}{2}\right)^{\nu}\frac{\Gamma(\nu)}{\nu} = \left(\frac{n}{2}\frac{1}{\nu}\right)Q_2$$

$$\simeq (1 - 2\nu_o)nQ_2 \qquad \text{(E10)}$$

Finally, by combining equations (E8), (E9), and (E10), one obtains

$$Z_{-\nu} \simeq [1 - (2mn\bar{\alpha}\varphi_o + n\tau_w^{2\nu_o})\tau_w]Q_2 \qquad \text{(E11)}$$

Similarly, the $Z_{-(\nu-1)}$ function follows

$$Z_{-(\nu-1)} \simeq -\frac{1}{2}\left(\frac{2}{n}\right)^{\nu-1}\frac{\Gamma(\nu)}{1-\nu} + \frac{1}{2}\left(\frac{2}{n}\right)^{1-\nu}\Gamma(1-\nu)\tau_w^{2(\nu-1)}$$

$$\simeq (1 - n\tau_w^{1-2\nu_o})\tau_w^{-2(1-\nu)}Q_2 \qquad \text{(E12)}$$

where

$$\frac{1}{2}\left(\frac{2}{n}\right)^{\nu-1}\frac{\Gamma(\nu)}{1-\nu} \simeq n[1 - 2(\varphi_o - 1)\nu_o]Q_2$$

From equation (E3b), one could directly obtain

$$C_{-(\nu-1)} \simeq \left[\frac{1}{2mn\bar{\alpha}} - n\tau_w^{2(1-\nu_o)}\right]\tau_w^{-2(1-\nu)}Q_2 \qquad \text{(E13)}$$

Through equations (E5) to (E13), K and M are reduced as given in equations (55) and (56) after several simplifications.

APPENDIX F

ASYMPTOTIC EXPANSION OF THE Z FUNCTION ($\tau_w \gg 1$)

Uniform asymptotic expansions of the modified Bessel function for large arguments (refs. 24 and 25) are

$$I_\nu(\nu\theta) \simeq \frac{1}{\sqrt{2\pi\nu}} \frac{e^{\nu\eta}}{(1+\theta^2)^{1/4}} \left[1 + O\left(\frac{1}{\nu}\right)\right] \tag{F1a}$$

$$K_\nu(\nu\theta) \simeq \sqrt{\frac{\pi}{2\nu}} \frac{e^{-\nu\eta}}{(1+\theta^2)^{1/4}} \left[1 - O\left(\frac{1}{\nu}\right)\right] \tag{F1b}$$

where

$$\eta = \sqrt{1+\theta^2} + \ln \frac{\theta}{1+\sqrt{1+\theta^2}} \tag{F1c}$$

Evaluation of $I_{\nu-k}(n\tau_w)$ and $K_{\nu-k}(n\tau_w)$

Since ν is

$$\nu = mn\bar{\alpha}\tau_w + \frac{1}{2}$$

$$n\tau_w \simeq (\nu - k)\frac{1}{m\bar{\alpha}}\left[1 + \frac{k - (1/2)}{\nu - k}\right] \tag{F2a}$$

let

$$z_o = \frac{1}{m\bar{\alpha}} \quad \text{and} \quad z = z_o\left[1 + \frac{k - (1/2)}{\nu - k}\right] \tag{F2b}$$

then

$$\sqrt{1+z^2} \approx \sqrt{1+z_o^2}\left[1 + \left(k - \frac{1}{2}\right)\frac{1}{\nu - k}\frac{z_o^2}{1+z_o^2}\right] \tag{F2c}$$

Similarly,

$$1 + \sqrt{1+z^2} \simeq \left(1 + \sqrt{1+z_o^2}\right)\left\{1 + \frac{k - (1/2)}{\nu - k}\frac{\sqrt{1+z_o^2}[z_o^2/(1+z_o^2)]}{1+\sqrt{1+z_o^2}}\right\}$$

and

$$\ln \frac{z}{1+\sqrt{1+z^2}} \simeq \left(\ln \frac{z_o}{1+\sqrt{1+z_o^2}}\right) + \frac{k-(1/2)}{\nu-k}\left(1 - \frac{z_o}{1+\sqrt{1+z_o^2}} \frac{z_o}{\sqrt{1+z_o^2}}\right) \tag{F2d}$$

From equation (F1c) it follows that

$$(\nu-k)\eta \simeq (\nu-k)\left(\sqrt{1+z_o^2} + \ln \frac{z_o}{1+\sqrt{1+z_o^2}}\right)$$

$$+ \left(k-\frac{1}{2}\right)\left(1 - \frac{1}{\sqrt{1+z_o^2}} \frac{z_o^2}{1+\sqrt{1+z_o^2}} + \frac{z_o^2}{\sqrt{1+z_o^2}}\right)$$

$$\simeq (\nu-k)\eta_o + \left(k-\frac{1}{2}\right)\mu_o \tag{F3a}$$

where

$$\left.\begin{aligned} \eta_o &= \sqrt{1+z_o^2} + \ln \frac{z_o}{1+\sqrt{1+z_o^2}} = \mu_o - \ln \beta_1 \\ \mu_o &= \sqrt{1+z_o^2} \end{aligned}\right\} \tag{F3b}$$

Therefore

$$I_{\nu-k}(n\tau_w) \simeq e^{[k-(1/2)]\mu_o} I_{\nu-k}(\nu-k)z_o \tag{F4}$$

Now, β_1 and β_2 from equations (28) can be also expressed as

$$\beta_1 = \frac{1+\mu_o}{z_o}, \qquad \beta_2 = \frac{-1+\mu_o}{z_o} \tag{F5}$$

Using equations (F4), (F1a), and the definition in (F3b), one can obtain the following asymptotic recurrence formula:

$$I_{\nu-k}(n\tau_w) \simeq \beta_1^{\,k} I_\nu(n\tau_w) \tag{F6}$$

Similarly, for $K_{\nu-k}(n\tau_w)$ as $\tau_w \to \infty$, one obtains

$$K_{\nu-k}(n\tau_w) \simeq e^{-[k-(1/2)]\mu_o} K_{\nu-k}(\nu-k)z_o \tag{F7}$$

The recurrence formula thus becomes

$$K_{\nu-k}(n\tau_w) \simeq \beta_2^{\,k} K_\nu(n\tau_w) \tag{F8}$$

Asymptotic Expansion of $C_{\nu-1}(\theta)$

As given in equation (C13a)

$$C_{\nu-1}(\theta) = \frac{1}{2}\left(\frac{2}{n}\right)^{\nu-1}\Gamma\left(\frac{1}{2}\right)\Gamma\left(\nu-\frac{1}{2}\right)\theta\left[I_{\nu-1}(n\theta)L_{\nu-2}(n\theta) - L_{\nu-1}(n\theta)I_{\nu-2}(n\theta)\right] \tag{F9}$$

The modified Struve function L_ν (ref. 25) for $\theta \gg 1$ is

$$L_\nu(n\theta) - I_{-\nu}(n\theta) \simeq \frac{1}{\pi}\sum_{k=0}^{\infty}\frac{(-1)^{k+1}\Gamma[k+(1/2)]}{\Gamma[\nu+(1/2)-k](n\theta/2)^{2k-\nu+1}} \tag{F10a}$$

$$(|\arg\theta| < \pi/2)$$

Let

$$\gamma_{k,\nu} = \frac{(-1)^{k+1}\Gamma[k+(1/2)]}{\Gamma[\nu+(1/2)-k](n\theta/2)^{2k-\nu+1}}$$

then

$$\gamma_{k,\nu} = \frac{-[k-(1/2)][\nu+(1/2)-k]}{(n\theta/2)^2}\gamma_{k-1,\nu} \tag{F10b}$$

As ν and $\theta \to \infty$, $\gamma_{k,\nu} \ll \gamma_{k-1,\nu}$; therefore, it is sufficient to take only the leading term in equation (F10a) as

$$L_\nu(n\theta) - I_{-\nu}(n\theta) \simeq \gamma_{0,\nu} = -\frac{1}{\Gamma(1/2)}\frac{(n\theta/2)^{\nu-1}}{\Gamma[\nu+(1/2)]} \tag{F11a}$$

With equation (F11a) the bracketed quantities in equation (F9) can be expressed (for simplicity, argument $n\theta$ is omitted) as

$$\left[I_{\nu-1}L_{\nu-2} - L_{\nu-1}I_{\nu-2}\right] \simeq \left[I_{\nu-1}I_{-(\nu-2)} - I_{-(\nu-1)}I_{\nu-2}\right]$$

$$-\left[\gamma_{0,\nu-1}I_{\nu-2} - \gamma_{0,\nu-2}I_{\nu-1}\right] \tag{F11b}$$

Since Wronskians (ref. 25) vanishes as $\theta \to \infty$

$$-W\left[I_{\nu-2}, I_{-(\nu-2)}\right] = \left[I_{\nu-1}I_{-(\nu-2)} - I_{-(\nu-1)}I_{\nu-2}\right]$$

$$= \frac{2}{\pi}\frac{1}{n\theta}\sin\pi(\nu - 2) \ll 1 \qquad \text{(F11c)}$$

It follows that

$$\left[I_{\nu-1}L_{\nu-2} - L_{\nu-1}I_{\nu-2}\right] \simeq \frac{1}{\Gamma(1/2)}\frac{(n\theta/2)^{\nu-2}}{\Gamma[\nu - (1/2)]}\left\{I_{\nu-2} - \left[\frac{\nu - (3/2)}{n\theta/2}\right]I_{\nu-1}\right\} \qquad \text{(F11d)}$$

If $\theta = \tau_w$ and $\tau_w \to \infty$, then, from equation (F6),

$$\left[I_{\nu-2} - \frac{\nu - (3/2)}{n\tau_w/2}\, I_{\nu-1}\right] \simeq I_\nu \qquad \text{(F11e)}$$

Finally, equation (F9), with equations (F11d) and (F11e), becomes

$$C_{\nu-1}(\tau_w) \simeq \frac{1}{n}\,\tau_w^{\nu-1}I_\nu(n\tau_w) = \frac{Z_\nu}{n\tau_w} \qquad \text{(F12)}$$

From equation (E3a) the same result is obtained for $\tau_w \ll 1$ and $\nu \gg 1$ since

$$C_{\nu-1}(\tau_w) \simeq \frac{\nu}{\nu - (1/2)}\frac{Z_\nu}{n\tau_w} \simeq \frac{Z_\nu}{n\tau_w}$$

An evaluation similar to the above procedure can be applied for $C_{-(\nu-1)}(\theta)$ except that one substitutes K_ν instead of I_ν; the results are

$$W\left[K_{\nu-1}, I_{-(\nu-1)}\right] = I_{-(\nu-1)}K_{\nu-2} + I_{-(\nu-2)}K_{\nu-1} = \frac{1}{n\theta}$$

and

$$\frac{1}{\Gamma(1/2)}\frac{(n\theta/2)^{\nu-2}}{\Gamma[\nu - (1/2)]}\left\{K_{\nu-2} + \left[\frac{\nu - (3/2)}{n\theta/2}\right]K_{\nu-1}\right\} \ll \frac{1}{n\theta} \qquad (\theta \to \infty)$$

which lead to

$$C_{-(\nu-1)}(\tau_w) \simeq \frac{1}{4}\left(\frac{2}{n}\right)^\nu \Gamma\left(\nu - \frac{1}{2}\right)\Gamma\left(\frac{1}{2}\right) \qquad \text{(F13a)}$$

This approximation can also be compared with the exact form of $\tau_w = \infty$ in integral tables (ref. 25).

$$\int_0^\infty t^\mu K_\nu(t)dt = 2^{\mu-1}\Gamma\left(\frac{\mu + \nu + 1}{2}\right)\Gamma\left(\frac{\mu - \nu + 1}{2}\right) \qquad R(\mu \pm \nu) > -1 \qquad \text{(F13b)}$$

Note that substituting $\mu = \nu$ in equation (F13b) gives the approximate formula found in equation (F13a). Note also that if $\nu \gg 1$, but $\tau_w \ll 1$, the following result is obtained after integrating equation (E1b)

$$C_{-(\nu-1)}(\tau_w) \simeq \frac{n\tau_w}{2(\nu - 1)} Z_{-\nu} \qquad \text{(F14)}$$

Further asymptotic expansion of the following functions are necessary to simplify the asymptotic evaluation of the flux function. Thus, as $\nu \to \infty$, the gamma function can be expressed as

$$\Gamma(\nu - k) \simeq \sqrt{2\pi}\, e^{-\nu} \nu^{\nu-k-(1/2)} \qquad \text{(F15a)}$$

and

$$\lim_{\nu\to\infty}\left(1 + \frac{x}{\nu}\right)^\nu \to e^x \qquad \text{(F15b)}$$

It follows that

$$Z^*_{-\nu} = \frac{1}{2}\left(\frac{2}{n}\right)^\nu \Gamma(\nu)$$

$$\simeq \sqrt{\frac{\pi e}{2\nu}}\left(\frac{2m\bar{\alpha}}{e}\tau_w\right)^\nu \qquad \text{(F16)}$$

Equation (F13) then becomes

$$C_{-(\nu-1)} \simeq \frac{(1/2)\Gamma(1/2)}{\sqrt{\nu}} Z^*_{-\nu} \qquad \text{(F17)}$$

From equation (F1a)

$$Z_\nu \simeq \frac{1}{\sqrt{2\pi\nu}} \frac{e^{-\mu_o/2}}{\sqrt{\mu_o}} \left(e^{\eta_o \tau_w}\right)^\nu$$

$$\simeq \frac{1}{\sqrt{2\pi\nu\mu_o e^{\mu_o}}} \left(\beta_2 e^{\mu_o \tau_w}\right)^\nu \qquad \text{(F18)}$$

Also from equation (F6) it is shown that

$$Z_{\nu-1} \simeq \frac{\beta_1 Z_\nu}{\tau_w} \tag{F19}$$

From equation (F1b) one obtains

$$Z_{-\nu} \simeq \sqrt{\frac{\pi}{2\nu}\frac{e^{\mu_o}}{\mu_o}}\,(\beta_1 e^{-\mu_o \tau_w})^\nu \tag{F20}$$

and from equation (F8),

$$Z_{-(\nu-1)} \simeq \frac{\beta_2 Z_{-\nu}}{\tau_w} \tag{F21}$$

With the asymptotic values derived above, the following relations hold:

$$\frac{mn\bar{\alpha}\tau_w C_{\nu-1}}{Z_\nu} \simeq \frac{1}{z_o} = \frac{1}{2}\,(1+\beta_1)(1-\beta_2) \tag{F22}$$

$$\frac{mn\bar{\alpha}\tau_w C_{-(\nu-1)}}{Z^*_{-\nu}} \simeq \frac{1}{2}\sqrt{\pi\nu} \gg 1 \tag{F23}$$

Since

$$e^{-n\tau_w} = e^{-[\nu-(1/2)]/m\bar{\alpha}} \simeq e^{z_o/2}(e^{-z_o})^\nu \tag{F24}$$

one obtains

$$e^{-n\tau_w} mn\bar{\alpha}\tau_w C_{-(\nu-1)} \simeq \frac{\pi}{4}\sqrt{2e^{1+z_o}}\left(\frac{2\tau_w}{z_o e^{1+z_o}}\right)^\nu \tag{F25}$$

Then

$$\frac{Z^*_{-\nu}}{Z_{-\nu}} \simeq \sqrt{\frac{\mu_o}{e^{\mu_o-1}}}\left(\frac{2}{1+\mu_o}\,e^{\mu_o-1}\right)^\nu \gg 1 \tag{F26}$$

since $\mu_o - 1 > 0$. Also one finds

$$\frac{e^{-n\tau_w} mn\bar{\alpha}\tau_w C_{-(\nu-1)}}{Z_{-\nu}} \simeq \frac{1}{2}\sqrt{\pi\mu_o e^{1+z_o-\mu_o}\nu}\left[\frac{2/(1+\mu_o)}{e^{1+z_o-\mu_o}}\right]^\nu \ll 1 \tag{F27}$$

since $1 + z_o - \mu_o > 0$. And

$$\frac{mn\bar{\alpha}\tau_w C_{-(\nu-1)}}{Z_{-\nu}} \simeq \frac{1}{2}\sqrt{\frac{\pi\mu_o}{e^{\mu_o-1}}}\left(\frac{2}{1+\mu_o}e^{\mu_o-1}\right)^{\nu} \gg 1 \qquad \text{(F28)}$$

From equation (F28) it is obvious now that

$$\frac{mn\bar{\alpha}\tau_w C_{-(\nu-1)}}{e^{-n\tau_w}Z_{-\nu}} \gg 1 \qquad \text{(F29)}$$

The values K_n and M_n (eqs. (61) and (62)) are readily evaluated from the asymptotic values presented above.

Calculation of Radiative Flux Function Γ

Coefficients c_1 and c_2 of the radiative flux function, Γ, can be evaluated from the previous results; thus,

$$c_1 = \frac{-k_2k_6 + k_4k_5}{\Delta}$$

$$\simeq \frac{4m(1-\beta_2)[(1/2) - R_w]Z_{-\nu} + 4m(\sqrt{\pi\nu}+1)[(1/2) - R_s]Z^*_{-\nu}}{(1+\beta_1)(\sqrt{\pi\nu}+1)Z_\nu Z^*_{-\nu}}$$

$$\simeq \frac{4m[(1/2) - R_s]}{(1+\beta_1)Z_\nu} \qquad \text{(F30a)}$$

Similarly, constant c_2 is evaluated as

$$c_2 = \frac{k_1k_6 - k_3k_5}{\Delta}$$

$$\simeq \frac{-4m(1 + \beta_1)[(1/2) - R_w]Z_\nu + (8/z_o)m[(1/2) - R_s]Z_\nu}{(1 + \beta_1)(\sqrt{\pi\nu} + 1)Z_\nu Z^*_{-\nu}}$$

$$\simeq \frac{-2m[(1 + \beta_2)/(1 + \beta_1) - 2(1 - \beta_2)R_s + 2R_w]}{(\sqrt{\pi\nu} + 1)Z^*_{-\nu}} \qquad \text{(F30b)}$$

Since the flux function is given as

$$\Gamma_\nu(\theta) = c_1Z_\nu(\theta) + c_2Z_{-\nu}(\theta) \qquad \text{(F31)}$$

it is necessary to examine the asymptotic behavior of the functions

$$\frac{Z_\nu(\theta)}{Z_\nu} \quad \text{and} \quad \frac{Z_{-\nu}(\theta)}{Z^*_{-\nu}}$$

for $1 \ll \tau \ll \tau_w$. Similar evaluation made for equation (F4) may be applied for obtaining the asymptotic form of $I_\nu(n\theta)$. Thus,

$$n\theta = n\tau_w(1 - \bar{\tau}) = \nu z_o(1 - \bar{\tau})\left(1 - \frac{1}{2\nu}\right) \qquad \text{(F32)}$$

Let $z^* = z_o(1 - \bar{\tau})$ and replace z_o in equation (F4) (with $k = 0$) by z^* so that

$$I_\nu(n\theta) \simeq e^{-(1/2)\mu^*} I_\nu(\nu z^*) \qquad \text{(F33a)}$$

where quantities pertaining to z^* are evaluated in a manner analogous to that for equations (F2c) and (F2d).

$$\mu^* = \sqrt{1 + (z^*)^2} \simeq \mu_o\left(1 - \frac{z_o^2}{1 + z_o^2}\,\bar{\tau}\right) \qquad \text{(F33b)}$$

$$\ln \frac{z^*}{1+\mu^*} \simeq \ln \beta_2 - \left(1 - \frac{\beta_2 z_o}{\mu_o}\right)\bar{\tau} = \ln \beta_2 - \frac{1}{\mu_o}\bar{\tau} \tag{F33c}$$

then

$$\eta^* \simeq (\mu_o - \ln \beta_1) - \left(\frac{z_o^2}{\mu_o} + \frac{1}{\mu_o}\right)\bar{\tau}$$

$$\simeq \eta_o - \mu_o \bar{\tau} \tag{F33d}$$

Thus, from equation (F1a) it is shown for $1 \ll \tau \ll \tau_w$ that

$$I_\nu(n\theta) \simeq \left(1 + \frac{1}{2}\frac{z_o^2}{1+z_o^2}\bar{\tau}\right) e^{-(1/2)(1/\mu_o)\bar{\tau}} e^{-\mu_o mn\bar{\alpha}\tau} I_\nu(n\tau_w)$$

$$\simeq e^{-\mu_o mn\bar{\alpha}\tau} I_\nu(n\tau_w) \tag{F34}$$

$$\frac{Z_\nu(\theta)}{Z_\nu} \simeq (1-\bar{\tau})^\nu e^{-\mu_o mn\bar{\alpha}\tau} = e^{-(1+\mu_o)mn\bar{\alpha}\tau}$$

$$\simeq e^{-n\beta_1\tau} \tag{F35}$$

Similarly, $K_\nu(n\theta)$ can be written as

$$K_\nu(n\theta) \simeq e^{\mu_o mn\bar{\alpha}\tau} K_\nu(n\tau_w) \tag{F36}$$

and so

$$\frac{Z_{-\nu}(\theta)}{Z_{-\nu}} \simeq (1-\bar{\tau})^\nu e^{\mu_o mn\bar{\alpha}\tau} \simeq e^{n\beta_2\tau} \tag{F37}$$

Therefore, from equation (F26), it becomes

$$\frac{Z_{-\nu}(\theta)}{Z^*_{-\nu}} = \frac{Z_{-\nu}(\theta)/Z_{-\nu}}{Z^*_{-\nu}/Z_{-\nu}} \simeq \mu_o^{-1/2}\left(\frac{1+\mu_o}{2}\right)^\nu e^{-n\beta_2(\tau_w-\tau)} \tag{F38}$$

For sufficiently large τ_w the value of equation (F38) is negligible compared to that of equation (F35), for example,

$$\bar{\tau} \ll \frac{1}{2}\left(\frac{z_o^2}{4 + z_o^2}\right) \tag{F39}$$

Thus, the asymptotic radiant flux function becomes

$$\Gamma_\nu(\theta) \simeq c_1 Z_\nu(\theta)$$

$$\simeq \frac{2m}{1 + \beta_1}(1 - 2R_s)e^{-n\beta_1\tau} \tag{F40}$$

APPENDIX G

CALCULATION OF RADIATIVE FLUX WITH PREHEATING INTERACTION

The energy equation in the preheating zone is, from equation (77),

$$\frac{\rho_\infty V_\infty h_s}{2\sigma T_s^4}\left(\frac{h^* - h_\infty}{h_s}\right) \approx \frac{1}{2\sigma T_s^4}(q^* - q_\infty) \tag{G1}$$

It follows that

$$\frac{h^* - h_\infty}{h_s} \simeq \lambda_a(\Gamma^* - \Gamma_\infty) \tag{G2}$$

where

$$\Gamma^* = q^*/2\pi B \tag{8a}$$

Defining Γ_{sp} as the radiative flux of the preheating zone at the shock wave and h_f as enthalpy just ahead of the shock front, one gets the relation

$$\frac{h_f - h_\infty}{h_s} \simeq \lambda_a(\Gamma_{sp} - \Gamma_\infty) \tag{87b}$$

Preheating increases the temperature behind the shock by the amount

$$\overline{T}_{sp}^{\,4} = 1 + \overline{\alpha}(\Gamma_{sp} - \Gamma_\infty) \tag{80}$$

Flux (coming from the hot shock layer) at the shock front is

$$\Gamma_{sp} = \overline{T}_{sp}^{\,4}(M_o + M_1 R_s^{\,\dagger} + M_2 R_w^{\,\dagger}) \tag{G3}$$

where $R_s^{\,\dagger} = R_s/\overline{T}_{sp}^{\,4}$ and $R_w^{\,\dagger} = R_w/\overline{T}_{sp}^{\,4}$. With equation (80) it follows that

$$\Gamma_{sp} = [1 + \overline{\alpha}(\Gamma_{sp} - \Gamma_\infty)]M_o + M_1 R_s + M_2 R_w \tag{G4}$$

The continuity of the flux function requires that (see sketch (a), main text)

$$\Gamma_{sp} = R_f - R_s \tag{G5}$$

The temperature ahead of the shock T_f is determined by

$$\bar{T}_f^4 = \bar{T}_r^4 + \bar{\alpha}_r[\Gamma_{sp} - \Gamma_\infty - (\Gamma_{sp} - \Gamma_\infty)_r] \tag{B10}$$

where $\bar{T}_r$ is the reference temperature derived from the assumption that only absorption by media is a major factor in the preheating zone (see appendix B, eqs. (B8) and (B10)). Thus, boundary fluxes of the preheating zone from equations (26) are

$$-\Gamma_{sp} = \bar{T}_f^4[M_0 + M_1R_f + M_2R_\infty]^* \tag{G6}$$

$$-\Gamma_\infty = \bar{T}_f^4[M_3 + M_4R_f + M_5R_\infty]^* \tag{G7}$$

where superscript * designates quantities in the preheating zone, and

$$R_f^* = R_f/\bar{T}_f^4$$

$$R_\infty^* = R_\infty/\bar{T}_f^4$$

It follows that

$$\Gamma_{sp} - \Gamma_\infty = -\bar{T}_f^4(M_0 - M_3)^* - (M_1 - M_4)^*R_f - (M_2 - M_5)^*R_\infty \tag{G8}$$

Now, one can solve the simultaneous equations given in equations (G3) through (G8) for $R_\infty = 0$, $R_w \approx 0$ and for given optical depths (τ_∞ and τ_w) of the preheating zone and shock layer, respectively, as

$$\Gamma_{sp} - \Gamma_\infty = \frac{-\bar{T}_g^4\left[M_0^*(1 + M_4^*) - M_3^*(1 + M_1^*) - \frac{(M_0 - M_3)^*}{1 + M_1}\right] + (M_1 - M_4)^* \frac{M_0}{1 + M_1}}{\Delta} \tag{G9}$$

where

$$\bar{T}_g^4 = \bar{T}_r^4 - \bar{\alpha}_r M_0[1 - 2E_3(\tau_\infty)]/\{1 - \bar{\alpha}M_0[1 - 2E_3(\tau_\infty)]\} \tag{G10}$$

and

$$\Delta = 1 + M_1^* - \frac{1}{1+M_1} + \bar{\alpha}_r\left[M_0^*(1+M_4^*) - M_3^*(1+M_1^*) - \frac{M_0^* - M_3^*}{1+M_1}\right] - \bar{\alpha}(M_1 - M_4)^* \frac{M_0}{1 + M_1} \tag{G11}$$

Then $\bar{T}_{sp}^4$ and $\bar{T}_f^4$ will be obtained from equations (80) and (B10), respectively. Thus, $\bar{T}_{sp}^4$ may be written in terms of known quantities as

$$\bar{T}_{sp}^{4} = \frac{(1+M_1^*) - \frac{1}{1+M_1} + \left[M_o^*(1+M_4^*) - M_3^*(1+M_1^*) - \frac{(M_o - M_3)^*}{1+M_1}\right](\bar{\alpha}_r - \bar{\alpha}\bar{T}_g^{4})}{\Delta} \tag{G12}$$

Boundary values are given by

$$R_f = -\frac{(\Gamma_{sp} - \Gamma_\infty) + \bar{T}_f^{4}(M_o^* - M_3^*)}{M_1^* - M_4^*} \tag{G13}$$

$$R_s = \frac{R_f - [1 + \bar{\alpha}(\Gamma_{sp} - \Gamma_\infty)]M_o}{1 + M_1} \tag{G14}$$

The terms Γ_{sp} and Γ_∞ can be obtained from equations (G6) and (G7) or are simply

$$\Gamma_{sp} = R_f - R_s \tag{G15}$$

$$\Gamma_\infty = \Gamma_{sp} - (\Gamma_{sp} - \Gamma_\infty) \tag{G16}$$

From equations (G15) and (G16), the radiative leakage parameter, which now includes emission effect, becomes

$$\Phi_\infty = \Gamma_\infty/\Gamma_{sp} \tag{G17}$$

Note that if the temperature jump due to preheating is not negligible ($\Gamma_{sp} - \Gamma_s \neq 0$), the following modifications are made to calculate the enthalpy and temperature distribution through the shock layer. Quantities K_5 and K_6 in equation (38a) are replaced by

$$K_5 = 2m\left[\frac{1}{2}(1 + \bar{\alpha}\Delta\Gamma_s) - R_s\right] - 2me^{-n\tau_w}\left[\frac{1}{2}(1 + \bar{\alpha}\Delta\Gamma_s) - R_w\right] \tag{G18}$$

$$K_6 = -2m\left[\frac{1}{2}(1 + \bar{\alpha}\Delta\Gamma_s) - R_w\right] + 2me^{-n\tau_w}\left[\frac{1}{2}(1 + \bar{\alpha}\Delta\Gamma_s) - R_s\right] \tag{G19}$$

where $\Delta\Gamma_s = \Gamma_{sp} - \Gamma_\infty$. However, the same result will be obtained, as one can see directly from the last equation, if the boundary values R_s and R_w are divided by $\bar{T}_{sp}^{4}$. Thus, from equation (G3), we define,

$$R_s^{\dagger} \equiv \frac{R_s}{\bar{T}_{sp}^{4}} = \frac{R_s}{1 + \bar{\alpha}\Delta\Gamma_s} \tag{G20}$$

$$R_w^{\dagger} \equiv \frac{R_w}{\overline{T}_{sp}^{\,4}} = \frac{R_w}{1 + \overline{\alpha}\Delta\Gamma_s} \tag{G21}$$

and the thermal function $(F_{sp} - F)^{\dagger}$ as given by equation (88a). The enthalpy and temperature distribution given as equations (89) and (90) will yield results identical to those derived from equations (G18) and (G19) since all other K in equation (38) are constants for given $\overline{\alpha}$ (constant) and τ_w.

APPENDIX H

CALCULATION OF RADIATIVE FLUX IN INJECTION AND ABLATION LAYERS

The general solution of radiative heat transfer for the two-layer problem, shock and injection layers, for example, has been presented in appendix A. The details of the analysis for both absorption and emission of injected gases on radiative heat to the wall is considered here. Since the characteristics of absorption coefficients for injected or ablated gases are not yet well known, the absorption coefficients simply appear in this analysis as a parameter, $(\rho\kappa)_b$, which is independent of temperature.

Injection Layer

For radiative transfer with gas injection from the body surface, injection rate, f_w, is an arbitrary parameter and is thus independent of the heating rate at the wall. For this case, the analysis of radiative heat transfer is straightforward.

Let flight conditions be fixed and assume the optical thickness τ_w (or τ_w^I) in the shock layer to remain unchanged during injection since the shock-layer structure is relatively insensitive to the presence of an injection layer. Note that assuming a given value of τ_w is equivalent to assigning a given body radius (see eqs. (74b) and (76a)). The following outline illustrates the calculation procedure:

(a) Assign (τ_w and $\bar{\alpha}$) in both regions: Region I (shock layer); for a given body radius (and flight condition) one can find τ_w and $\bar{\alpha}$. Region II (injection layer); optical thickness, τ_{wb}, is assumed. The injection rate, f_w, is also assumed, and one finds $\bar{\alpha}_b$ from equation (99).

(b) Calculate R_w^I and R_w^{II} from equations (A14) and (A15).

(c) Calculate the absorption coefficient, which corresponds to quantities $(\tau_w, \bar{\alpha}, R_s, R_w)^{II}$, by equations (74b) and (95b):

$$\frac{(\rho\kappa)_b}{(\rho\kappa)_s} = \frac{(\rho\kappa)_b L_{bo}}{(\rho\kappa)_s k_s \sqrt{\frac{\rho_\infty}{\rho_s}\frac{M_\infty}{M_b}}\, f_w R} \tag{H1}$$

where

$$(\rho\kappa)_b L_{bo} = \tau_{wb} \int_0^1 (\rho/\rho_w)^{1/2}\, d\bar{\tau} \tag{74b}$$

(d) Calculate Γ_{wb} and Φ_{wb} from equations (A17) and (91).

By repeating procedures (a) through (d) for other values of τ_{wb} and f_w, we can obtain radiative blockage function Φ_{wb} as a function of the injection rate with the absorption coefficient ratio $(\rho\kappa)_b/(\rho\kappa)_s$ as the parameter for a given body radius.

It is interesting to note that Φ_w has nearly a single correlation curve as presented in figure 10(a).

Ablation Layer

For an ablating surface, the ablation rate, f_w, is coupled with radiative heat at the wall Γ_{wb}. Thus, some simple algebraic iteration is required to solve equation (98). Using the approximation given by equation (92), one can calculate on initial input value of $\bar{\alpha}_b$, from equations (98) and (99), by

$$\bar{\alpha}_b \simeq \frac{\bar{T}_w^4 \left(\frac{\partial \bar{T}^4}{\partial \bar{h}}\right)_w}{\frac{h_s}{\zeta}\Gamma_{wo}} 2E_3(\tau_{wb}) \tag{H2}$$

for given τ_{wb}. Similar procedures (as outlined in the previous section) are then used to calculate R_w^I, R_w^{II}, and Γ_{wb}. This Γ_{wb} provides a new ablation rate, f_w, and thus, previous calculations are repeated until the value of f_w converges. Only two or three iterations are necessary for good convergence. Even the results obtained by using equation (H2) as an initial input show sufficient accuracy. With this ablation rate one can compute the absorption coefficient ratio from equation (H1). Thermodynamic properties of carbon are obtained from reference 36.

APPENDIX I

EQUILIBRIUM AIR PROPERTIES

Thermodynamic charts are presented for flight speeds to 30 km/sec in figure 13. These charts give the pressure and temperature behind and the density ratio across the normal shock wave, and can be used to obtain reference properties for the present solutions. These properties were computed from the thermodynamic charts of references 34 and 35.

Radiative properties for equilibrium air are presented in figure 14. Figure 14(a) presents $E_t/2$, one-half the emission rate per unit volume, for optically thin air. This chart was prepared by combining the calculations of reference 37 for low temperature and reference 38 for higher temperatures. Figure 14(b) presents Planck mean absorption coefficients from the same references used in the present analysis. The relation between emission rate and absorption coefficients is $E_t = 4\rho_s \kappa_s \sigma T_s^4$. The absorption coefficients for equilibrium air are not well established over the whole temperature range.

REFERENCES

1. Allen, H. J.: Hypersonic Aerodynamic Problems of the Future. AGARDograph 68, Pergamon Press, Oxford, 1963, pp. 1-41.

2. Rose, P. H.: Future Problems in Re-entry Physics. Proceedings of Second Manned Space Flight Meeting, AIAA-NASA, New York, April 1963, AIAA, New York, 1963, pp. 279-294.

3. Riddell, Frederick R.; and Winkler, Howard B.: Meteorites and Re-Entry of Space Vehicles at Meteor Velocities. ARS J., vol. 32, no. 10, Oct. 1962, pp. 1523-1530.

4. Yoshikawa, Kenneth K.; and Chapman, Dean R.: Radiative Heat Transfer and Absorption Behind a Hypersonic Normal Shock Wave. NASA TN D-1424, 1962.

5. Goulard, Robert: Preliminary Estimates of Radiative Transfer Effects on Detached Shock Layers. AIAA J., vol. 2, no. 3, March 1964, pp. 494-502.

6. Hanley, G. M.; and Korkan, K. D.: Approximate Inviscid, Nonadiabatic Stagnation Region Flow Field Solution. AIAA J., vol. 3, no. 8, Aug. 1965, p. 1537.

7. Howe, John T.; and Viegas, John R.: Solutions of the Ionized Radiating Shock Layer Including Reabsorption and Foreign Species Effects and Stagnation Region Heat Transfer. NASA TR R-159, 1963.

8. Wilson, K. H.; and Hoshizaki, H.: Inviscid, Nonadiabatic Flow About Blunt Bodies. AIAA J., vol. 3, no. 1, Jan. 1965, pp. 67-74.

9. Kourganoff, V.: Basic Methods in Transfer Problems. Clarendon Press, Oxford, 1952.

10. Krook, Max: On the Solution of Equation of Transfer. I. Astrophys. J., vol. 122, no. 3, Nov. 1955, pp. 488-497.

11. Kondo, J.: Radiation and Dissociation in a Hypersonic Stagnation Point Flow. Paper presented at the Joint Meeting of Phys. Soc. Japan and Am. Phys. Soc., Honolulu, Sept. 1965.

12. Wang, K. C.: Radiating Shock Layer. Martin RR-67, June 1965.

13. Thomas, P. D.: The Transparency Assumption in Hypersonic Radiative Gasdynamics. AIAA J., vol. 3, no. 8, Aug. 1965, pp. 1401-1407.

14. Zel'dovich, Ia. B.: Shock Waves of Large Amplitude in Air. Soviet Phys. JETP, vol. 5, no. 5, Dec. 1, 1957, pp. 919-927.

15. Raizer, Iu. P.: On the Structure of the Front of Strong Shock Wave in Gases. Soviet Phys. JETP, vol. 5, no. 6, Dec. 15, 1957, pp. 1242-1248.

16. Klimishin, I. A.: Determination of Build-Up of Radiation Intensity Prior to the Emergence of a Shock Wave at the Surface of a Star. Soviet Astron.-AJ, vol. 6, no. 6, May-June 1963, pp. 782-783.

17. Heaslet, Max. A.; and Baldwin, Barrett S.: Predictions of the Structure of Radiation-Resisted Shock Wave. Phys. Fluids, vol. 6, no. 6, June 1963, pp. 781-791.

18. Nemchinov, I. V.; and Tsikulin, M. A.: Evaluation of Heat Transfer by Radiation for Large Meteors Moving at Great Velocity in the Atmosphere. Geomagnetics and Aeronomy, vol. 5, 1965, pp. 512-520.

19. Cresci, Robert J.; and Libby, Paul A.: The Downstream Influence of Mass Transfer at the Nose of a Slender Cone. J. Aerospace Sci., vol. 29, no. 7, July 1962, pp. 815-826.

20. Katzen, Elliott D.; and Kaattari, George E.: Inviscid Hypersonic Flow Around Blunt Bodies. AIAA J., vol. 3, no. 7, July 1965, pp. 1230-1237.

21. Heaslet, Max. A.; and Fuller, Franklyn B.: Approximate Predictions of the Transport of Thermal Radiation Through an Absorbing Plane Layer. NASA TN D-2515, 1964.

22. Placzek, G.: The Function $E_n(x) = \int_1^\infty e^{-xu} u^{-n} du$. Rep. MT-1, Natl. Res. Council of Canada, Div. of Atomic Energy, Dec. 2, 1946.

23. Chin, Jin H.; and Hearne, L. F.: Shock-Layer Radiation for Sphere-Cones With Radiative Decay. AIAA J., vol. 2, no. 7, July 1964, pp. 1345-1346.

24. McLachlan, N. W.: Bessel Functions for Engineers. Clarendon Press, Oxford, First ed., 1934.

25. Abramowitz, M.; and Stegun, I. A., eds.: Handbook of Mathematical Functions With Formulas, Graphs, and Mathematical Tables. Natl. Bur. Std., Applied Math., Series 55, Washington, G.P.O., 1964.

26. Viegas, John R.; and Howe, John T.: Thermodynamic and Transport Property Correlation Formulas for Equilibrium Air From 1,000° K to 15,000° K. NASA TN D-1429, 1962.

27. Hayes, W. D.; and Probstein, R. F.: Hypersonic Flow Theory. Applied Mathematics and Mechanics, vol. 5, New York, Academic Press, 1959, p. 158.

28. Telenin, G. F.; and Tinyakov, G. P.: Investigation of Supersonic Flow About a Sphere of Air and Carbon Dioxide in Thermochemical Equilibrium. Soviet Phys-Doklady, vol. 9, no. 11, May 1965, pp. 954-957.

29. Yoshikawa, K. K.: Linearized Theory of Heat Transfer in Hypersonic Flight. Paper presented at Fifth National Congress of Applied Mech., June 1966.

30. Romeo, David J.; and Sterrett, James R.: Flow Field for Sonic Jet Exhausting Counter to a Hypersonic Mainstream. AIAA J., vol. 3, no. 3, March 1965, pp. 544-546.

31. Kaattari, George E.: The Effect of Simulated Ablation-Gas Injection on the Shock Layer of Blunt Bodies at Mach Numbers of 3 and 5. NASA TN D-2954, 1965.

32. Matting, Fred W.: General Solution of the Laminar Compressible Boundary Layer in the Stagnation Region of Blunt Bodies in Axisymmetric Flow. NASA TN D-2234, 1964.

33. Goulard, R.: The Coupling of Radiation and Convection in Detached Shock Layers. J. Quant. Spectr. Radiative Transfer 1, no. 3/4, Dec. 1961, pp. 249-257.

34. Moeckel, W. E.; and Weston, K. C.: Composition and Thermodynamic Properties of Air in Chemical Equilibrium. NASA TN D-4265, 1958.

35. Fenter, F. W.: Thermodynamic Properties of High Temperature Air. L. T. V. Rep. RE-IR-14, 1961.

36. Krieger, F. J.: The Thermodynamics of the Graphite-Carbon Vapor System. Rand Corp. RM-3326-PR, Sept. 1962.

37. Kivel, B.; and Bailey, K.: Tables of Radiation From High Temperature Air. Avco Rep. 21, 1957.

38. Armstrong, B. H.: Mean Absorption Coefficients of Air, Nitrogen, and Oxygen From 22,000° to 220,000°. Lockheed Aircraft Corp. LMSD-49759.

TABLE I.- EXPONENTIAL CONSTANTS, n

τ_w	n	τ_w	n
0	2.000	.40	1.736
.002	1.990	.50	1.709
.004	1.986	.60	1.686
.006	1.982	.70	1.667
.008	1.978	.80	1.651
.010	1.974	.90	1.636
.012	1.970	1.00	1.623
.014	1.966	2.00	1.548
.016	1.963	3.00	1.519
.018	1.959	4.00	1.507
.020	1.956	5.00	1.503
.040	1.929	6.00	1.501
.060	1.907	7.00	1.500
.080	1.889	8.00	1.500
.10	1.873	9.00	1.500
.20	1.812	10.00	1.500
.30	1.769	∞	1.500

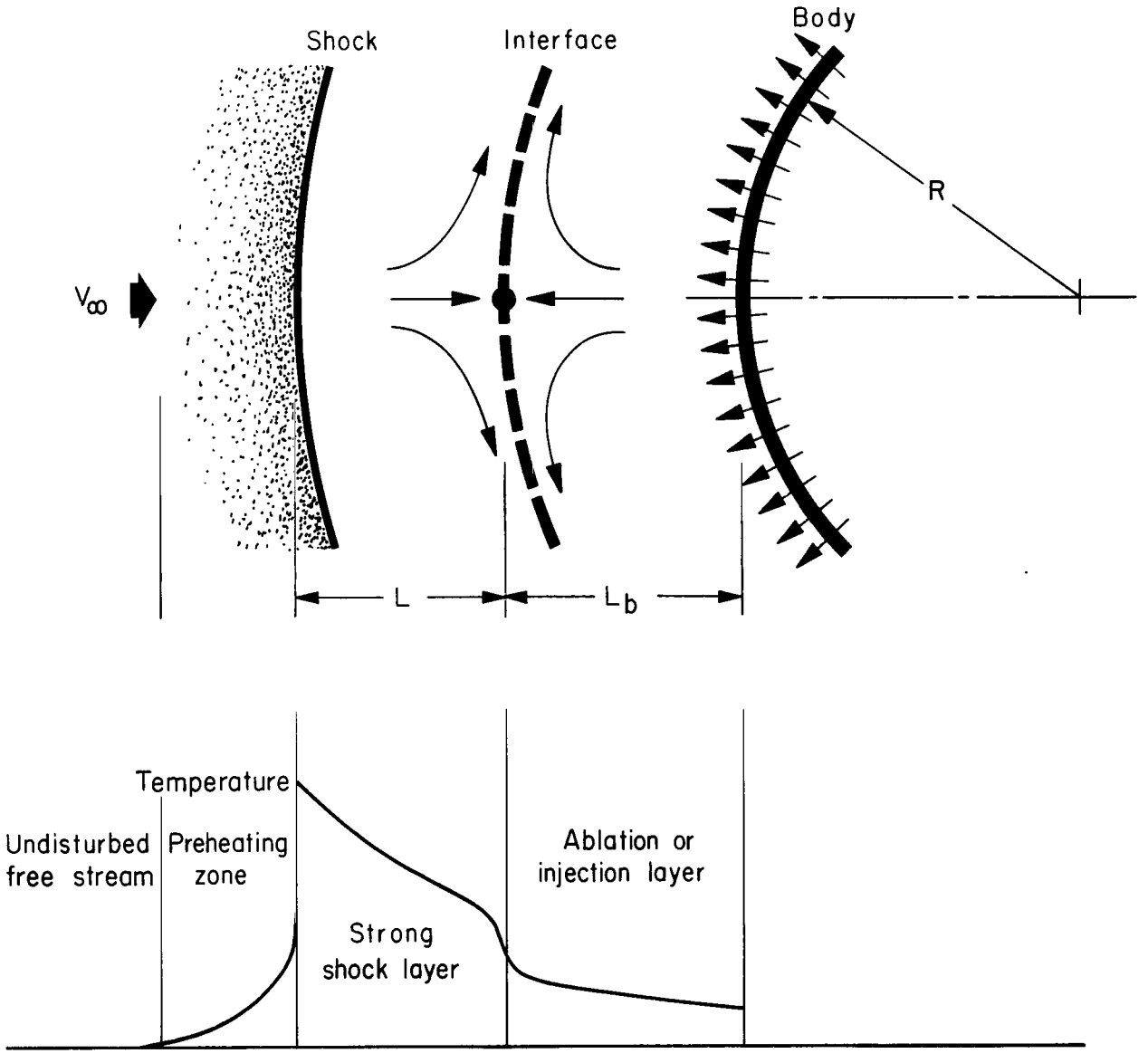

(a) Geometry of flow.

Figure 1.- Nonadiabatic flow model.

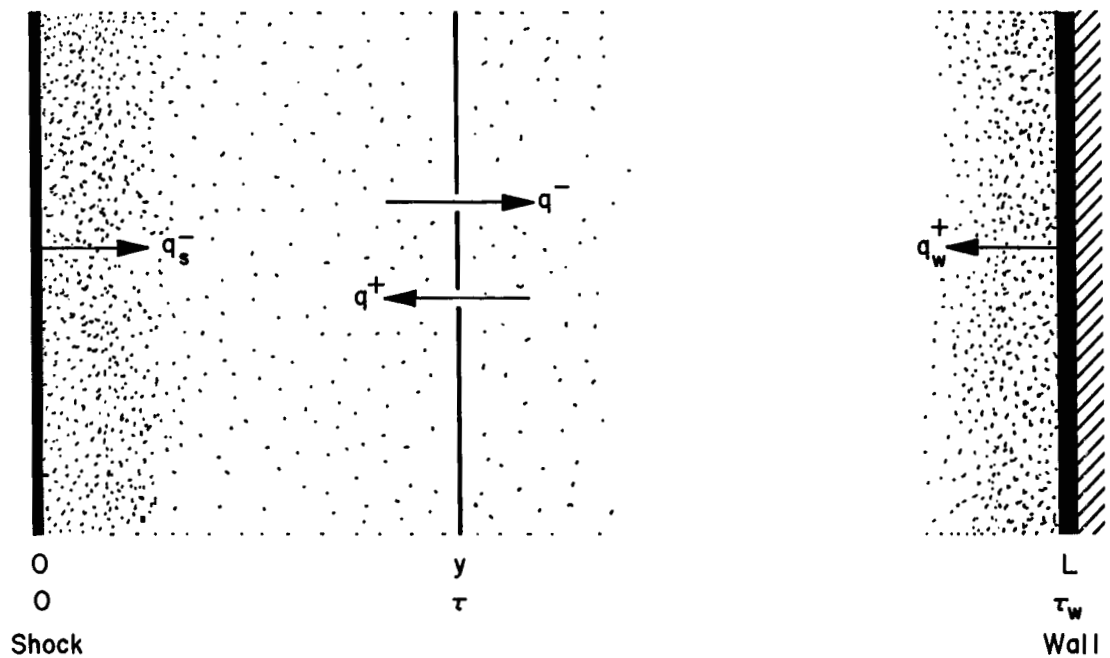

(b) Nomenclature.

Figure 1.- Concluded.

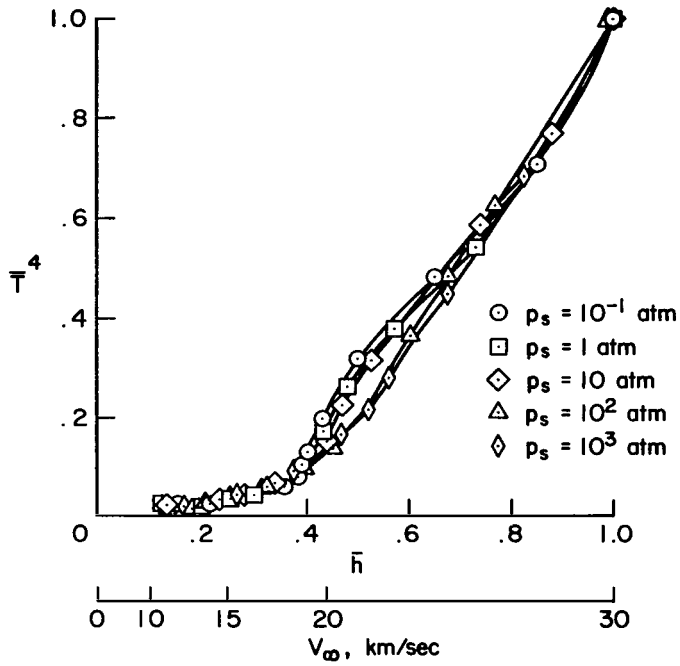

(a) Reference speed, V_∞ = 30 km/sec.

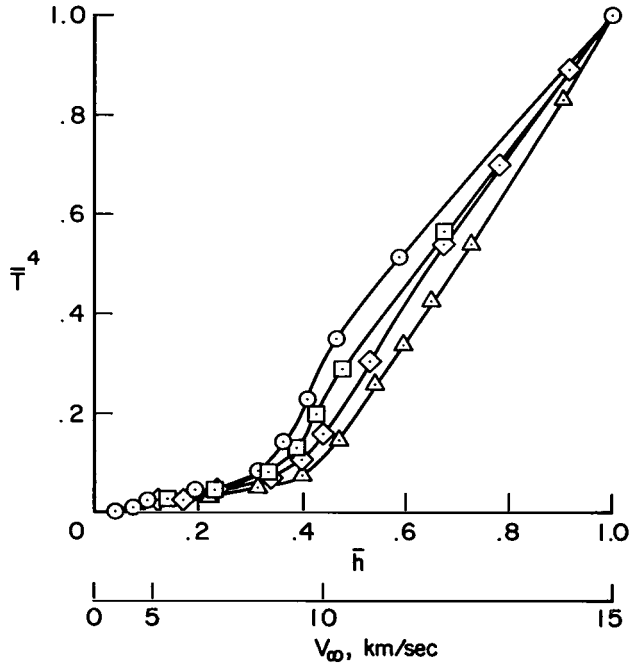

(b) Reference speed, V_∞ = 15 km/sec.

Figure 2.- Relationship between $\bar{T}^4$ and enthalpy.

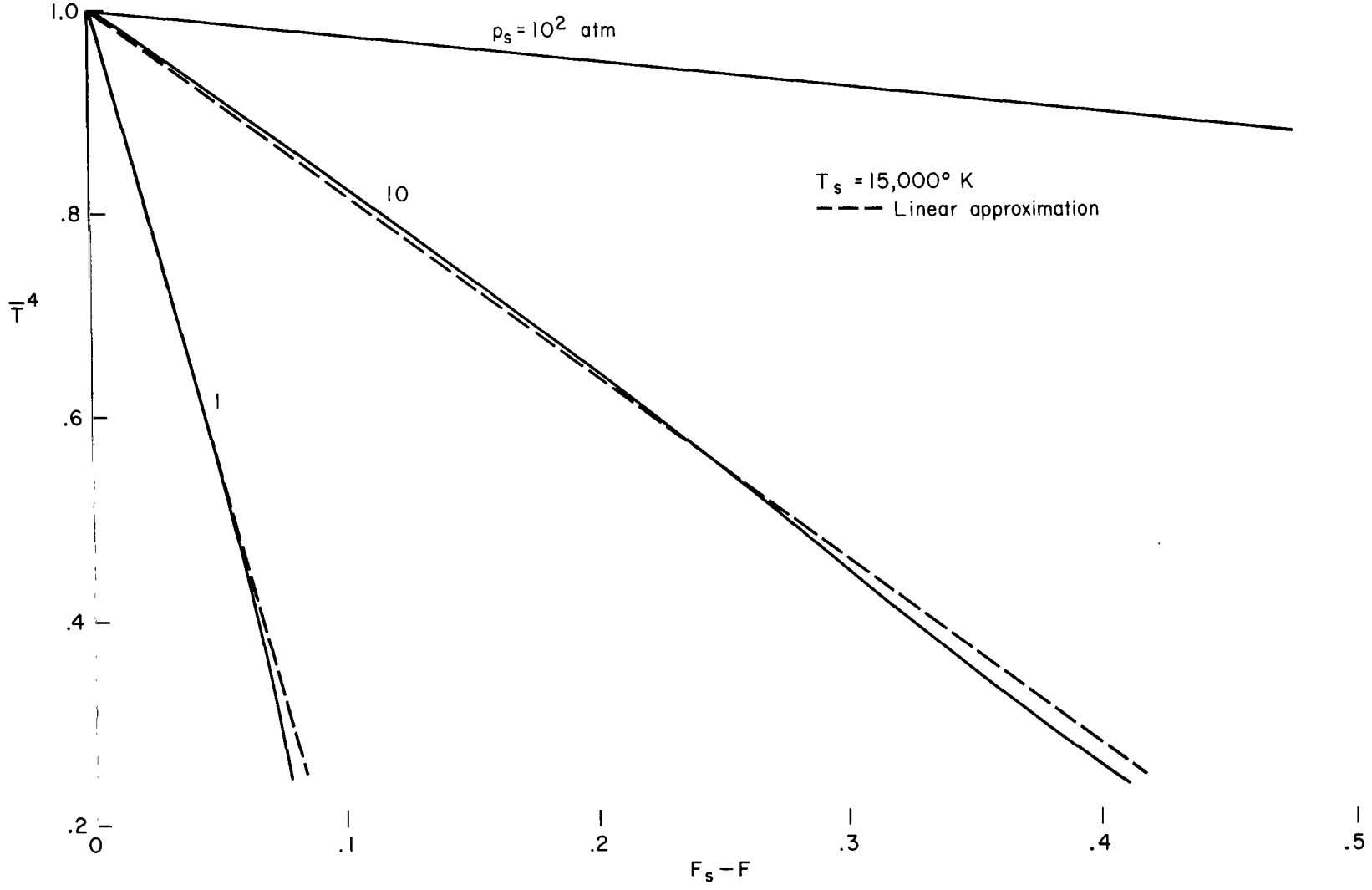

(c) Reference T_s = 15,000° K.

Figure 2.- Concluded.

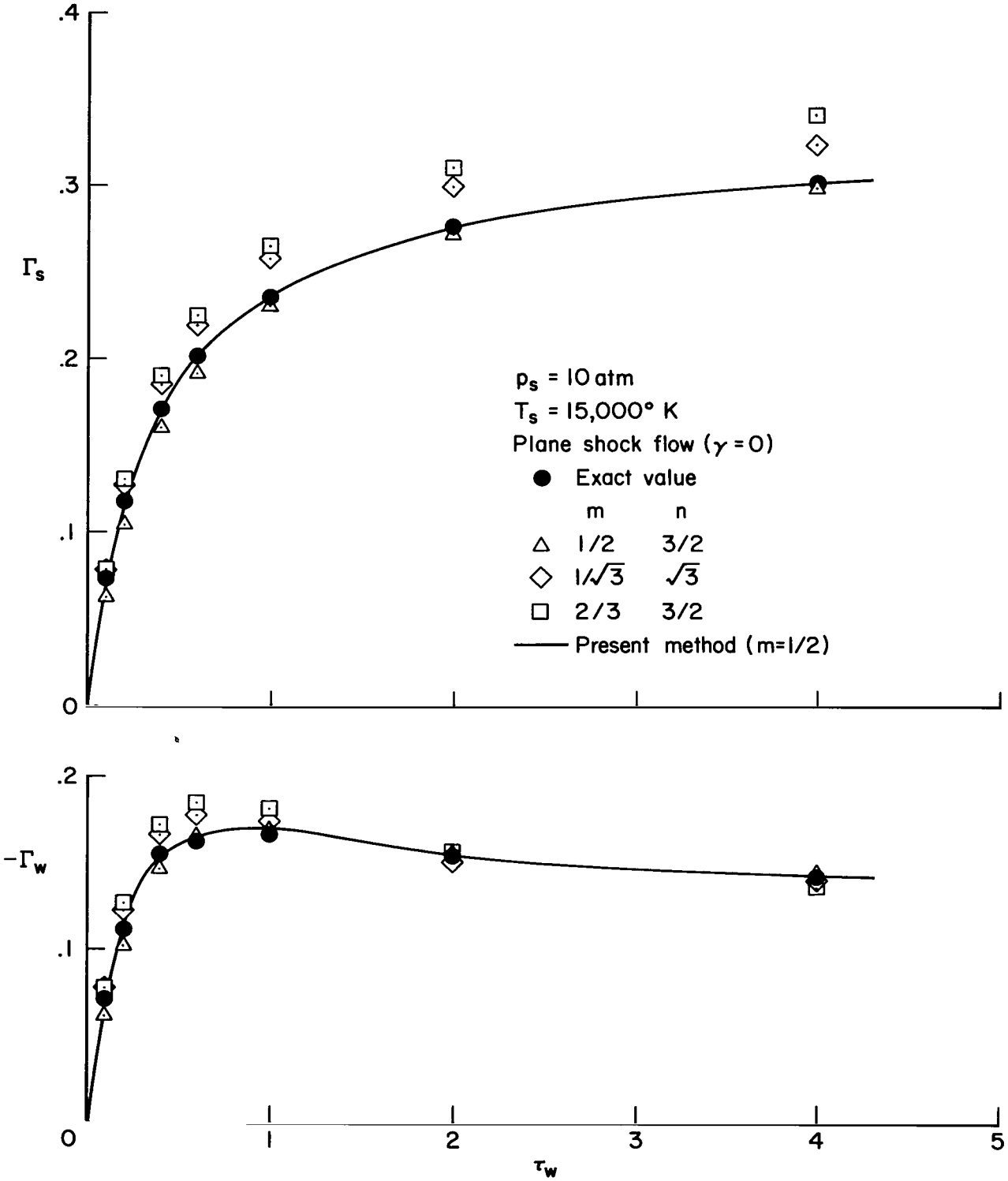

(a) Radiative heat fluxes for plane shock flow.

Figure 3.- Comparison of exact and approximate solutions.

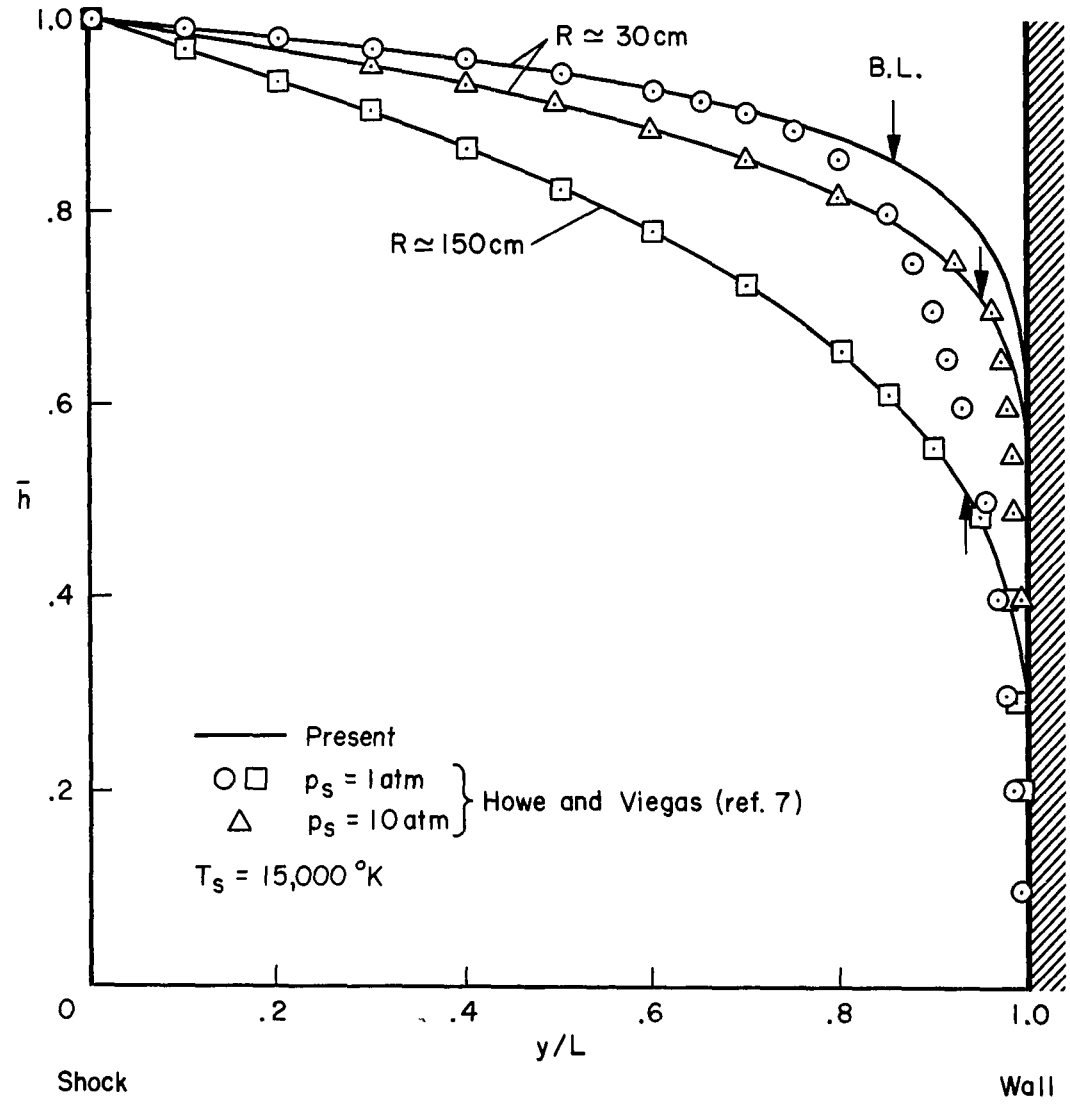

(b) Enthalpy distribution in stagnation flow.

Figure 3.- Continued.

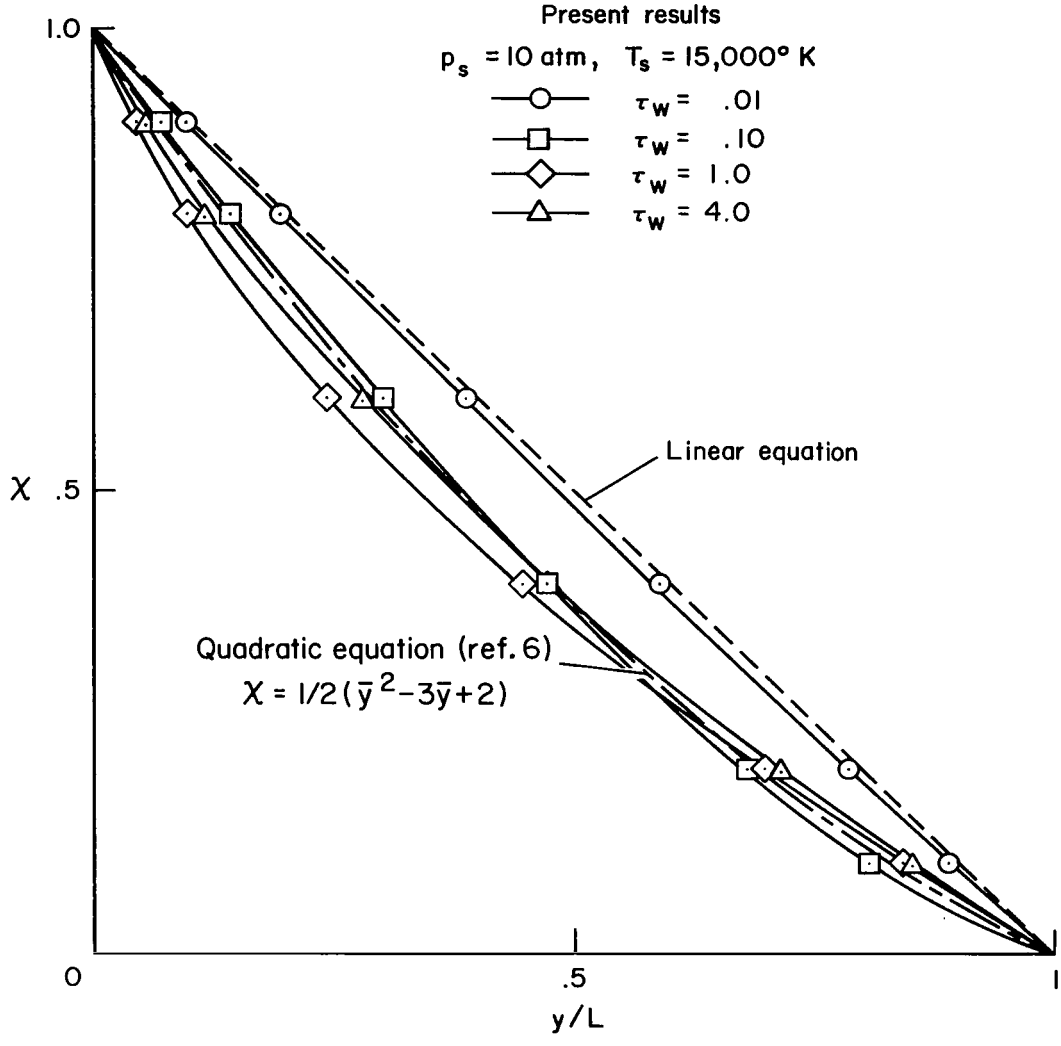

(c) Mass-flow distribution.

Figure 3.- Concluded.

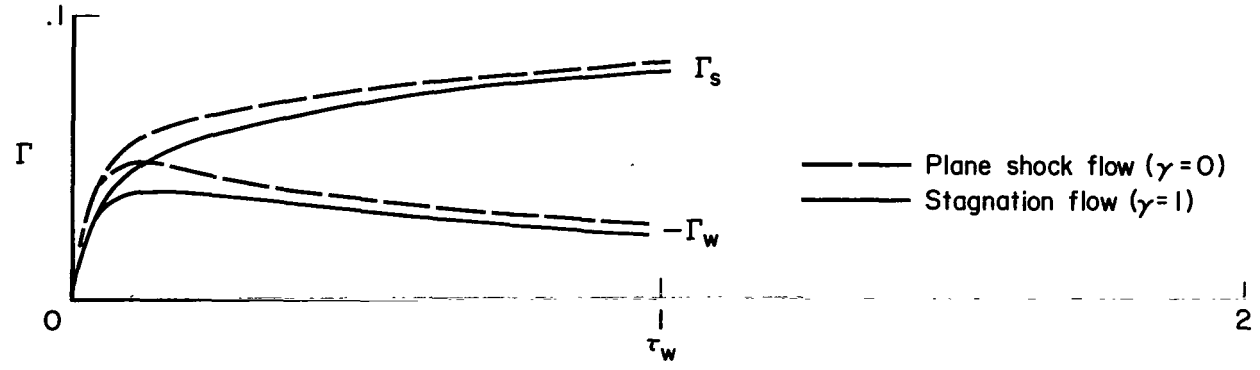

(a) p_s = 1 atm, T_s = 15,000° K

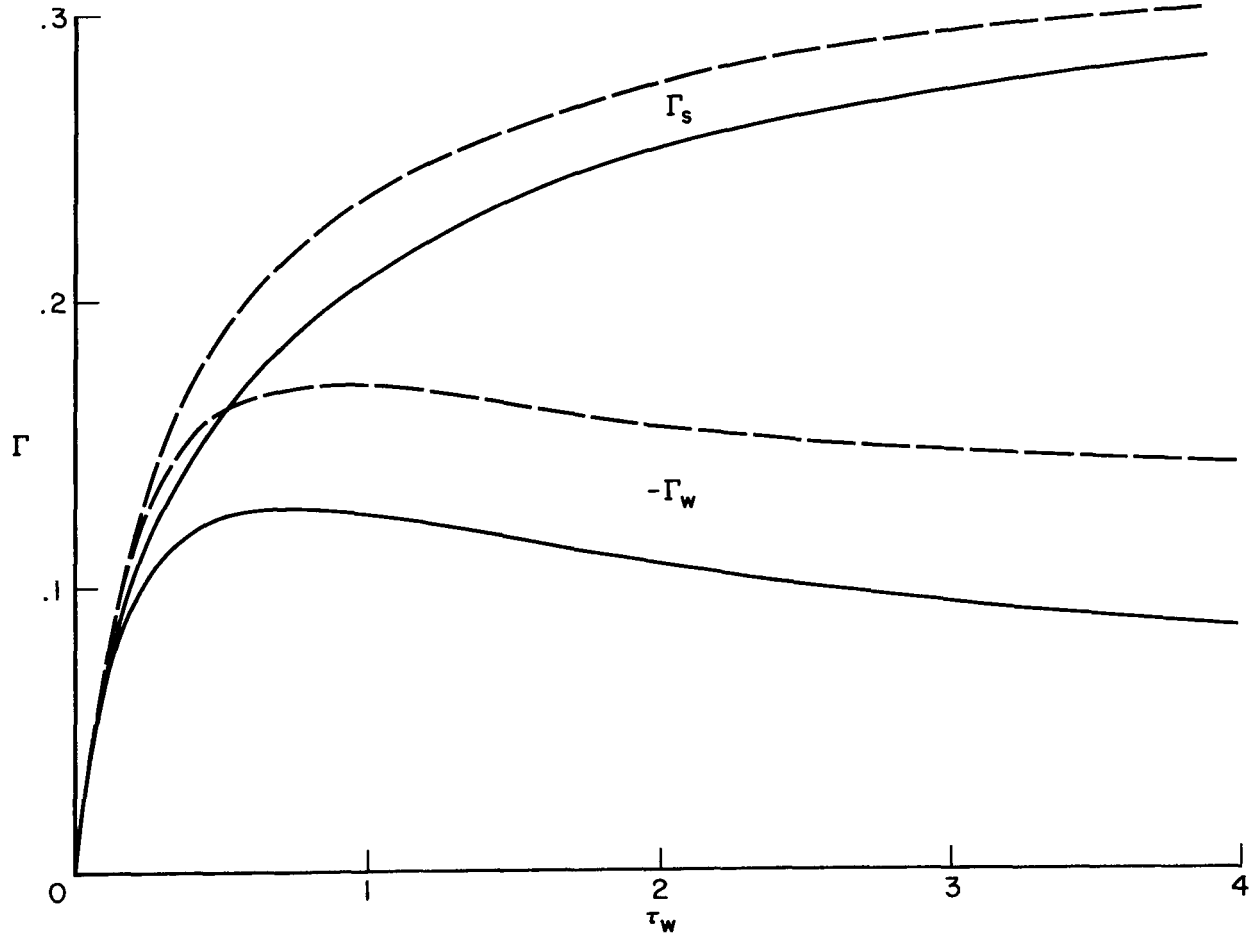

(b) p_s = 10 atm, T_s = 15,000° K

Figure 4.- Radiative heat fluxes at the shock and at the wall.

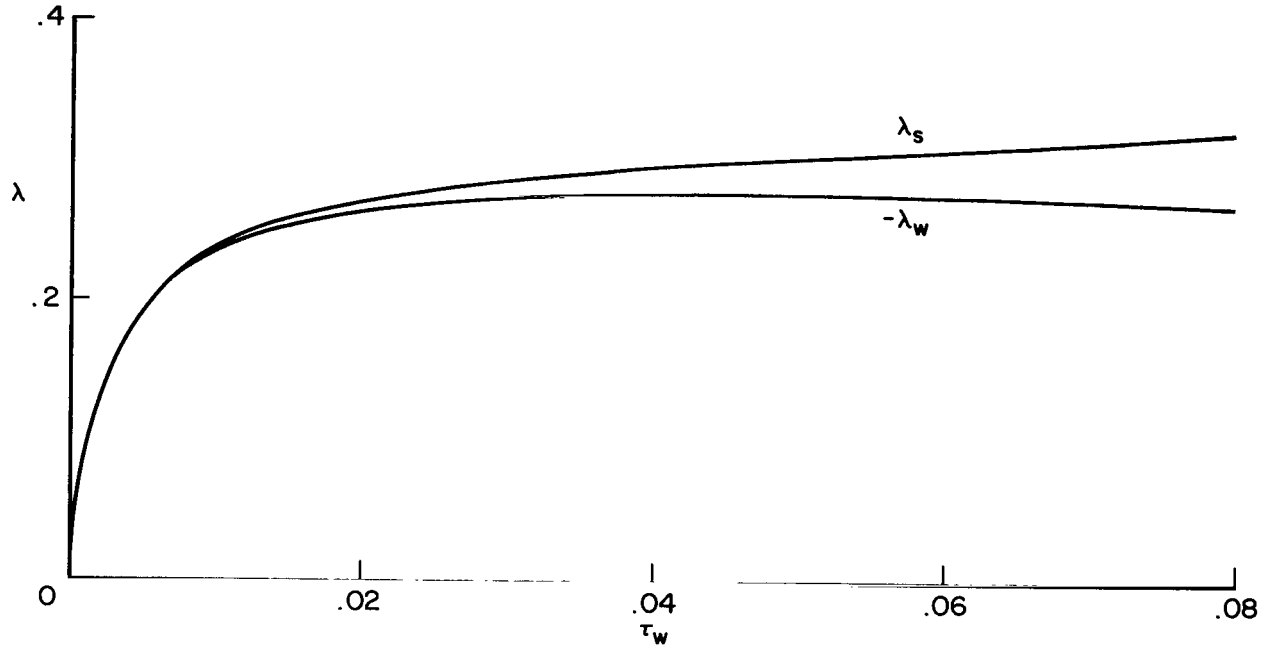

(a) $V_\infty \simeq 30$ km/sec, $H \simeq 67$ km.

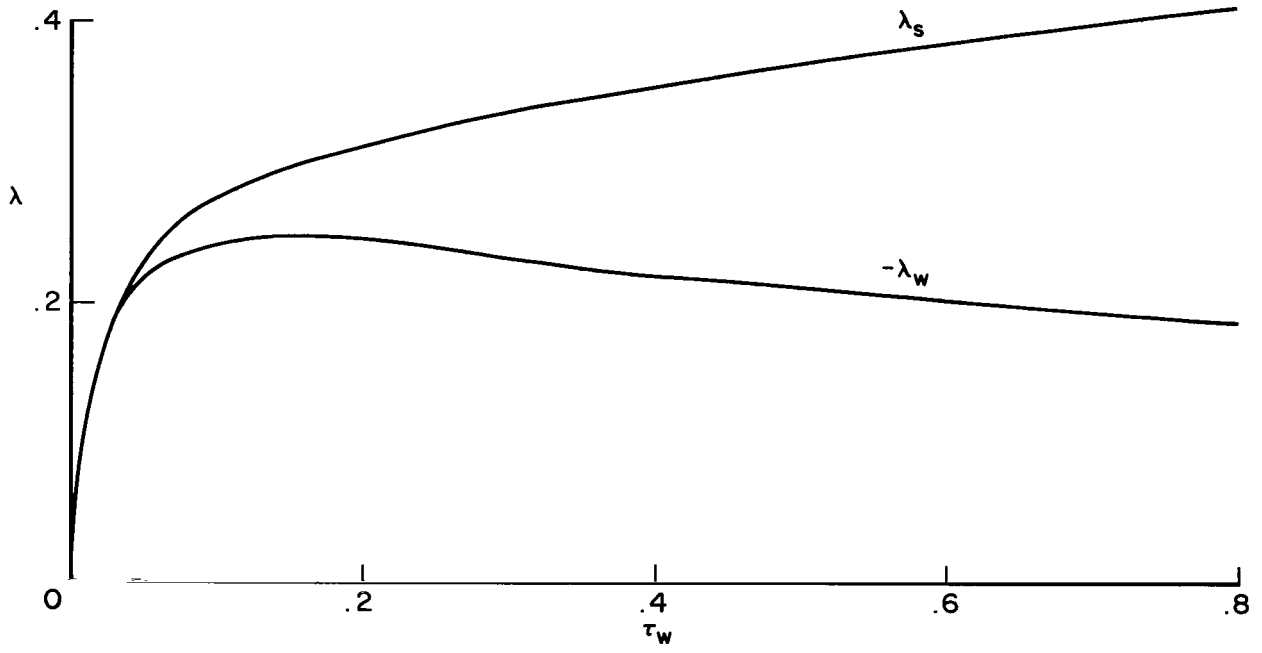

(b) $V_\infty \simeq 30$ km/sec, $H \simeq 49$ km.

Figure 5.- Radiative heat at the shock and at the wall ($\gamma = 1$).

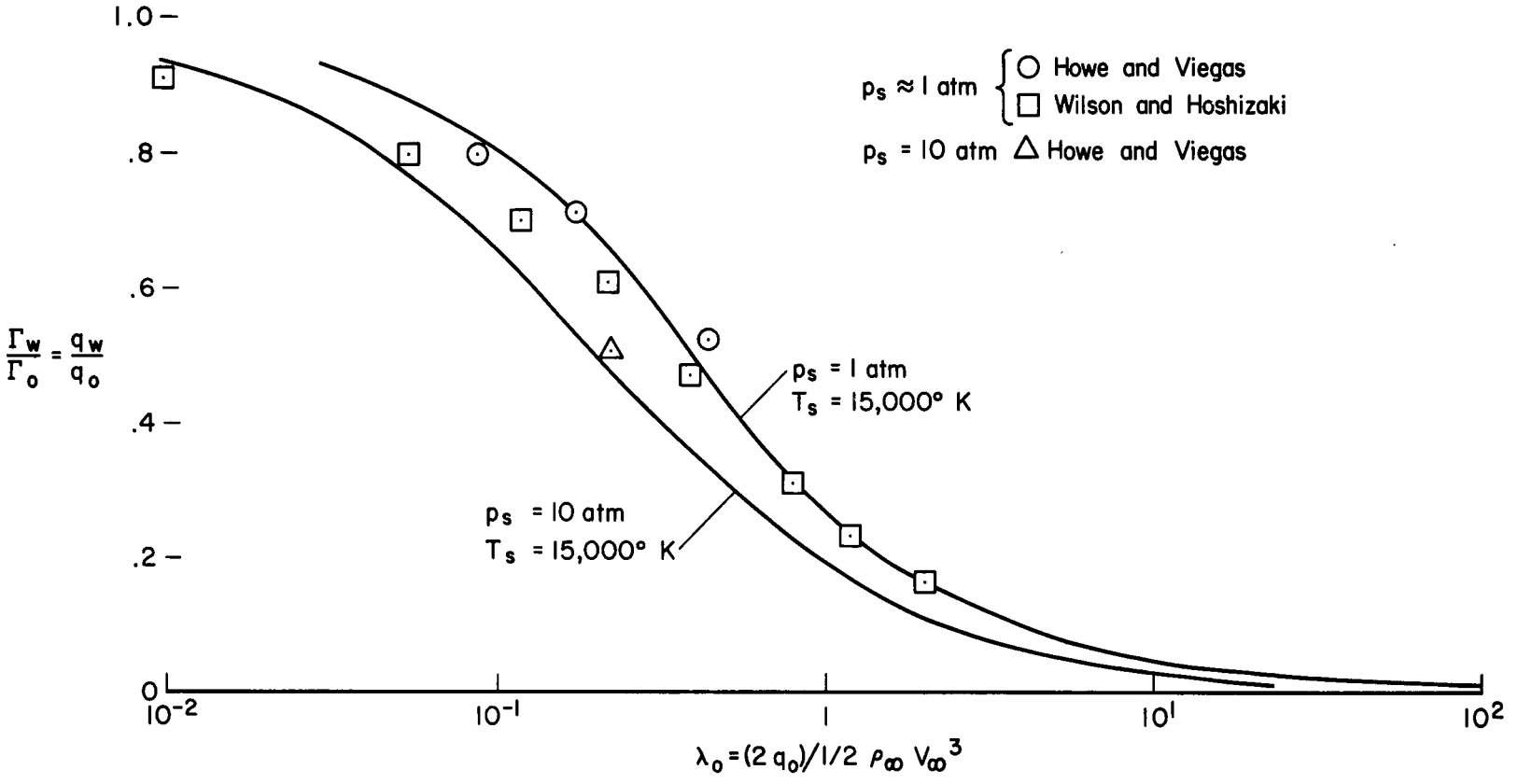

(c) Effect of nonadiabatic flow on radiative heat at the wall.

Figure 4.- Concluded.

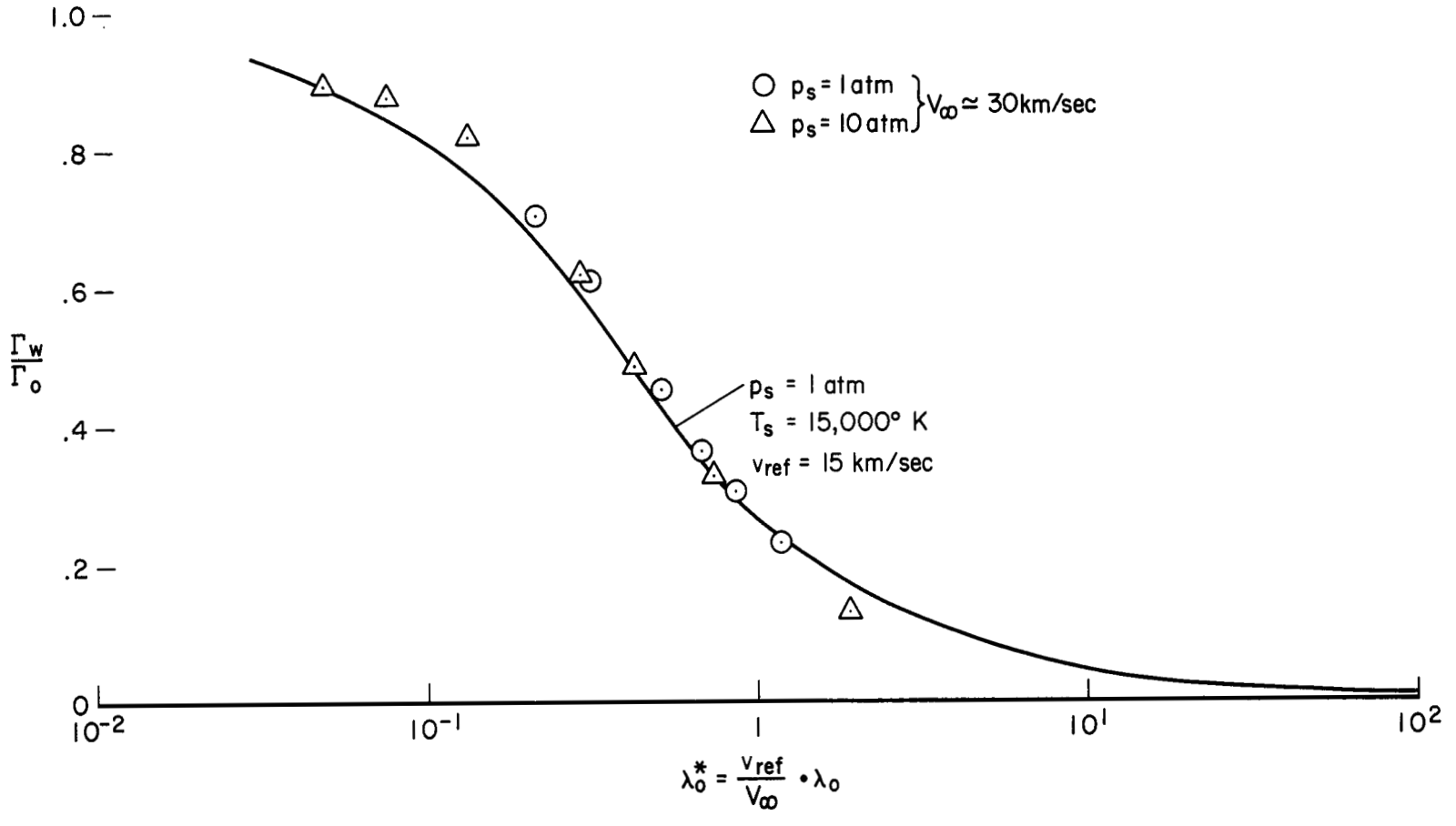

(c) Effect of nonadiabatic flow on radiative heat at the wall.

Figure 5.- Concluded.

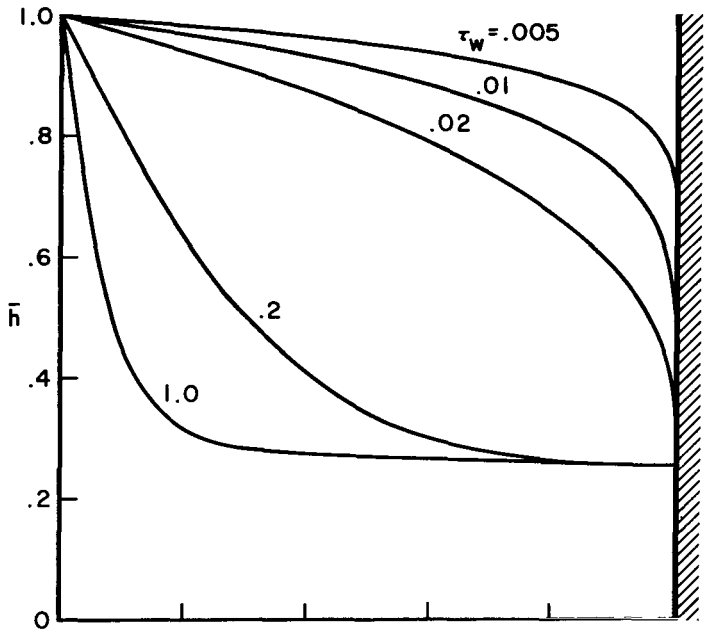

(a) p_s = 1 atm, T_s = 15,000° K

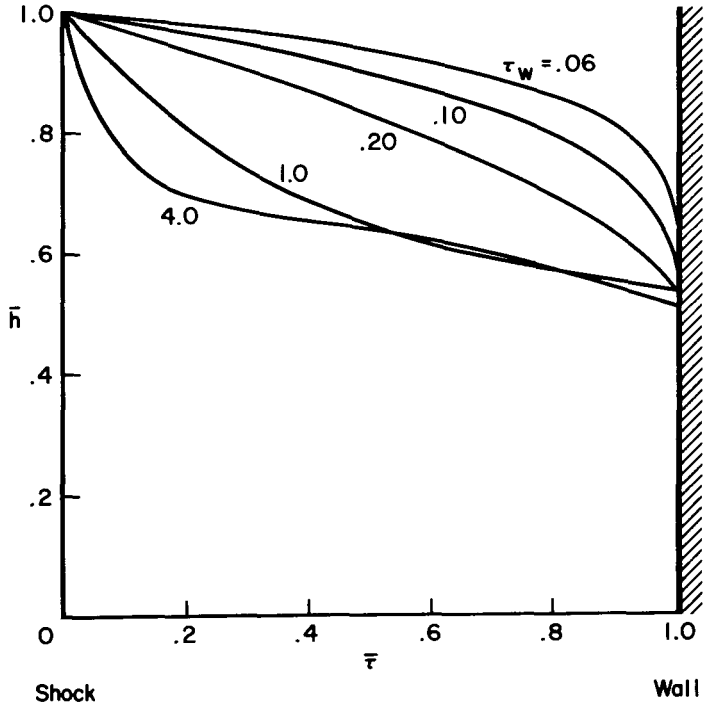

(b) p_s = 10 atm, T_s = 15,000° K

Figure 6.- Enthalpy distribution as a function of optical thickness (γ = 1).

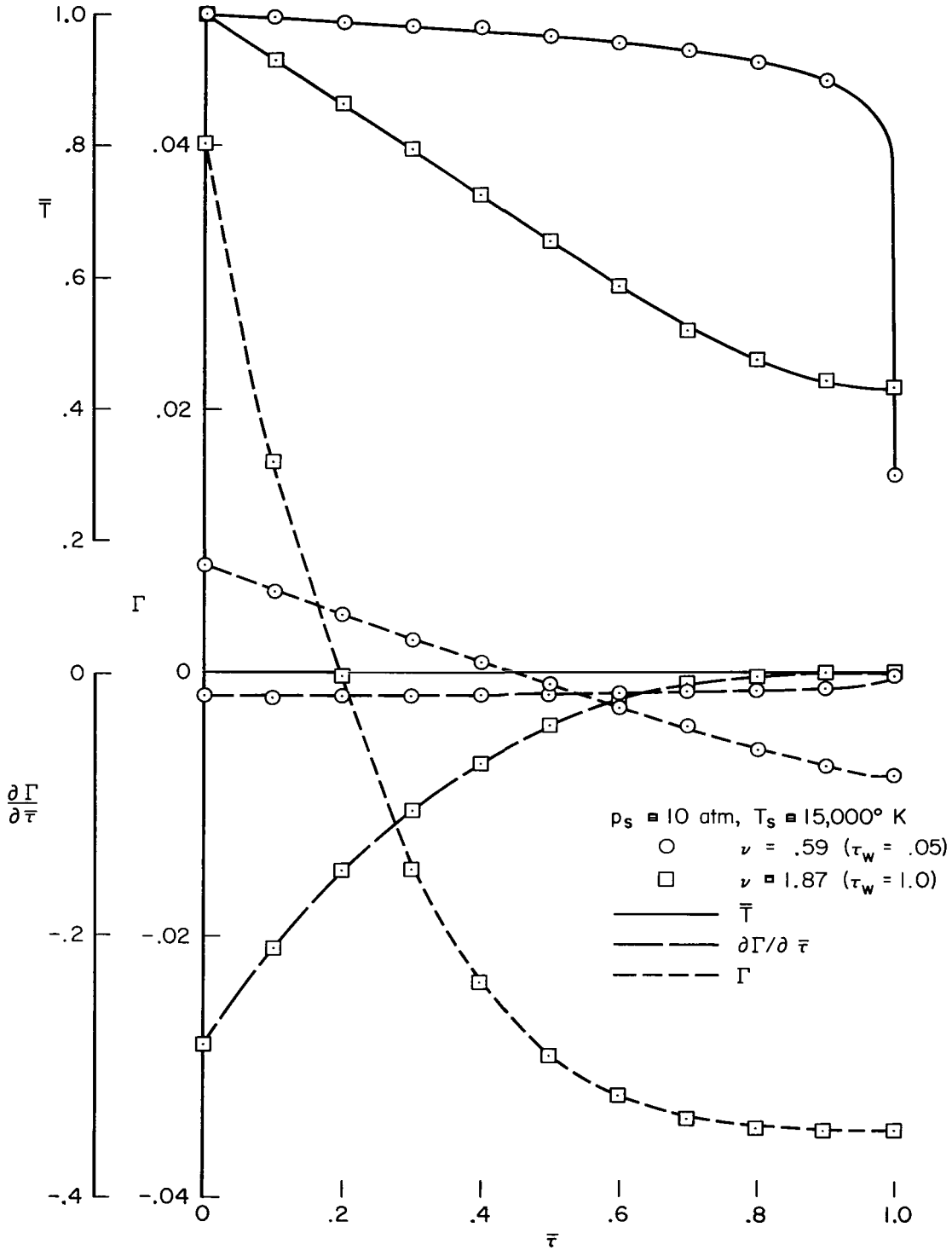

Figure 7.- Distributions of temperature, radiative heat flux, and heat-flux derivative in shock layer.

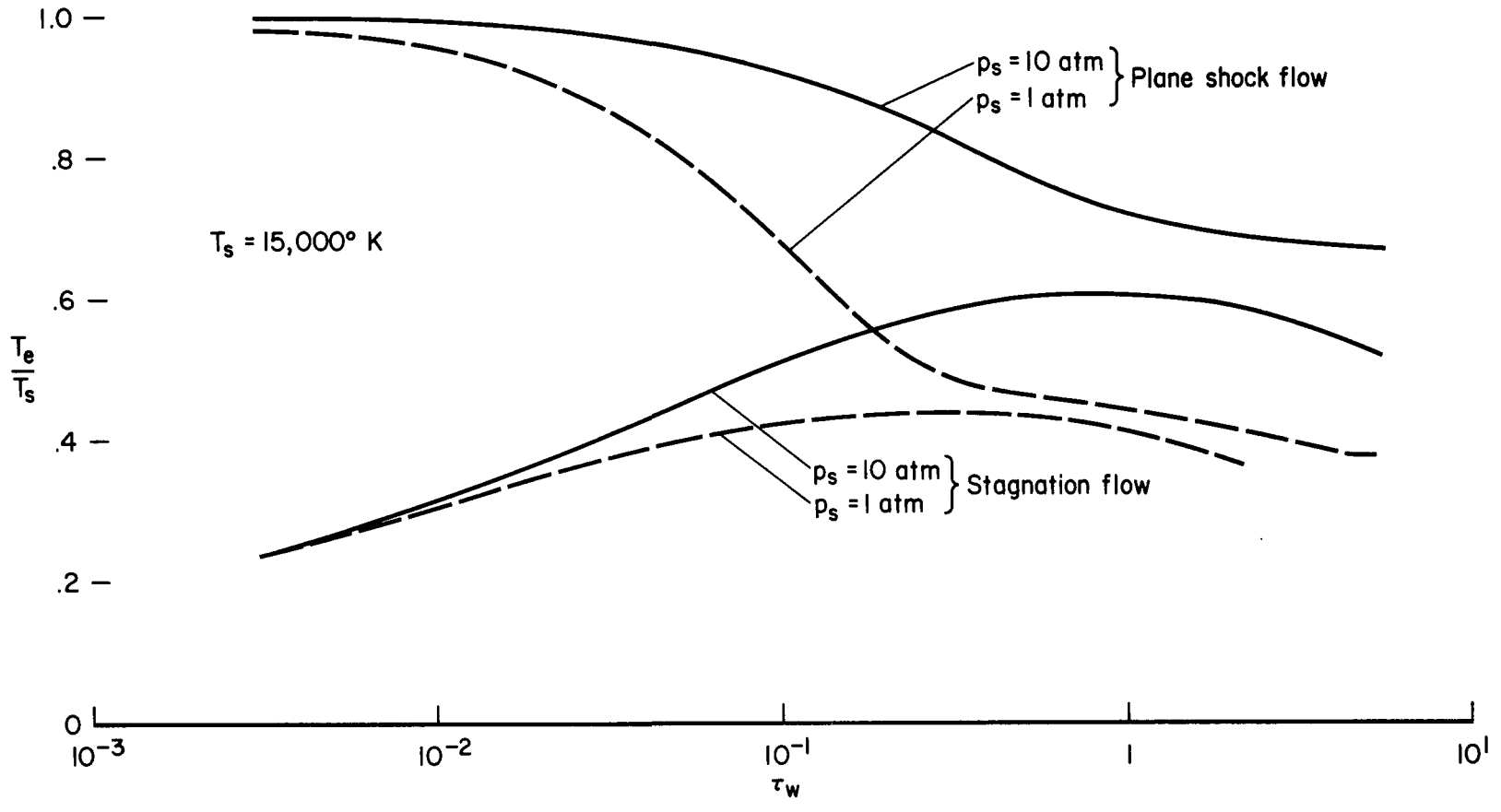

Figure 8.- Effect of absorption in shock layer on gas temperature at the wall.

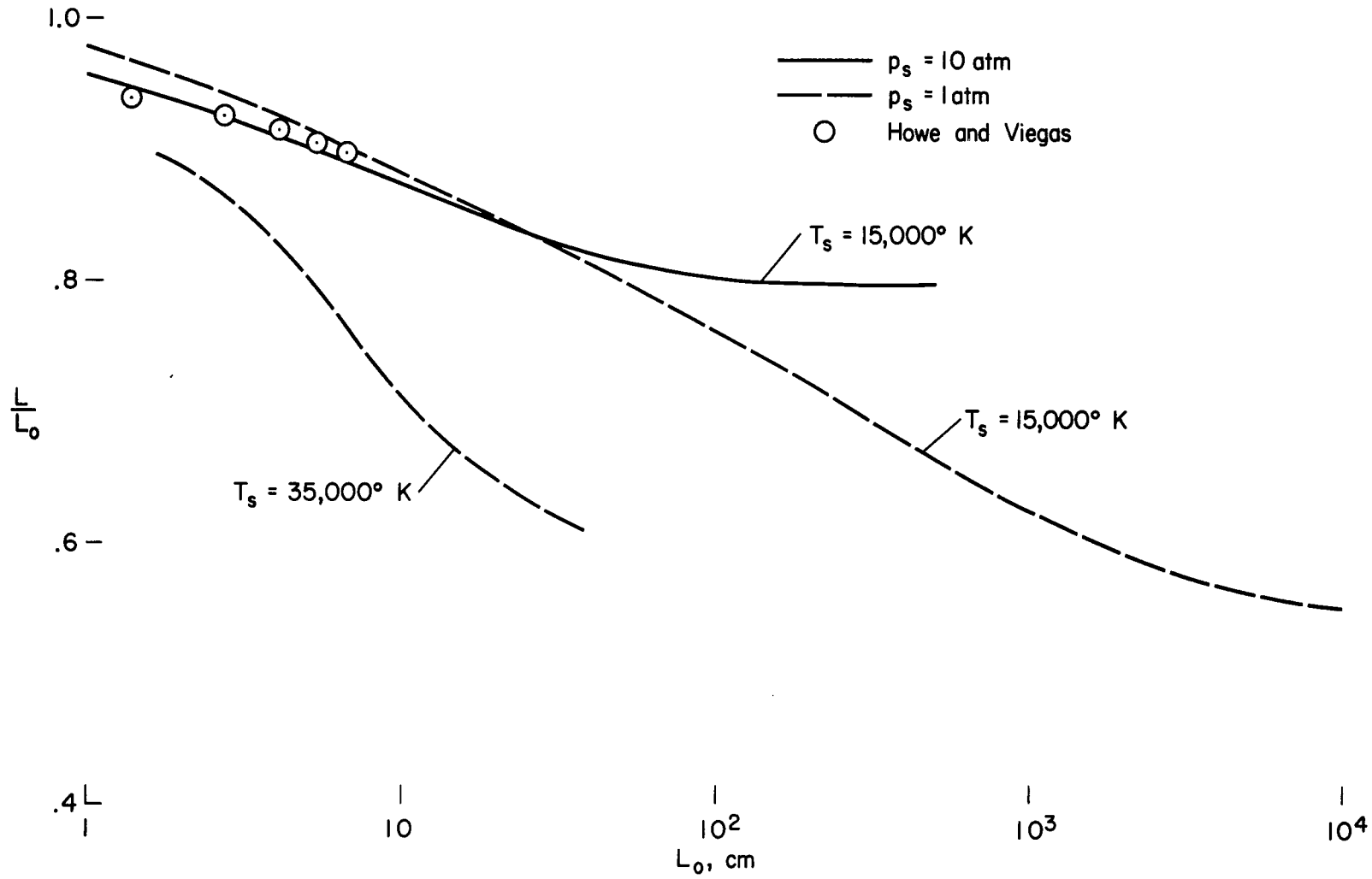

Figure 9.- The effect of nonadiabatic flow on shock-standoff distance.

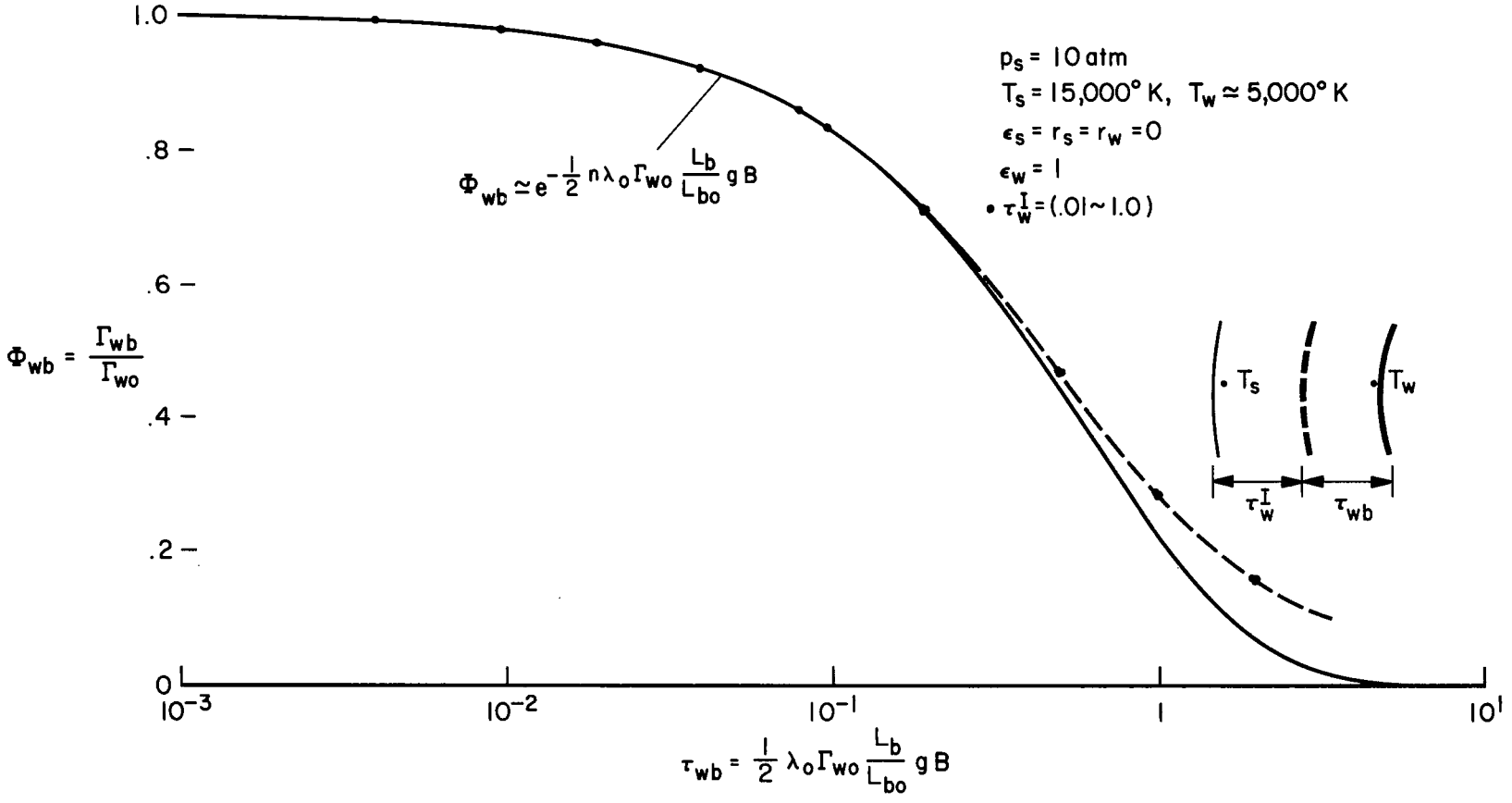

(a) Injection layer.

Figure 10.- Effect of absorption in injection and ablation layer on radiative heat flux to the wall.

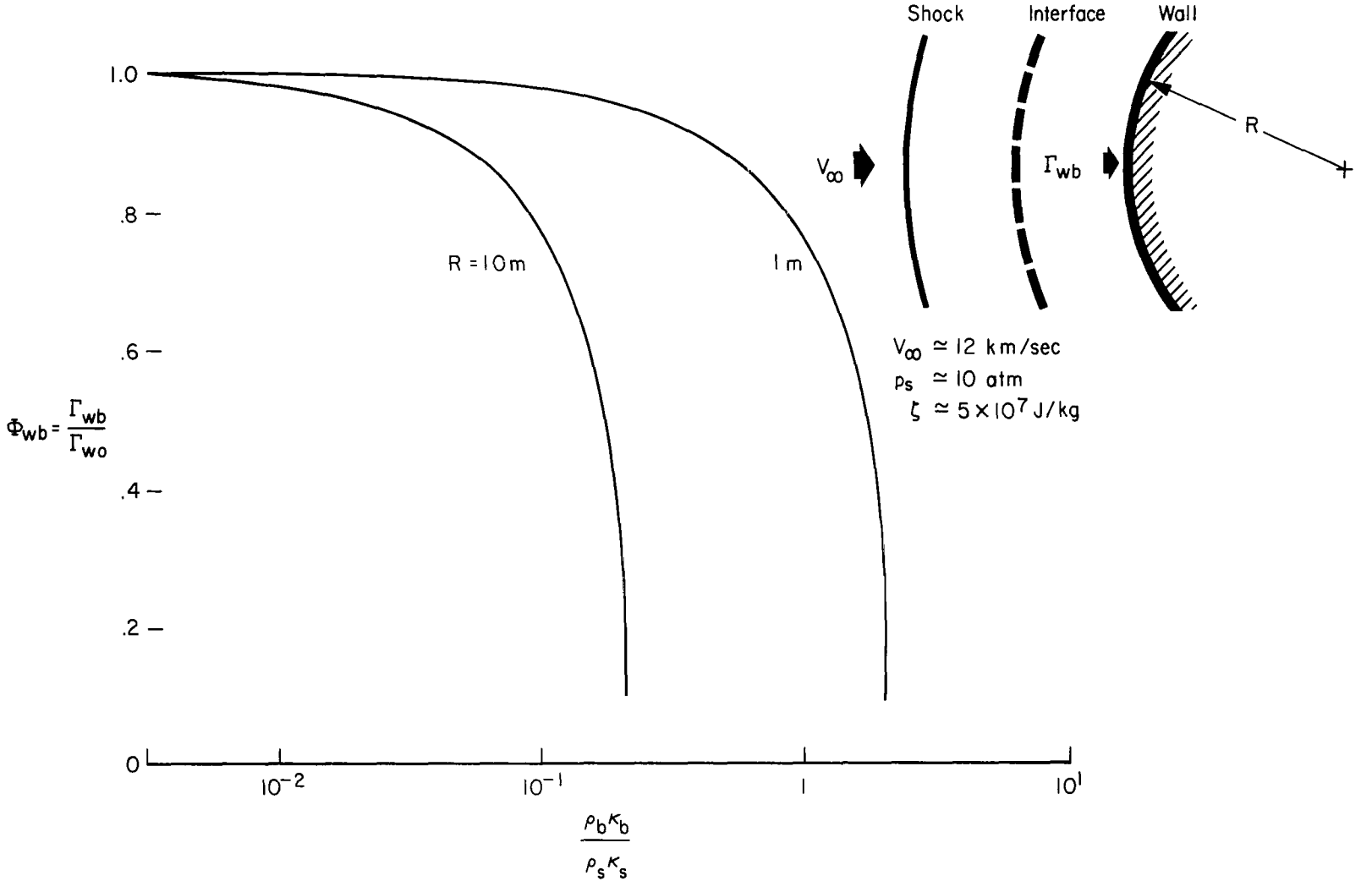

(b) Ablation layer.

Figure 10.- Concluded.

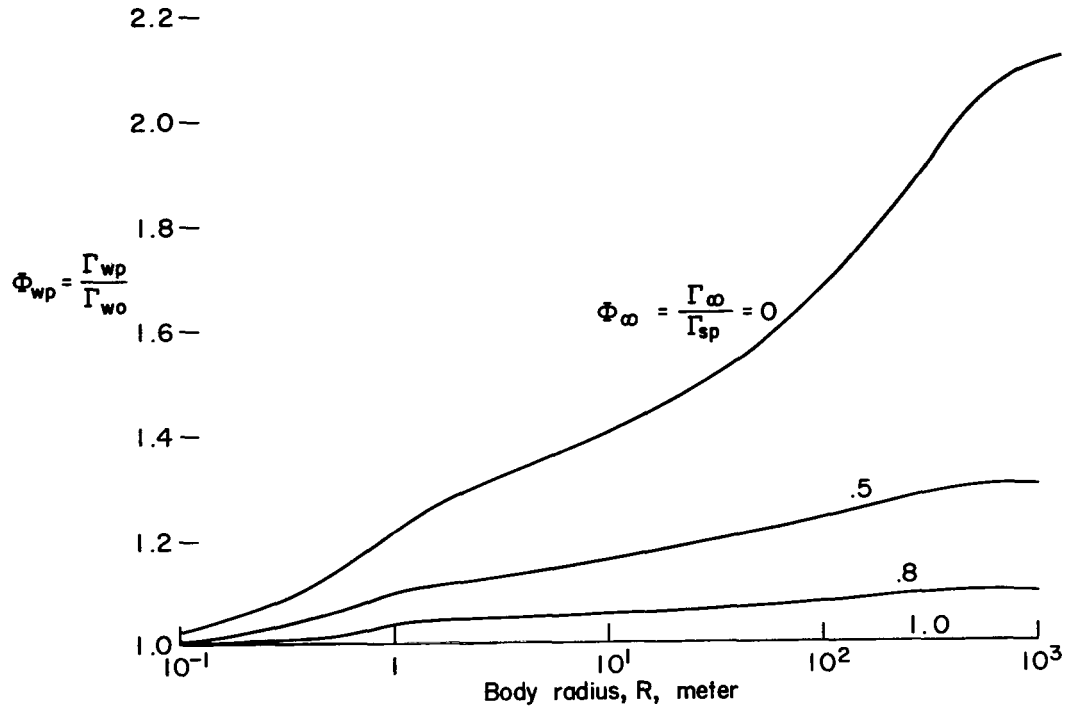

(a) p_s = 1 atm, T_s = 15,000° K ($V_\infty \simeq$ 15 km/sec, H ≃ 58 km).

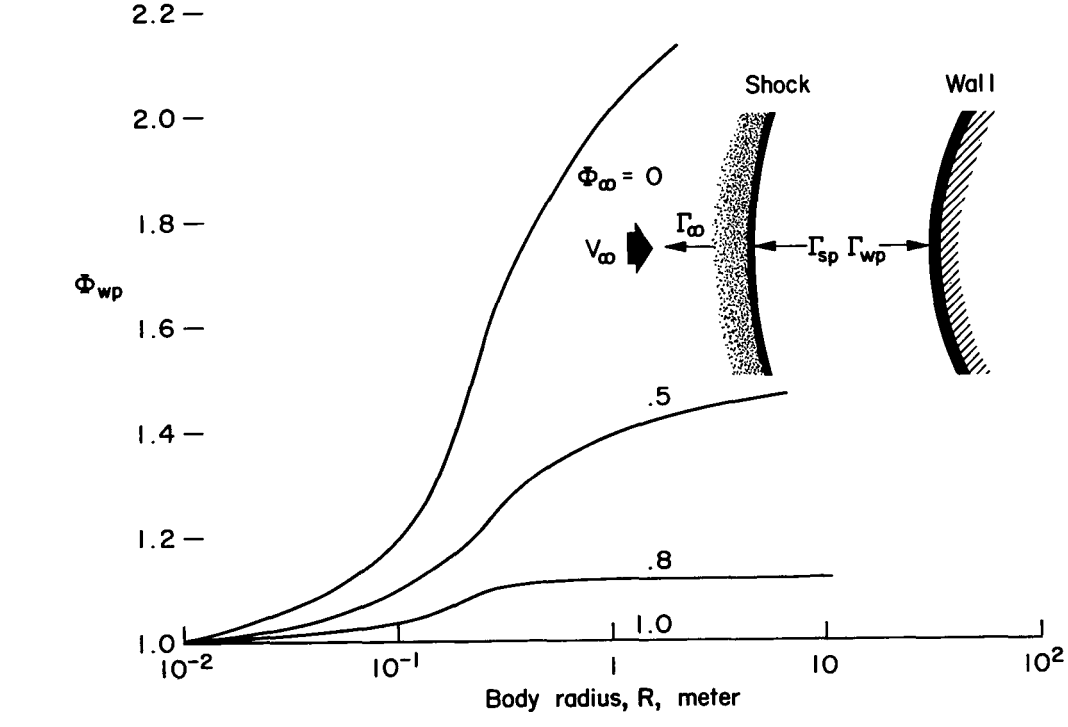

(b) p_s = 10 atm, T_s = 40,000° K ($V_\infty \simeq$ 30 km/sec, H ≃ 49 km).

Figure 11.- Effect of preheating on radiative heat to the wall.

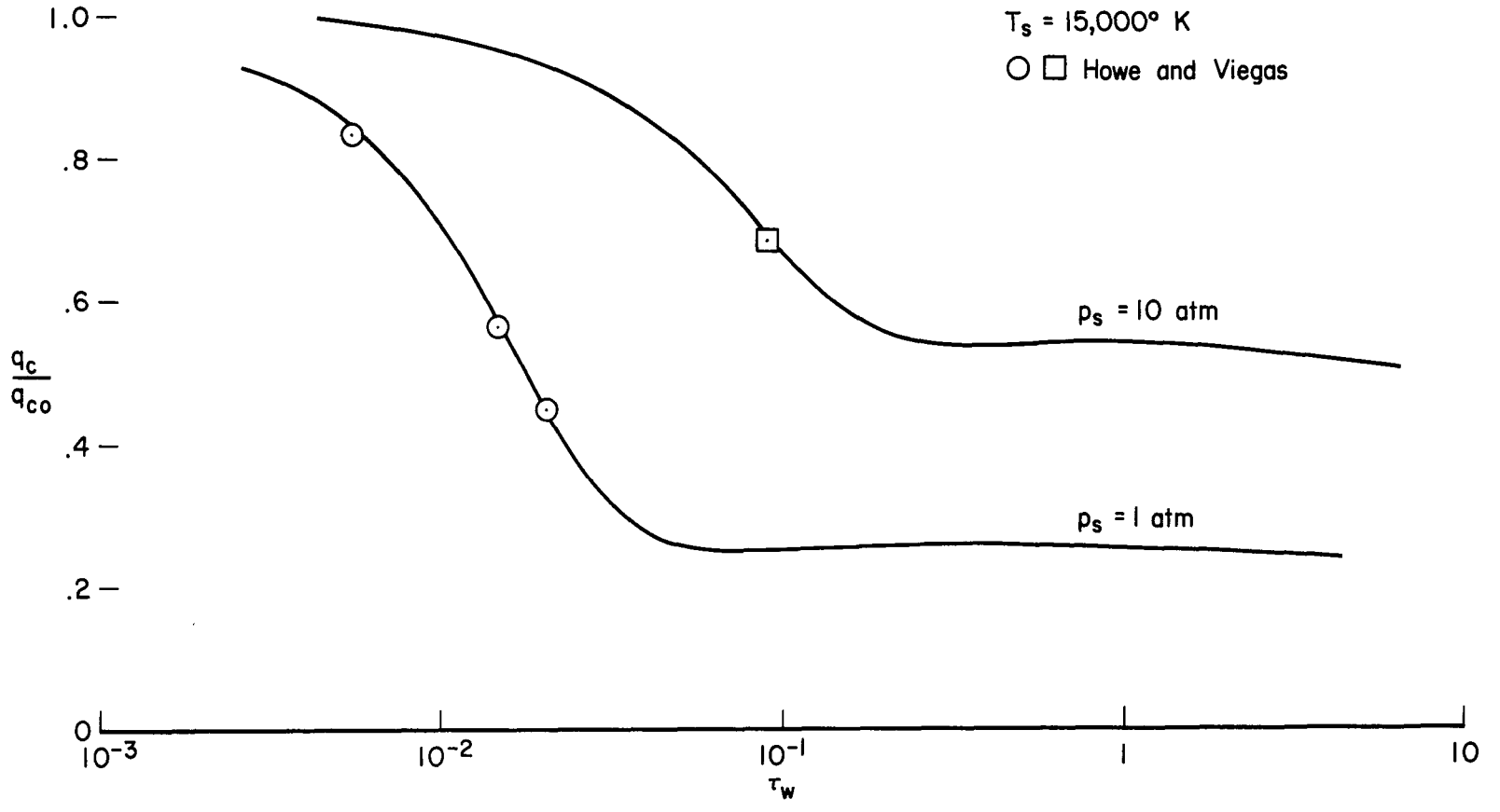

Figure 12.- The effect of radiative heat on convective heat to the wall.

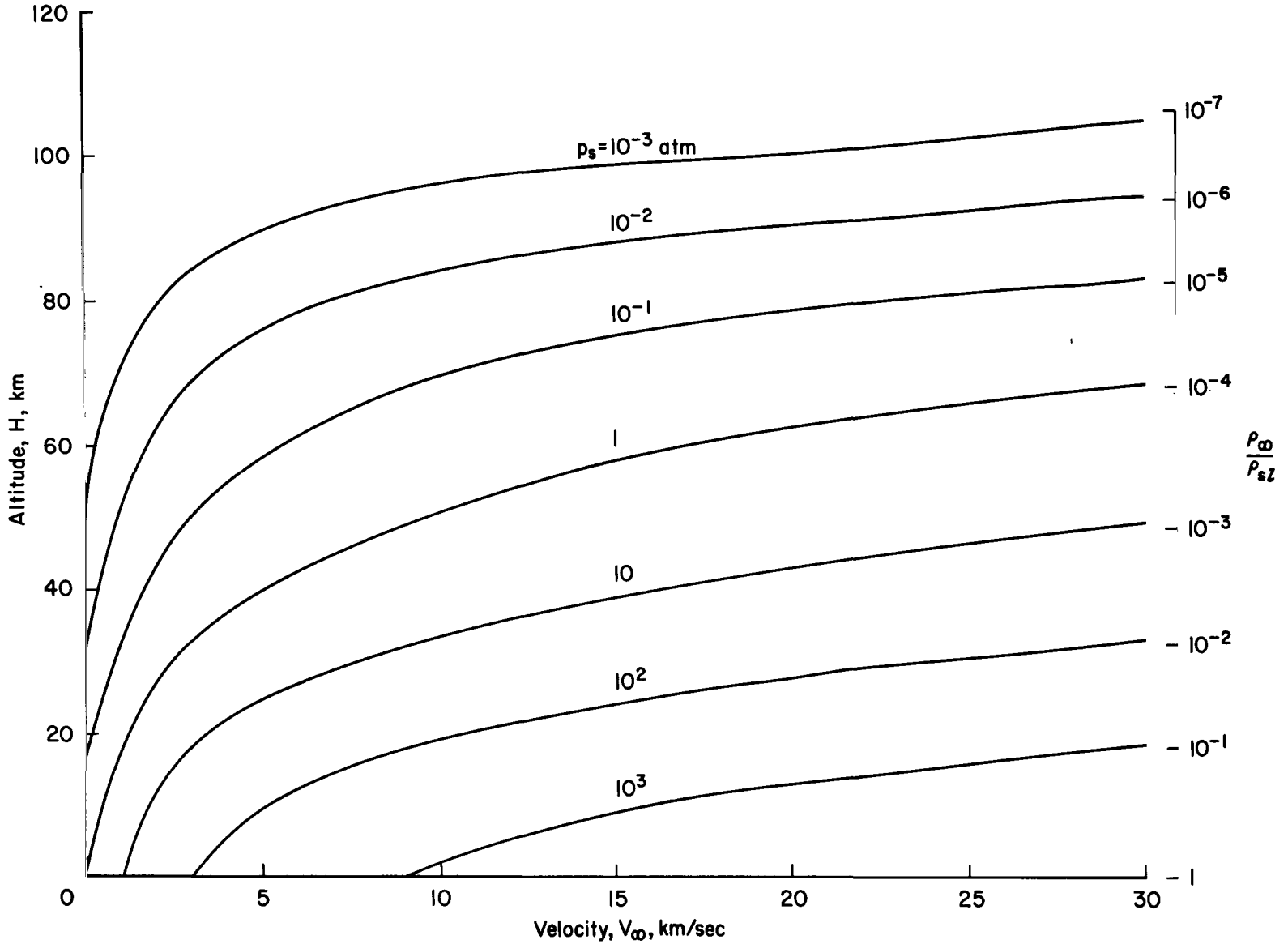

(a) Pressure.

Figure 13.- Thermodynamic properties behind shock for equilibrium air.

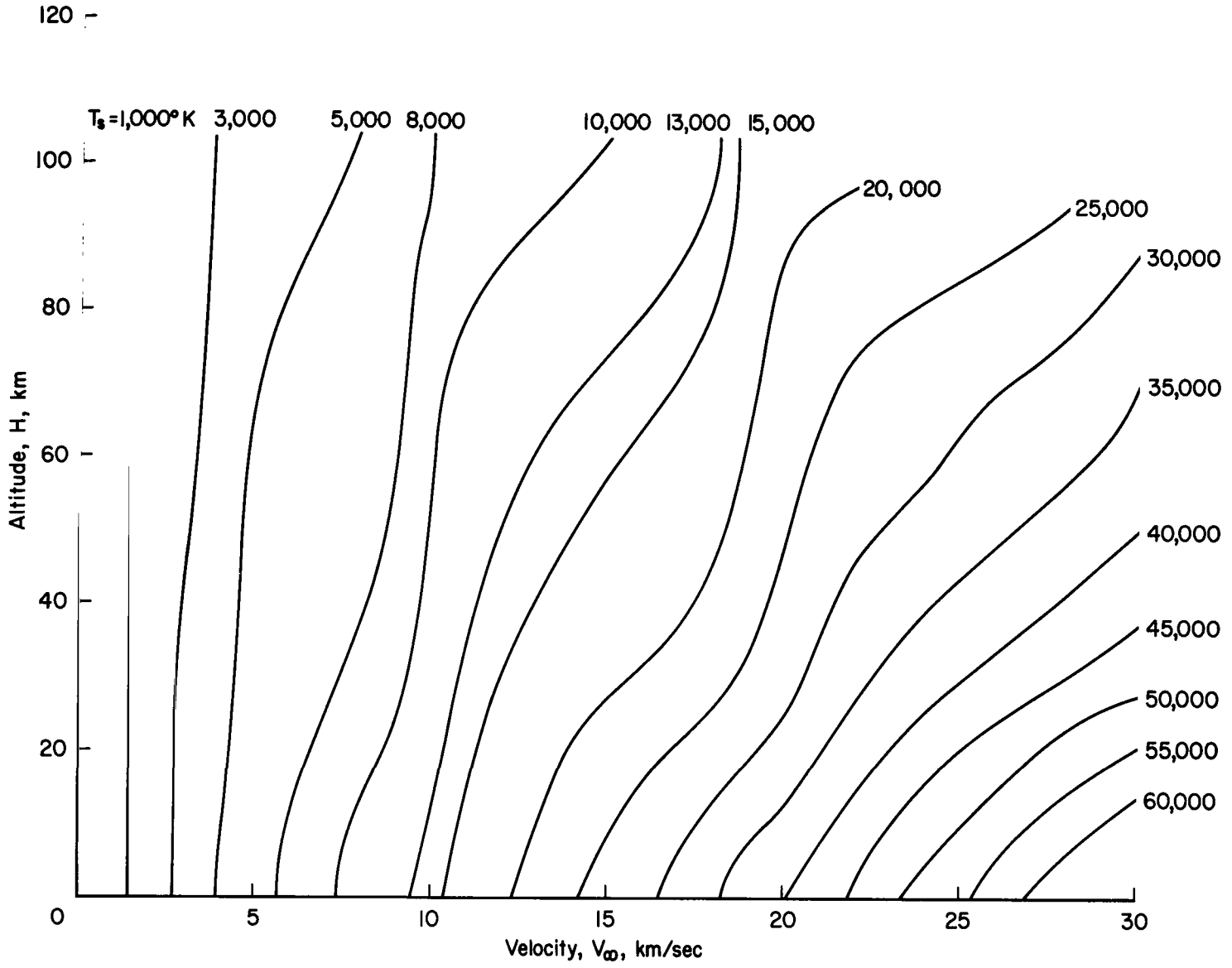

(b) Temperature.

Figure 13.- Continued.

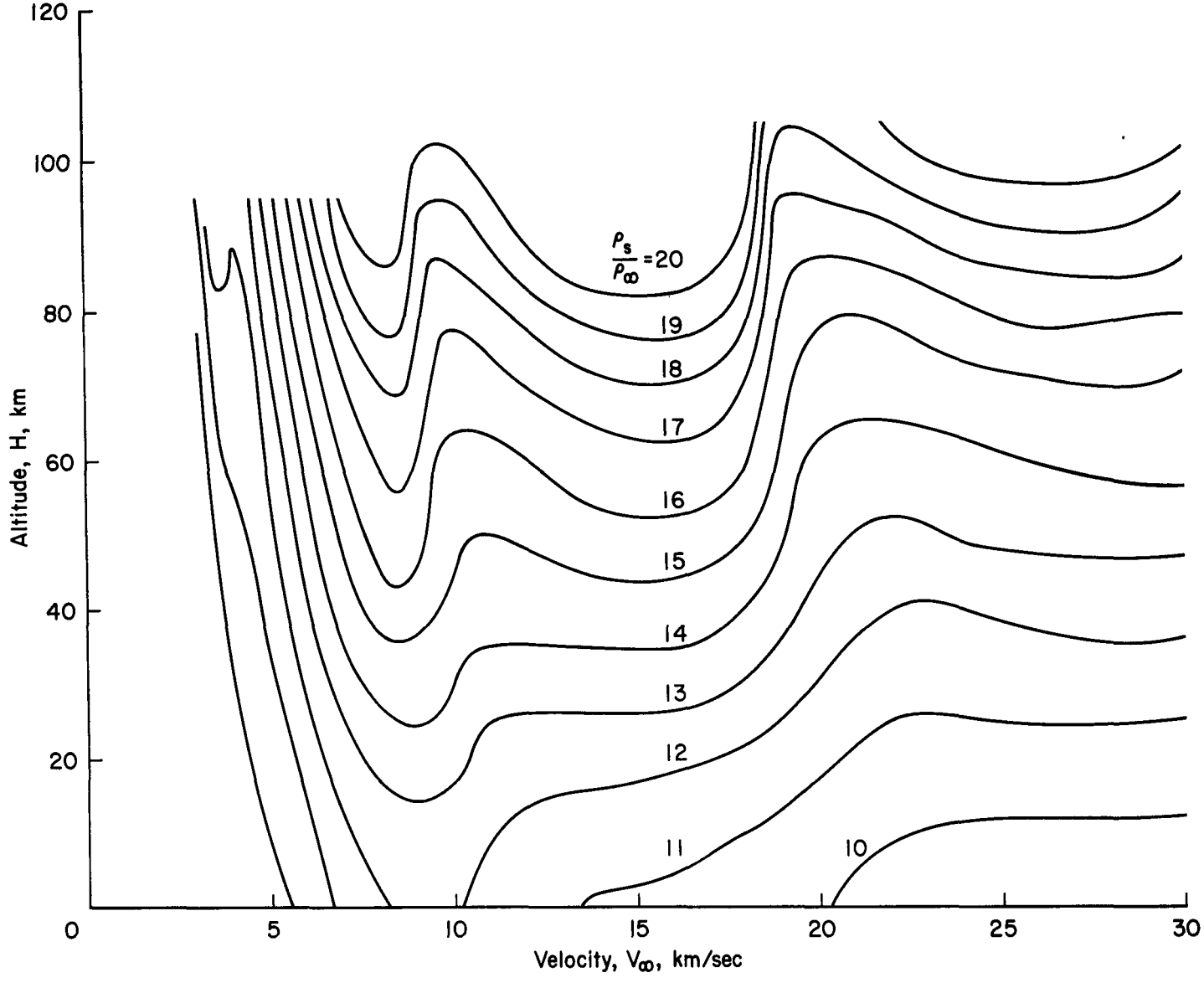

(c) Density ratio across shock.

Figure 13.- Concluded.

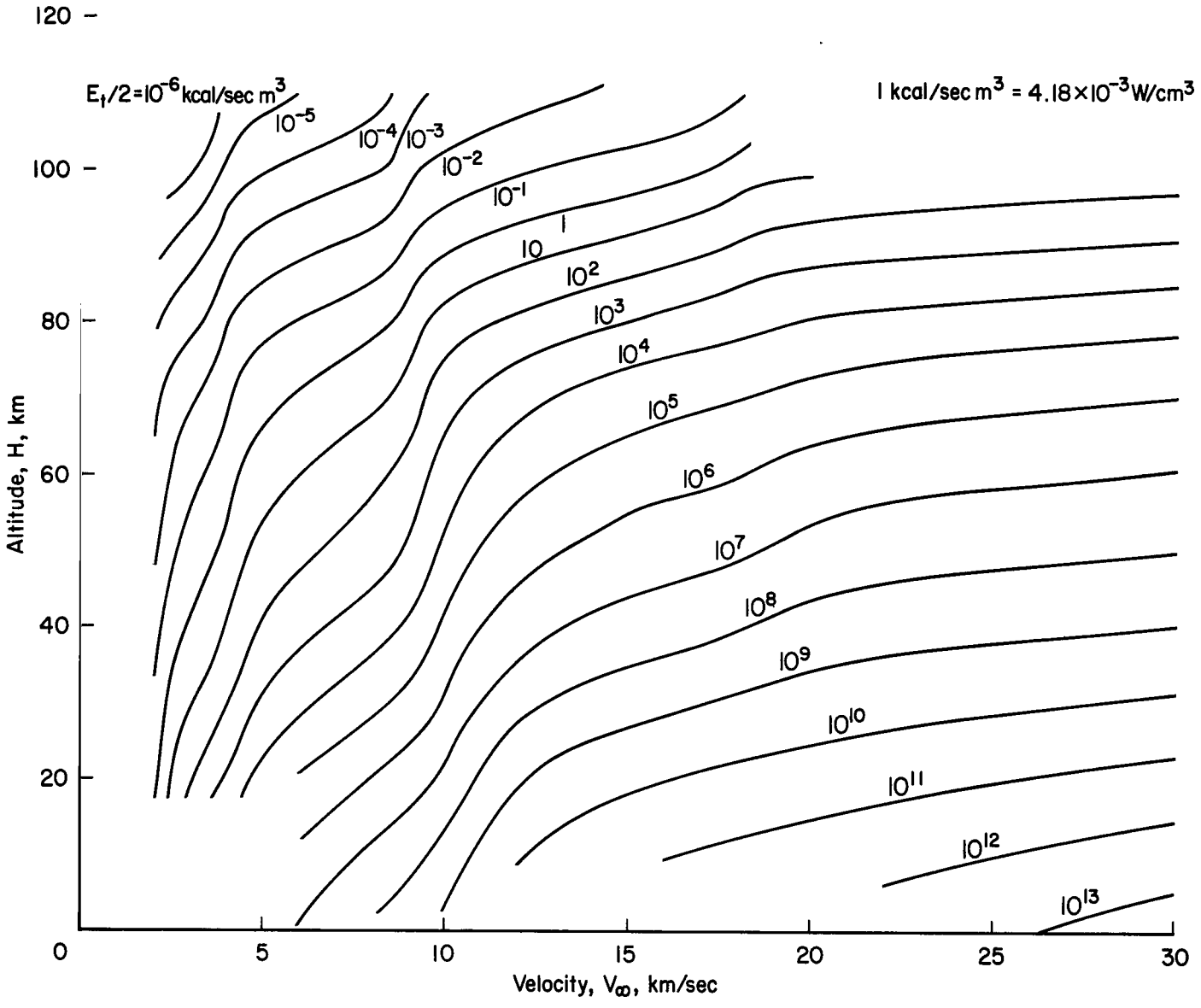

(a) Radiative intensity.

Figure 14.- Radiative properties behind shock for equilibrium air.

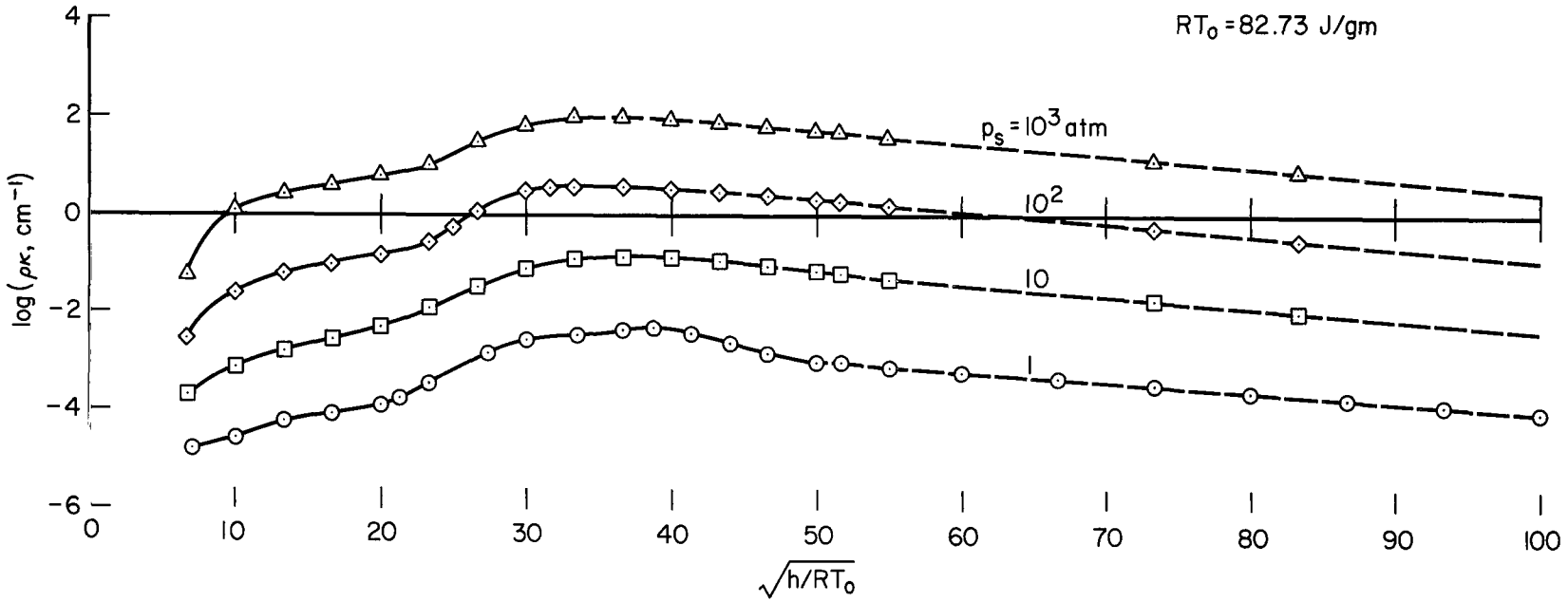

(b) Planck mean absorption coefficient.

Figure 14.- Concluded.

"The aeronautical and space activities of the United States shall be conducted so as to contribute . . . to the expansion of human knowledge of phenomena in the atmosphere and space. The Administration shall provide for the widest practicable and appropriate dissemination of information concerning its activities and the results thereof."

—NATIONAL AERONAUTICS AND SPACE ACT OF 1958

NASA SCIENTIFIC AND TECHNICAL PUBLICATIONS

TECHNICAL REPORTS: Scientific and technical information considered important, complete, and a lasting contribution to existing knowledge.

TECHNICAL NOTES: Information less broad in scope but nevertheless of importance as a contribution to existing knowledge.

TECHNICAL MEMORANDUMS: Information receiving limited distribution because of preliminary data, security classification, or other reasons.

CONTRACTOR REPORTS: Scientific and technical information generated under a NASA contract or grant and considered an important contribution to existing knowledge.

TECHNICAL TRANSLATIONS: Information published in a foreign language considered to merit NASA distribution in English.

SPECIAL PUBLICATIONS: Information derived from or of value to NASA activities. Publications include conference proceedings, monographs, data compilations, handbooks, sourcebooks, and special bibliographies.

TECHNOLOGY UTILIZATION PUBLICATIONS: Information on technology used by NASA that may be of particular interest in commercial and other non-aerospace applications. Publications include Tech Briefs, Technology Utilization Reports and Notes, and Technology Surveys.

Details on the availability of these publications may be obtained from:

SCIENTIFIC AND TECHNICAL INFORMATION DIVISION

NATIONAL AERONAUTICS AND SPACE ADMINISTRATION

Washington, D.C. 20546